Australian Government

Wine Australia

Developing a phone-based imaging tool to inform on fruit volume and potential optimal harvest time



FINAL REPORT to

WINE AUSTRALIA

Project Number: **CSU 1501**

Principal Investigator: **Dr Leigh Schmidtke**

Research Organisation: **National Wine and Grape Industry Centre, Charles Sturt University**

Date: **June 2018**

Project CSU 1501

Developing a phone-based imaging tool to inform on fruit volume and potential optimal harvest time.

Chief Investigator:
Dr Leigh Schmidtke

Institution:
National Wine and Grape Industry Centre
Charles Sturt University
Lock Bag 588
Wagga Wagga
New South Wales 2678

Copyright Statement:

Copyright © Charles Sturt University 2018

All rights reserved. Apart from any use permitted under the Copyright Act 1968, no part of this report may be reproduced by any process without written permission from Charles Sturt University.

Disclaimer:

The document may be of assistance to you. This document was prepared by the author in good faith on the basis of available information. The author, the National Wine and Grape Industry Centre and Charles Sturt University cannot guarantee completeness or accuracy of any data, descriptions or conclusions based on information provided by others.

The document is made available on the understanding that the author, the National Wine and Grape Industry Centre and Charles Sturt University accept no responsibility for any person acting on, or relying on, or upon any opinion, advice, representation, statement of information, whether expressed or implied in the document, and disclaim all liability for any loss, damage, cost or expense incurred or arising by reason of any person using or relying on the information contained in the document or by reason of error, omission, defect or mis-statement (whether such error, omission or mis-statement is caused by or arises from negligence, lack of care or otherwise).

The product trade names in this publication are supplied on the understanding that no preference between equivalent products is intended and that the inclusion of a product does not imply endorsement by the National Wine and Grape Industry Centre or Charles Sturt University over any other equivalent product from another manufacturer.

Table of Contents

Table of Contents **3**

List of Figures **5**

List of Tables **8**

Abbreviations **9**

1 Abstract **10**

2 Executive summary **11**

3 Acknowledgements **14**

4 Background **14**

5 Project aims and performance targets **16**

6 Pre-development investigation and analysis **18**

6.1 Preliminary data collection and investigation 18

6.1.1 Initial image collection *18*

6.1.2 Computer analysis on images *19*

6.2 New GrapeCS-ML database for development 24

6.2.1 Computer vision and machine learning for viticulture technology *24*

6.2.2 Datasets 1-5 in the new GrapeCS-ML database 29

6.3 Machine learning for app development 36

6.3.1 Pre-investigation and initial design of algorithms for app development *36*

6.3.2 Simulation results on machine learning *41*

6.4 Preliminary results on berry heterogeneity, spatial distribution and maturation within single bunches (cv. Shiraz) 42

6.4.1 Introduction to study *43*

6.4.2 Materials and methods *43*

6.4.3 Results *44*

7 Android app development **48**

7.1 Code design and structure 48

7.2 User interface and functionality 49

7.3 Code and platform considerations 51

7.4 Circle detection and app flow 51

7.5 Berry size measurement 55

7.6 Tint measurement 55

7.7 File and data management 55

7.7.1 Data structure and analysis *55*

7.7.2 Data management - Dashboard *57*

8 Post-development analysis and testing **59**

8.1 Apps analysis on images 59

8.1.1 Analysis and testing of app and Dyostem™ for berry hue *60*

8.1.2 Analysis and testing of app and Dyostem™ for berry volume *64*

8.2 Small scale vinification and grape berry analysis 67

8.2.1 Grape sampling for Dyostem™ and app calibrations *67*

8.2.2 General analyses of grape maturity, yeast available nitrogen and basic wine parameters *68*

9 Outcomes and conclusions **82**

10 Recommendations **83**

11 Appendices **85**

Appendix 1: Communications **85**

11.1 Publications in international peer review journals: 85

11.2 Book Chapters (Conference Proceedings): 85

11.3 Oral communications at conferences: 85

11.4 Reports for the industry 85

11.5 Oral communications for the industry 85

11.6 Posters: 85

Appendix 2: Intellectual property **88**

Appendix 3: References **89**

Appendix 4: Staff **93**

Appendix 5: MATLAB codes for desktop **94**

Appendix 6: OpenCV and Java codes for phone app **109**

Appendix 7: Picture taking protocol **110**

List of Figures

Figure 1: Sample images of captured grape berries with (top pictures) and without (bottom pictures) using the calibration card. 19

Figure 2: Sample images of grape berries located using the MATLAB desktop program. 20

Figure 3: Sample images of grape berries located using the MATLAB desktop program 21

Figure 4: Sample images of grape berries located using the MATLAB desktop program 22

Figure 5: Berry size and colour estimation from colour calibration card 23

Figure 6: Berry size estimation from common object (coin)..... 23

Figure 7: Berry size estimation from reference probe 24

Figure 8: Berry size and colour estimation from colour calibration card 24

Figure 9: Issues for colour casting conditions 25

Figure 10: Preliminary prototype app running on the Android smartphone 25

Figure 11: Shiraz berry growth and ripening curves. Image first published in (Rogiers et al., 2017) 33

Figure 12: Dataset 1 – Sample images from dataset 1 at various stages of development 33

Figure 13: Dataset 2 – Sample images from dataset 2 including a volume reference 34

Figure 14: Dataset 2 – Sample images from dataset 2 showing development following veraison and includes a colour reference 34

Figure 15: Dataset 3 – Sample images from dataset 3 at various stages of bunch development. 35

Figure 16: Dataset 3 – Sample images from dataset 3 at various stages of bunch development 35

Figure 17: Dataset 4 – Sample images from dataset 4 at various stages of bunch development. 36

Figure 18: Dataset 5 – Images and corresponding segmented bunch regions 37

Figure 19: Image processing and machine learning algorithm flows for white cultivars..... 38

Figure 20: Image processing and machine learning algorithm flow for red cultivars 39

Figure 21: Path 1 – Early Stage image processing and machine learning flow for red cultivars 40

Figure 22: Path 2 – Middle Stage image processing and machine learning flow for red cultivars 41

Figure 23: Path 3 – Late Stage image processing and machine learning flow for red cultivars 42

Figure 24: Berry spatial distribution according to their seed number within a ripe bunch. The arrows show the rachis and small branches with the counted number of berries on each. Our results did not show differences between warm (a) and temperate (b) climates. 46

Figure 25: Berry number per class of pericarp fresh mass (g) and the associated seed number. The results show that berry from the same fresh mass could have a different seed number. No real differences are evident between warm (a) and temperate (b) climates. 47

Figure 26: Selected berry composition parameters ordered for fresh weight. An apparent association between berry seed number (vertical axis) and berry mass is evident. No specific association between berry seed number and berry water content or dry weight mass is evident 47

Figure 27: Seed content and berry colour at veraison: comparison between green, pink and red berries. The ripest berries in terms of anthocyanins biosynthesis (berry colour) had the highest seed content 48

Figure 28 a, b: Principal Component Analysis loadings (a) and scores (b) plot of berry composition. PC2 shows a clear separation of samples according to berry seed number. Associated with berry seed number are highly loaded variables for pericarp mass and total dry weight of seeds. Of interest is the lack of position of sugar (g/g) in PC2 (near the origin) inferring a disassociation between berry sugar accumulation and seed number..... 49

Figure 29: Code design and structure of app..... 50

Figure 30: NWGIC app screen 51

Figure 31: Image capture with reference probe 51

Figure 32: Data record 52

Figure 33: Berry detection and sampling 52

Figure 34: Sampled berries for analysis 52

Figure 35: Distribution of berry volume 53

Figure 36: App berry detection image processing and machine learning pipeline 54

Figure 37: Dashboard on Excel spreadsheet for viewing app analysis results 60

Figure 38: Sample data from global spreadsheet used for the app analysis results 61

Figure 39: Photograph images for Chardonnay grape bunches (2018 harvest) taken in daylight 62

Figure 40: Photograph images for Chardonnay grape bunches (2018 harvest) taken in artificial shade 63

Figure 41: Comparison of phone app and Dyostem for Chardonnay bunch hue (2018 harvest) in daylight..... 65

Figure 42: Comparison of phone app and Dyostem for Chardonnay bunch hue (2018 harvest) in shade 66

Figure 43: Sample bunch image taken in daylight and artificial shade with corresponding app berry detections. The measured hue values from the app are also shown 67

Figure 44: Comparison of phone app and Dyostem for Chardonnay volume (2018 harvest) in daylight. 68

Figure 45: Comparison of phone app and Dyostem for Chardonnay volume (2018 harvest) in shade 69

Figure 46: Chardonnay grape berry maturation data for the Cumulus vineyard - Vintage 2017..... 75

Figure 47: Chardonnay grape berry maturation data for the Gundagai vineyard - Vintage 2017. Samples from 15 and 20 February are from early maturation blocks; 21 and 28 February samples from mature blocks..... 76

Figure 48: Sensory descriptive ratings for Chardonnay wines - Vintage 2017 77

Figure 49: Principal Component Analysis biplot of sensory descriptive ratings for Chardonnay wines. 78

Figure 50: Cumulus vineyards Sauvignon Blanc maturity data - Vintage 2017 81

Figure 51: See Saw vineyards Sauvignon Blanc maturity data - Vintage 2017 82

Figure 52: Descriptive sensory analysis of Sauvignon Blanc wines harvested at early and mature levels of grape maturation at two vineyards - Vintage 2017 83

Figure 53: Principal Component Analysis biplot of sensory descriptive ratings for Sauvignon Blanc wines 84

Figure 54: Gundagai vineyard Shiraz grape maturity data - Vintage 2017 86

Figure 55: Cumulus Vineyards Shiraz maturity data - Vintage 2017 87

Figure 56: Avoid non-uniform illumination: note the top of the bunch is in the shade compared to the

bottom (left). Uniform illumination is better (right) 116

Figure 57: Another example of non-uniform illumination: some of the berries are lit brightly by the sun..... 117

Figure 58: Blue colour cast in the original photograph (left). The same image after being colour-corrected using the ColourChecker card (right). 117

Figure 59: An example where the camera is held too high 118

List of Tables

Table 1: Summary of five datasets collected for computer vision and machine learning..... 32

Table 2: Classification rate (%) for white berry cultivars using various machine learning approaches and colour spaces 43

Table 3: Classification rate (%) for red berry cultivars using various machine learning approaches and colour spaces. 43

Table 4: Grape sampling for small lot wine making. 70

Table 5: Reference standards for sensory descriptive analysis 73

Table 6: Chardonnay grape analysis at harvest and finished wine data..... 77

Table 7: Sensory descriptive analysis mean ratings for Chardonnay wines. Letters in each row indicate significant differences between wines..... 79

Table 8: Sauvignon Blanc grape analysis at harvest and finished wine data. 83

Table 9: Mean sensory ratings for Sauvignon Blanc wines. Different letters infer a significant difference..... .85

Abbreviations

CHT	Circular Hough Transform
FFNN	Feed-forward neural network
HSI	Hue-Saturation-Intensity colour space
HSV	Hue-Saturation-Value colour space
k-NN	k nearest neighbour
LAB	Lightness and a b colour space
RGB	Red-Green-Blue colour space
RRD	Ridge ring detector
SVM	Support vector machine
TSS	Total Soluble Solids
VIVC	Vitis International Variety Catalogue
YCbCr	Luminance-chrominance colour space

1 Abstract

The objective of this project was to investigate the feasibility of developing a smartphone-based imaging tool for berry quality assessment that can be conveniently used within vineyards to provide real time and in-field evaluation of grape berry size and colour. After taking a photograph of the grape bunch on the vine, the smartphone application analyses the image, detects and samples the visible berries, and determines the volume and hue distributions of the sampled berries. Results are reported for the analysis of grape bunch images from Australian vineyards.

The resulting app (called **WineOz SmartGrape**) is programmed for use on an Android smartphone platform and can be downloaded from the app store using the following link: https://play.google.com/store/apps/details?id=com.nwgic.grapeyield

The app is intended to be used to monitor the spatial and temporal data collected for vineyard blocks and is best used when interfaced to a dashboard which can be downloaded from the NWGIC web site along with instructions:

http://www.csu.edu.au/nwgic/research/wineoz-smartgrape-mobile-application

Challenges and recommendations for smartphone imaging in the field are also discussed.

2 Executive summary

This project arises from two developments: a deepening understanding of the chemistry associated with grape maturation; and rapid development of mobile imaging techniques, especially associated with smartphones.

The mature development of mobile phones with high-quality cameras, well-developed software environments, image processing, and statistical analysis (including machine learning) for data and image classification could offer a less expensive means to measure berry skin colour, fruit volume and distribution, grape berry homogeneity versus heterogeneity. That forms the justification for the present project.

White grape colour transition (from green to yellow, and yellow to orange) during the ripening is linked to chlorophylls and carotenoids degradation, and the formation of C13 norisoprenoids. Deloire 2013, showed that using a Dyostem™ instrument (Vivelys and Montpellier SupAgro, France) to measure berry volume and skin colour in white cultivars could help the harvest decision process to achieve desirable wine styles. However, this technique is expensive, slow, destructive, and cannot be deployed in the vineyard. Other techniques such as optical fibre evanescent field absorption (FEFA) have been used to measure grape colour but they also rely on specialised equipment and the destruction of grapes.

The link between sugar accumulation and flavour development in the berry is often non-existent, compound and environment dependent, and highly influenced by harvest time. Berry size can be manipulated most efficiently with irrigation strategies and is one of the key determinants of berry shrinkage. Heterogeneity in berry volume significantly alters grape composition and can only be rectified by expensive sorting techniques in the winery. Thus, the development of in-field decision support tools will assist vineyard managers to more effectively operate commercial vineyards for irrigation management and harvest decisions for specific wine styles.

This project commenced by determining the feasibility of using desktop computing systems for berry detection and colour measurements of images of bunches of grapes. A colour reference card located within the image allowed for colour correction algorithms to be applied and served as a depth of field calibration for accurate berry size estimation. Initial image analysis showed good correlations between berry measures from the image and laboratory measures for berry size and colour in white varieties, and berry size for red varieties. Several reference items were trialled for depth of field calibrations and for the purposes of this project a probe that could be inserted into the target bunches was chosen. Inserting a probe into the bunch of grapes

facilitates image capture as the camera operator is not required to hold or place an object in the image area; the probe is not obscured by fingers or the hands of the operator and the probe can be easily removed and reused. Berry illumination is an important consideration to image capture prior to analysis as colour casting arises from differentially shaded portions of the vine canopy, which in turn is influenced by the degree of cloud cover, light angle and time of day. Several image databases have been created for grape bunches at varying levels of maturity and for several cultivars, along with traditional measures of grape composition. These databases will provide a valuable resource for the development of machine learning algorithms for future projects.

To determine the spatial and temporal variability of fruit composition within a single bunch, an investigation to characterise bunch heterogeneity at two developmental stages (veraison and full maturity immediately prior to harvest) was undertaken. Berry position within bunches and branches did not influence berry composition, however, berry seed number was strongly correlated with sugar concentration fresh and dry mass of the pericarp and skin colour at veraison.

Smartphone app development was undertaken to incorporate image capture, berry detection, colour and size measures within the Android Studio with OpenCV. This App can be operated using Android version 4.0.3 (Ice Cream Sandwich). To assist in the development of the user interface, feedback from industry representatives was sought prior to final GUI development. User data incorporating vineyard, block and grape cultivar can be entered prior to image capture and running berry detection algorithms. A considerable investment of time to overcome the programming challenge of incorporating image detection and machine learning algorithms from a desktop to a smartphone computing environment was required for this project.

The resulting Android platform App (**WineOZ SmartGrape**) can be downloaded from the app store and interfaced with an Excel™ based dashboard to monitor the temporal and spatial data created with the image analysis features of the software. The app can be downloaded from: https://play.google.com/store/apps/details?id=com.nwgic.grapeyield

The dashboard, along with instructions and guidelines for imaging, is available from the NWGIC web site:

http://www.csu.edu.au/nwgic/research/wineoz-smartgrape-mobile-application

The berry detection pipeline was developed within this project using a sequential process that makes use of five stages of detection:

1. Colour image capture with reference probe detection.
2. Greyscale conversion.
3. Equalisation of the grayscale image to a standardised distribution of colour.
4. Berry detection using a circle detection algorithm.
5. Berry detection filtering using a support vector machine learning algorithm.

While the image undergoes a greyscale transformation, pixel colour information within each detected berry is retained and this is used to determine the medium berry colour within the HSV colour scale. Berry size estimation is determined using a ratio of pixels across the reference probe and detected circle following image analysis. Once berry diameter has been determined an estimate of berry volume is calculated using a standard sphere formula. Metadata collected during image capture allows spatial and temporal data curation within three separate data files which are easily linked to an Excel™ dashboard to display results within a desktop environment.

Ground truthing of the app results to the industry standard measures for berry size and colour was undertaken in the 2018 growing season for Chardonnay grapes growing in the Riverina. A suite of grape bunch images was collected in full sunlight and with shading to assess the impact of illumination on berry detection and colour measures. Good comparison for berry hue angle obtained from the smartphone app and a Dyostem™ instrument were obtained for bunches in full sunlight, however, such correlations were not evident for partially shaded or fully shaded bunches. These results were obtained without any colour correction applied to the images and demonstrated a requirement for this feature to be incorporated into future versions of the app. Berry volume estimates were poorly correlated with Dyostem™ values and a number of factors are important when comparing these methods. The Dyostem™ instrument is a proprietary system and the methods used for calculation of berry volume could not be determined. Attempts to access the source code for the instrument and requests to the instrument manufacturer to obtain this information were not successful. Some berry water loss and deformation may have arisen from the berries as these were measured up to 24 hours after their collection. The number of pixels that represented the reference probe diameter (0.8 cm) may vary from image to image depending on camera position and proximity to the probe. This variance associated with the pixel diameter of the probe translates to a significant ratio difference used for berry volume calculations. This arises due to the small size of the probe and can be corrected by enlarging the probe diameter.

Small lot winemaking of Chardonnay and Sauvignon Blanc at early and advanced levels of grape maturity were undertaken to explore the link between berry colour assessment and wine style. Clear and demonstrably different sensory profiles of the wines were noted by a trained sensory panel at the early and mature stages of grape development. Importantly, changes in the wine sensory profiles were correlated to a change in berry hue angle, demonstrating the opportunity to use grape berry colour as a predictor of wine style and establishing a sufficient body of evidence to support future research to move the outcomes of this project from a proof of concept to a mature decision support tool for practical vineyard management.

3 Acknowledgements

The activities and investigations described in this report were supported by funding from Wine Australia. Charles Sturt University, through the National Wine and Grape Industry Centre (NWGIC), provided considerable cash support and in-kind contributions of staff time, expertise, laboratory and wine making facilities.

This project could not have proceeded without the invaluable input, allocation of resources, ready access to vineyards and assistance provided to NWGIC researchers by our industry partners. We would like to thank Marty Gransden from Cumulus Wine, Justin Jarrett from See Saw, and Christian De Camps at Gundagai Vineyards for providing access to the vineyards.

The National Wine and Grape Industry Centre is a research centre at Charles Sturt University, created as an alliance with the New South Wales Department of Primary Industry and the New South Wales Wine Industry Association. Input and support from the external partners of the NWGIC is gratefully acknowledged.

4 Background

Since the advent of the smartphone just over a decade ago, a fundamental shift has occurred in the way individuals interact with, obtain, analyse and interpret data, and apply technology. Improvements in computing power, incorporation of a multitude of sensors with higher fidelity, improved connectivity, and access to faster upload and download speeds has resulted in smartphones and smart devices becoming ubiquitous within most populations.

Smartphone ownership in Australia is estimated at around 88% of the entire population with ownership amongst those aged 18-35 years well over 91%, representing an ownership level approaching market saturation (Drumm et al., 2017). Commensurate with improved computing

power of smartphone and tablet devices, along with higher ownership rates, a plethora of apps has been developed, and most professions would now have some smartphone app for which the developers purport its use to improve work related functions.

The agricultural sector has been a particularly active area for app development. Interestingly, many apps that target various agricultural enterprises make use of camera and global positioning sensors (Pongnumkul, Chaovalit, & Surasvadi, 2015), suggesting that spatial and temporal data domains, along with data management and interpretation, will be important features of successful apps that facilitate decision support systems.

Numerous smartphone apps targeting the viticultural industry have been described with significant focus on disease detection and management for economically important pathogens including botrytis (Hill et al., 2014), *Erysiphe necator* (powdery mildew) (Birchmore et al., 2015); flower (Aquino et al., 2015; Millan et al., 2017) and yield estimation (Font et al., 2015; Kicherer et al., 2015; Liu, Marden, & Whitty, 2013); vine vigour and canopy architecture (De Bei et al., 2016) to name a few.

The timing of grape harvest is often decided by viticulturists and winemakers using various criteria. Even when the harvest decision is determined by a range of objective measures of grape maturity (e.g. Brix, titratable acidity, phenols and anthocyanins/colour), these indices give no information about the grape aromatic potential or the resulting wine flavour profiles (Calderon-Orellana et al., 2014; Deloire, 2014).

The link between sugar accumulation and flavour development in the berry is poorly defined, compound and environment dependent, and highly influenced by harvest time (Antalick et al., 2015; Bindon et al., 2013; Kalua & Boss, 2009; Šuklje et al., 2017). Berry size can be manipulated most efficiently with irrigation strategies (Etchebarne, Ojeda, & Hunter, 2010; Ojeda et al., 2002) and is one of the key determinants of berry shrinkage (Rogiers & Holzapfel, 2015). Heterogeneity in berry volume significantly alters grape composition (Šuklje et al., 2012) which can only be rectified by expensive sorting techniques in the winery, while berry shrivel, a major issue for Shiraz (Šuklje et al., 2016), can lead to significant yield losses.

White grape colour transition (from green to yellow, and yellow to orange) during the ripening is linked to chlorophylls and carotenoids degradation, and formation of C13 norisoprenoids (Crupi, Coletta, & Antonacci, 2010; Kwasniewski et al., 2010). C13 norisoprenoids contribute positively to wine sensory properties with floral aromas (Benkwitz et al., 2012). It is also well known that carotenoids and chlorophyll concentrations decline after veraison, which is evident by grape colour changes, and overexposure to sunlight will cause sunburn (Greer, Rogiers, & Steel, 2006).

The Dyostem™ tool that measures berry colour and size was successfully used in several wineries in Europe, South America and South Africa (Deloire, 2013) to assist in determining appropriate harvest dates by providing a potential means to link berry colour with wine aromatic profiles. The technique is expensive, slow and destructive. It is not portable and cannot be deployed in the vineyard.

The purpose of the work described in this research project was to determine the feasibility of developing a smartphone app that can be conveniently used within vineyards to provide real time evaluation of grape berry size and colour.

5 Project aims and performance targets

The main aim of this project was to develop a portable, phone-based imaging tool that allows growers and winemakers to non-destructively measure the volume and the colour of grape berries (red and white varieties) in the vineyard, in real-time. The growers/winemakers will be able to assess and prevent berry dehydration (to limit crop loss and fruit heterogeneity) and assess the maturation degree of white grapes (skin colour from green to yellow and orange; Deloire 2014).

The mobile phone software application to be developed will measure the:

- colour of berries (hue angle), calibrated against a standard colour scale for red and white varieties;
- number of berries;
- sizes/volumes of berries; and
- distribution of fruit colour and volume.

The project aims and planned outputs were as follows:

Planned Output as per Grant Application	Target Date
Post Doc (Dr Elena Kraeva-Deloire) appointed mid January 2016 Programmer (Dr Feng Lu Ge) appointed mid January 2016 Commercial vineyards secured: Cumulus, See Saw	January 2016
Berry sampling for chemical analyses achieved in early February 2016 by A. Deloire and E. Kraeva-Deloire. Harvest for small scale vinification.	March 2016
In field test photographs of berries and bunches completed in early February 2016 by N. Bordes and B. Pailthorpe.	March 2016
Small scale vinifications completed.	April 2016

Database of photographs and data from specific cultivars collated for machine learning algorithms.	April 2016
Machine learning algorithm: initial development completed	July 2016
Wine bottling achieved.	July 2016
Alpha version of Android app to selected growers and winemakers.	September 2016
Chemical measures of grape and wine composition completed.	November 2016
Wine sensory scores and profiling completed.	December 2016
Field testing of the Android application: first phase completed.	March 2017
In field test photographs of berries and bunches completed in Orange by N. Bordes and B. Pailthorpe.	March 2017
Beta version of Android app.	April 2017
Berry sampling for chemical analyses achieved.	April 2017
Harvest for small scale vinification achieved.	April 2017
Small scale vinification completed.	April 2017
Photographs and data from specific cultivars assembled.	July 2017
Wine bottling completed.	July 2017
Comprehensive suite of fruit and wine chemical analysis completed.	November 2017
Objective sensory scores of wines completed.	November 2017
Software refined and tested.	November 2017
Training on the utilisation of the app completed.	November 2017
Android app released for use.	December 2017
Final report submitted.	December 2017

6 Pre-development investigation and analysis

This section presents investigations and analysis activities that were undertaken before the app development. These activities included capturing berry images from vineyards and performing an initial analysis, initiating a berry image database to aid in the machine learning development, and reviewing existing work in the literature. Preliminary results on berry heterogeneity, spatial distribution and maturation within single bunches are also presented at the end of the section.

6.1 Preliminary data collection and investigation

6.1.1 Initial image collection

Figure 1 shows a sample of grape berry images that were captured for initial investigation. Images were captured using a colour calibration card (top pictures) and without the calibration card (bottom pictures), from two vineyards (Cumulus and See Saw) in Orange. The colour card allows for both colour and size calibration. The colour card allows the image to be corrected for changes in illumination by passing the images to calibration software from the manufacturer of the card. The card also allows for a form of size calibration due to the fact that each colour square has a fixed dimension of 0.95 cm × 0.95 cm. The sizes of the berries can then be estimated by calculating the radius of the berry in the picture and then using the size calibration ratio.

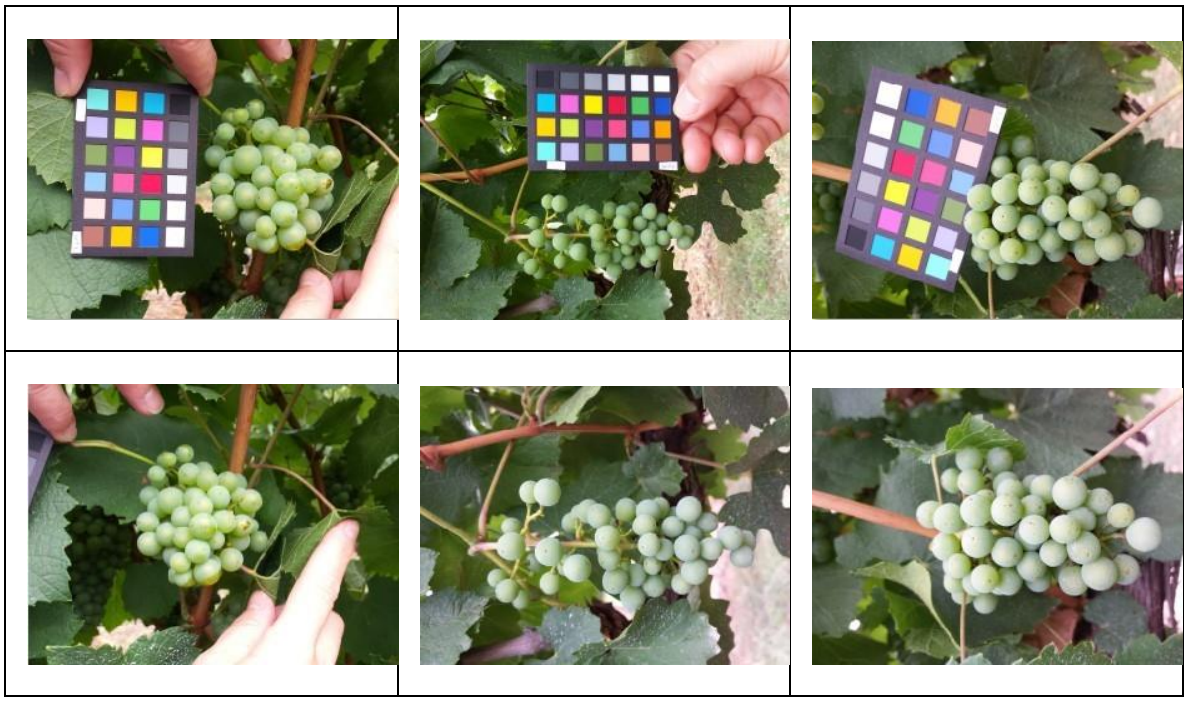


Figure 1: Sample images of captured grape berries with (top pictures) and without (bottom pictures) using the calibration card.

6.1.2 Computer analysis on images

Preliminary investigations and computer analysis were then carried out on the berry images using desktop-based techniques. The objectives of the preliminary investigations were to establish the feasibility of the approaches before the actual development of the smartphone application. The investigations were performed using the MATLAB™ software development environment using the Image Processing and Machine Learning toolboxes.

The first investigation involved using image processing and machine learning techniques to find the location of the grape berries in the images. We used the MATLAB™ function imfindcircle and incorporated the function into a program for detecting the location of berries. The MATLAB™ program for the desktop analysis is shown in Appendix 5 of this report. Given a range of radii, the imfindcircle function locates circular objects in the images which fall within the radii range. The function returns a list of circular objects containing the centres and the radii. The assumption in the approach is that grape berries from certain cultivars such as Chardonnay, Sauvignon Blanc and Shiraz can be modelled as circular objects. Figure 2 shows sample images of Chardonnay berries detected using the desktop MATLAB™ program. The top two images were from Cumulus and the bottom two images were from the See Saw vineyard.



Figure 2: Sample images of grape berries located using the MATLAB desktop program.

As shown in Figure 2, the desktop program was able to give the location of the grape berries (highlighted with the red circle) for images captured in different lighting conditions (e.g. sunlight and shade) and image resolutions.

Having successfully located the berries, the next stage of the analysis was to investigate the feasibility to calculate the volume and hue tint angle distributions. These could then be compared with results measured from Dyostem™. Figure 3 shows a sample result. The top figure shows an image of Chardonnay with the detected berries using the desktop algorithm. The bottom left figure shows the volume distribution which was measured from Dyostem™, and the bottom right figure shows the calculated volume distribution by the desktop MATLAB™ program. As shown in the figure, two peaks can be seen near 0.65 and 0.8-0.9 cm^3 for both the measured and calculated berry volumes showing good correspondence between the approaches. These calculated results were from sampling about 60% of the berries presented at the bunch surface.

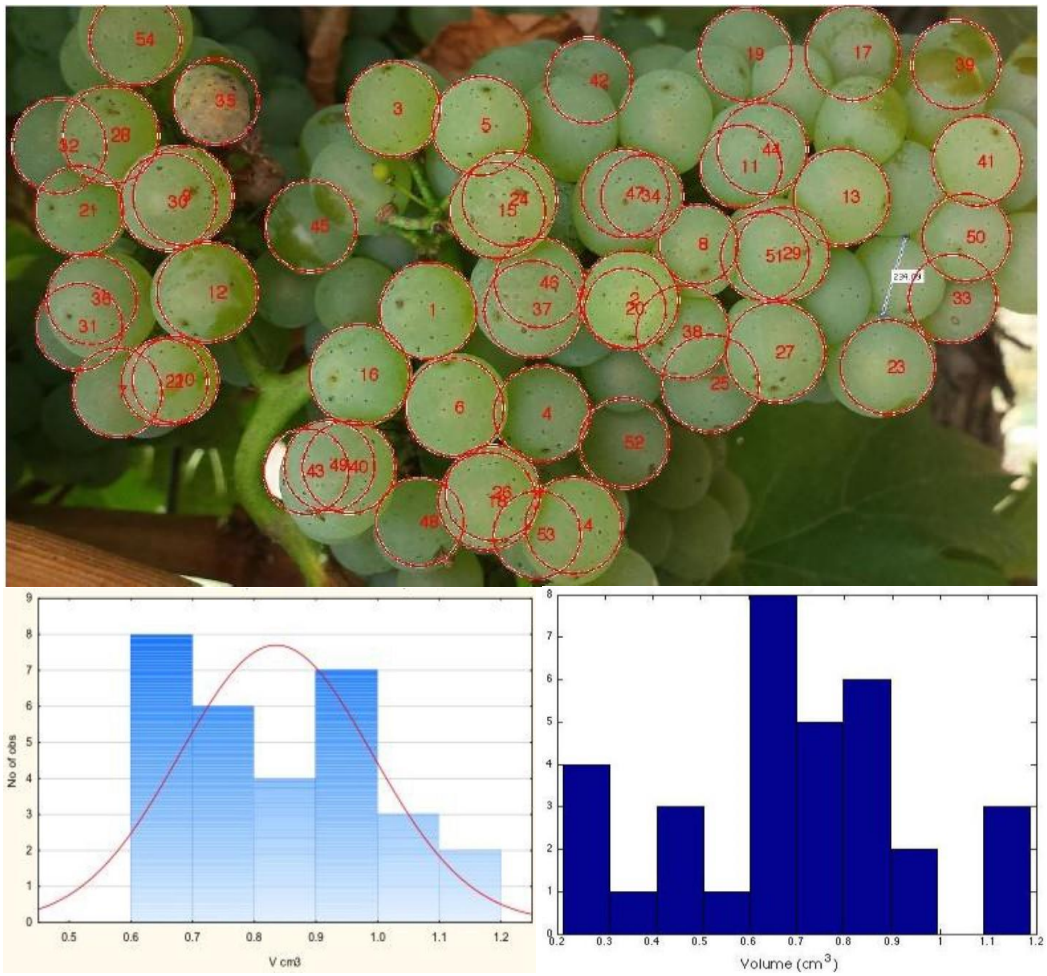


Figure 3: Sample images of grape berries located using the MATLAB desktop program.

The calculated berry hue angles were also compared with the measured results from Dyostem^{TM}. Figure 4 shows the hue tint angle distribution which was calculated for the Chardonnay berry image in Figure 3. The tint angle was in the 90-100 range suggesting that the grapes were not ripe. The Dyostem^{TM} measured tint angle was 82-100.

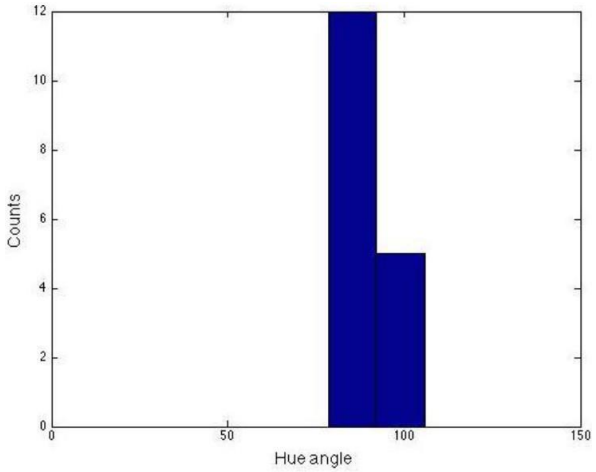


Figure 4: Sample images of grape berries located using the MATLAB desktop program.

We also investigated how to determine the sizes of the grape berries in the real world from the images taken. Figure 5 to Figure 7 show three options that were considered for estimating berry sizes and colour. Figure 5 shows the first approach using the colour calibration card. The advantages of using the colour calibration card is that it allows the berry images to be adjusted for different illumination conditions to determine the berry tint angles. At the same time, berry sizes (circular diameters) can also be estimated by comparing the sizes of the berries in the image with the lengths of the colour squares on the card. Each square on the card measures 0.95 cm × 0.95 cm. This approach using the calibration card would give good measurements for berry size and colour. However, a significant practical disadvantage of the approach is that it becomes tedious for grapegrowers to hold the calibration card while taking the photograph of the grape berries.

The second approach we considered involved using a small common object (e.g. coin) to serve as the size reference, as shown in Figure 6. Holding a coin while taking the photograph with the smartphone is less tedious when compared to the need to hold the calibration card. The coin can also be attached to a string hung on a vine cane, to avoid needing to hold the object. The disadvantage of the coin approach is that only size calibration can be performed. It is not possible to calibrate the colours in the image for different illumination conditions. The third – and preferred - approach was to use a reference probe which could be inserted into a grape

bunch. This allows the user to focus on capturing the image of the grape bunch without needing to hold the reference probe. Figure 7 shows the reference probe inserted into a bunch. The probe would be inserted into the centre of the bunch. The reference probe we used had a diameter of 0.8 cm for size calibration. Furthermore, some basic colour calibration could also be obtained by having a colour pattern on the reference probe. Section 10 - Recommendations gives further details on using the reference probe for both size and colour calibrations.



Figure 5: Berry size and colour estimation from colour calibration card.



Figure 6: Berry size estimation from common object (coin).



Figure 7: Berry size estimation from reference probe.

Some other issues we considered during the preliminary investigation related to illumination conditions and colour casting. Figure 8 shows bunches imaged under different illumination conditions and Figure 9 shows some issues for colour casting conditions. The incidence of day, time of the day, and lighting conditions introduce a colour cast to digital photographs, and to be able to measure the colour of the berries accurately, the colour cast has to be eliminated. This can be done using a colour calibrated card. Our final preliminary investigation before moving on to the app development phase was to develop a prototype app on an Android phone to verify the feasibility of our approach for implementation on a smartphone. Figure 10 shows the preliminary prototype app running on the Android phone.

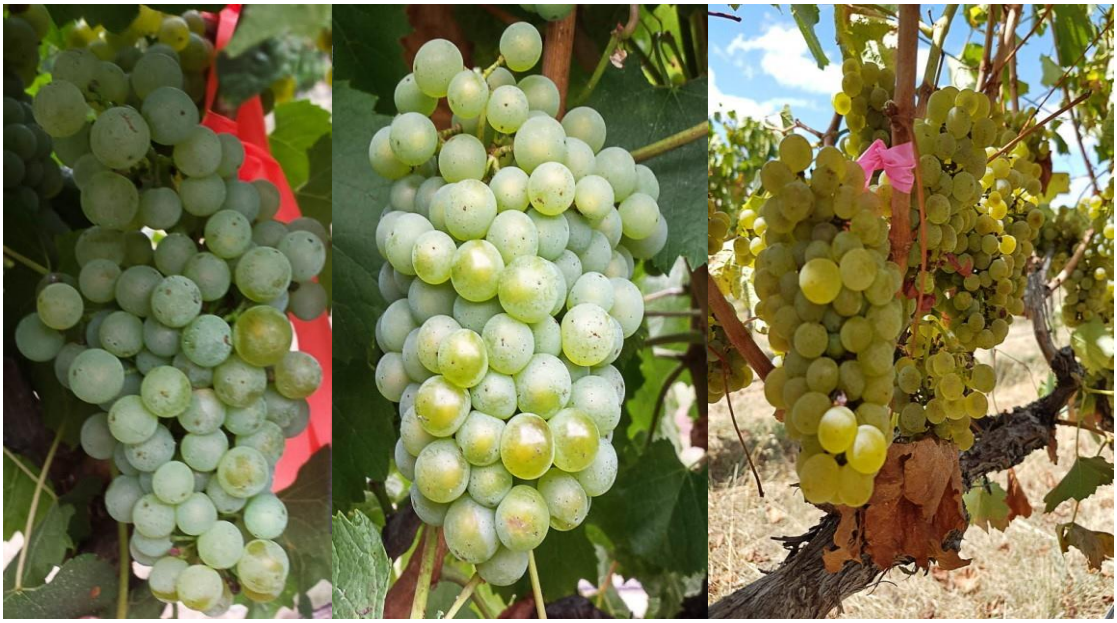


Figure 8: Berry size and colour estimation from colour calibration card.



Figure 9: Issues for colour casting conditions.

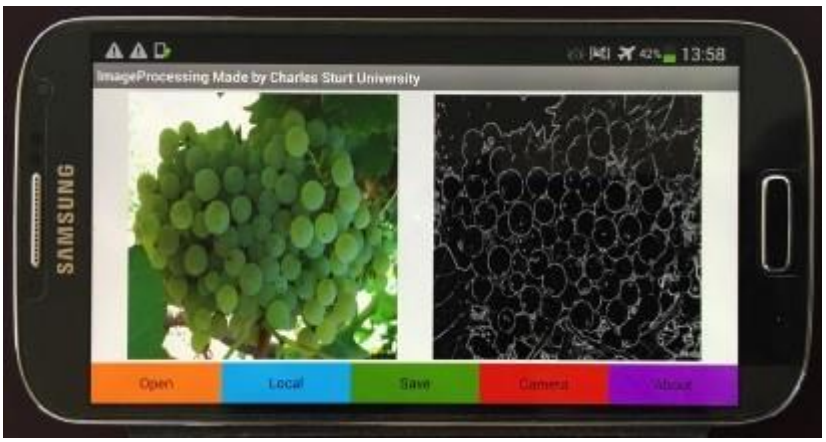


Figure 10: Preliminary prototype app running on the Android smartphone.

6.2 New GrapeCS-ML database for development

6.2.1 Computer vision and machine learning for viticulture technology

This section presents a review of recent research relevant to the application of computer vision, machine vision, image processing and machine learning research for viticulture technology focusing on topics relevant to this research project.

The methods can be broadly divided into two main approaches: (i) laboratory-based techniques; and (ii) in-field techniques. Laboratory-based techniques have the advantage of controlled lighting conditions and in the case for accurate berry detection, the problem of obstruction by leaves and other bunches is avoided. The drawback, however, is that these methods are destructive. The more challenging approach is to perform berry detection in-field in a non-destructive manner. In this case, the illumination conditions cannot be controlled, and there is the additional obstruction problem. For each representative viticulture topic, we will first discuss the laboratory-based approaches that have been proposed, followed by the in-field approaches. We also attempt to present a chronological sequence based on the publication year. Details on the grape variety are also included.

Yield estimation or forecasting is of critical importance in the wine industry. Traditionally, yield forecasts have been generated by counting vine number, bunch number per vine and includes the manual and destructive sampling of bunches to determine their weight, berry size, and berry numbers. Details of yield estimations involving traditional methods such as the lag phase method and others can be found in Brittany & Michelle (2017) and Sabbatini et al. (2017). The manual process is labour intensive, expensive, and inaccurate. For each selected vine, the hand-harvested bunches are weighed and counted. From these data, the average number of bunches per vine and the average weight per bunch can be calculated and this information is then

extrapolated to the vineyard on the basis of the number of vines per acre. The method can be inaccurate if the yield is unevenly distributed across the vineyard. Traditional manual sampling methods are destructive because a subsample of the bunches, or berries are removed from the vine.

Laboratory-based techniques for harvest yield estimation can be found in the works by Battany (2008) and Tardaguila et al. (2012). Battany (2008) used a flatbed scanner to take images of detached Pinot Noir berries. The grayscale images were converted to binary and watershed segmentation was used to separate the joined berries and counted. Their approach was more accurate and faster than manual berry counting, but also involved destructive harvesting. In practice, this would also require subjective sampling which may cause inaccuracies for yield estimation. Tardaguila et al. (2012) proposed a methodology to determine the size and weight of grapes by extracting the morphology of a grape using the Freeman chain code algorithm. Their method was not developed for grape bunches but for individual berries under laboratory conditions. Although significant progress has been made, the approach is still impractical for the accurate and rapid measurement of berry size and weight in the field.

Field-based techniques for harvest yield estimation can be found in the work of Dunn & Martin (2004), Chamelat et al., (2006), Rabatel & Guizard, (2007), Ries et al., (2011), Reis et al., (2012), Nuske et al., (2011) and Nuske et al., (2012). An early approach was proposed by Dunn & Martin (2004), who studied the relationship between fruit weight and the ratio of fruit pixels to total pixels from 16 colour RGB images of the canopy of Cabernet Sauvignon grapevines as the vine was progressively harvested. Threshold and tolerance values were then set manually to select the ‘fruit’ pixels from a single image. These values were then used for the subsequent analysis of the remaining images, and the segmented ‘fruit’ pixels were counted. Using this approach, their experiments accounted for 85% of the variation in yield for the various levels of fruit removal. Chamelat et al., (2006) developed an approach that combined shape detection with colour information using a semi-supervised Support Vector Machine (SVM) classifier to detect red grape bunches. Their technique allowed the detection of the grape bunches in different orientations and sizes with a 99% success rate.

The method by Rabatel & Guizard (2007) used a watershed algorithm to detect the separation of berry contours from luminance discontinuities with ellipse model fitting of the contour arcs using the least square algorithm. Their method could detect two thirds of the visible berries on the vine. The authors concluded that the size estimation would be more accurate by introducing adaptive thresholding in the watershed algorithm and the model fitting using a multivariate semi-supervised classification.

A different approach was proposed by Ries et al., (2011) to detect bunches from white and red grape cultivars using night captured images. Colour segmentation and mapping was implemented to generate a binary image. Morphological dilation was applied to fill in holes between pixels and small regions were removed. The orientation of each bunch and the stem location was determined from the pixel distribution and density around the bunch centre. The authors reported a false detection rate of 9% for all images used in their experiment. The authors extended the work in 2012 (Reis et al, 2012) to differentiate between white and red grapes and achieved classification rates of 97% and 91% for red and white grapes respectively.

Nuske et al., (2011) proposed an automated computer vision method based on shape and visual texture to identify and count green grape berries against a green leaf background. Their approach used a visible light camera mounted on a small vehicle driven along the rows in a vineyard. Their algorithm was comprised of several components to enable berry detection. They first used the radial symmetry transform to identify berry locations. Then, a combination of colour and texture features followed by the k-Nearest Neighbour classifier was used to classify the detected points. The final stage removes false positive detections for berries that do not have at least five berries in close proximity. Their approach can predict yield to within 9.8% of the actual crop weight. The authors performed an extension of the work in 2012 (Nuske et al., 2012) by utilising calibration data obtained from previous harvests and a small set of handpicked samples. This approach achieved a 4% and 3% improvement in yield estimation accuracy above the previous harvest calibration and the handpicked samples respectively.

Murillo-Bracamontes et al., (2012) proposed an advanced approach to segment and identify individual grapes from the image of a cluster using the circular Hough transform. Their method was robust enough to detect partially occluded berries. False detections were reduced using colour information. A group of researchers in Spain (Diiago et al., 2012) proposed a grapevine yield and leaf area estimation technique using supervised classification in RGB images based on the Mahalanobis distance parameter to characterise the grapevine canopy and assess the leaf area and yield. Their classification methodology is able to discriminate among seven different classes (grape, wood, background and leaf (with four classes based on increasing leaf age)). Their results revealed a high performance of 92% accuracy for leaves and 98% for clusters. Their method is more successful than other approaches due to its capability to identify various classes of tissue.

Farias et al., (2012) proposed an image acquisition and processing framework for in-field grape and leaf detection and quantification. Their framework had six steps: (1) image segmentation based on Fuzzy C-Means with Gustafson Kessel (FCM-GK) clustering; (2) obtaining the centroids

which are the FCM-GK outputs as seeding for k-Means clustering; (3) Cluster identification generated by k-Means using SVM; (4) Morphological operations over grape and leaf clusters to fill holes and eliminate small clusters; (5) a Scale-Invariant Feature Transform (SIFT) to create a mosaic image to avoid overlapping regions among images; and (6) Finding centroids in the grape bunches by calculating the areas of leaves and grapes. The performance of their method is more successful than that of Diiago et al., (2012) since the method accounts for illumination artefacts and automatically clusters the training data.

The work by Liu et al., (2013) aimed to accurately estimate the weight of fruit on the vine. They first photographed manually harvested bunches in a laboratory environment to provide a baseline for the accuracy of the weight calculation. The authors investigated several approaches for classification (colour histogram, RBF thresholding, and fuzzy clustering and SVM). The authors concluded that two important parameters affect the performance of the histograms: (i) the colour space used, and (ii) the number of bins in the histogram. Their results showed that RGB thresholding gave a true positive rate of 87%, with a false positive rate of 5%, whilst fuzzy clustering and SVM results in a true positive rate of 97%, with a false positive rate of 16%.

In 2014, Nuske et al., (2014a and 2014b) proposed extended work that was centred on a vehicle-mounted vision system. Their algorithms processed images by exploiting three prominent visual cues (shape, colour and texture) using a classifier that detects berries which have similar colour to the background of vine leaves. Methods were also introduced to maximise the spatial variance and the accuracy of the yield estimates by optimising the relationship between image measurements and yield. The experimental results conducted over four growing seasons for wine and table grapes demonstrated yield estimates that capture up to 75% of spatial yield variance and with an average error between 3% and 11% of total yield.

Another approach was proposed by Font et al., (2015) for yield estimation using the analysis of high-resolution images obtained with artificial illumination at night. Their work first assessed different pixel-based segmentation approaches to detect red grapes to obtain the best estimation of the cluster areas in these illumination conditions. They used various methods including threshold-based, Bayesian classifier, Mahalanobis distance, histogram segmentation and linear colour model segmentation, and investigated the RGB and HSV colour spaces. Their results showed that the best segmentation method for non-occluded red table grapes was threshold segmentation in HSV colour space, resulting in 10% estimation error after morphological filtering. The authors proposed two procedures for yield estimation: (1) The number of pixels corresponding to a cluster of grapes is computed and converted directly into a

yield estimate; and (2) The area of a cluster of grapes is converted into a volume. The results with these proposed methods gave yield errors of 16% and 17% respectively.

Liu et al., (2015b) presented a work using a combination of texture and colour information with SVM classification. The bunch segmentation method has three stages (image pre-processing, training using a training dataset and testing segmentation on the test dataset). Morphological operations are performed in HSV colour space on both training and testing images to extract the initial bunch hypotheses. A shape filter is then applied to exclude incorrectly identified bunches.

A new approach for yield estimation was proposed by Liu et al., (2015a) to estimate the 3D structure of grape bunches from a single image. The proposed 3D model based on a single image is appropriate for a bunch with distinguishing shoulders, but it cannot achieve a good estimation of berry numbers on a bunch with overlapping shoulders. Their experiments on two varieties revealed an average accuracy of 87.3% relative to the actual number of berries on a bunch.

Researchers in China aimed to detect the grape clusters in a vineyard using image processing and machine learning (Luo et al., 2015). They proposed an image segmentation method based on an improved artificial swarm optimisation fuzzy clustering. The fitness function of the artificial colony was improved based on the objective function of the fuzzy C-average clustering (FCM) algorithm. Image segmentation was then performed based on the maximum membership principle. They conducted their experiment on black grape images taken under normal light illumination and an accuracy of 90.33% was achieved. Luo et al. continued their research by proposing grape image segmentation based on artificial bee colony and fuzzy clustering and the AdaBoost framework (Luo et al., 2016). In the initial step, the effective colour components of grape clusters were extracted to construct the linear classification models based on a threshold. In the second component, an advance classifier was constructed by using the AdaBoost framework. The authors used 900 testing samples to verify the performance and an accuracy rate of up to 96.56% was achieved. They also tested the performance of their work using 200 images captured under three various illuminations in the vineyard and the average detection rate was 93.74%.

Casser (2016) applied feed-forward neural networks (FFNN) to address the problem of colour-based grape detection for in-field images. The authors considered four classes (night time red berries, night time white berries, day time red berries and day time white berries). Different light conditions on grape varieties were investigated and the influence of different colour models was also examined. Their simulation results showed that an average classification rate of

93% could be achieved. The comparison with SVM revealed that FFNN could slightly outperform SVM in computation time.

A recent approach for a smartphone application was proposed by Aquino et al., (2017). The grape cluster is placed in front of a dark cardboard for analysis. The authors proposed a new image analysis algorithm based on mathematical morphology and pixel classification for grapevine berry counting. The methodology has two main stages. Initially, images were downsized and converted to the CIELab colour space. In the first stage, a set of berry candidates was extracted from the image using morphological filtering. The bright spots produced by light reflection from the berry surface were detected by finding the regional maxima of illumination. In the second stage, false positives (FP) were eliminated. This elimination process was performed by means of pixel classification using a classifier input with a set of key descriptors, and trained by supervised learning. This process involved a set of six morphological and statistical descriptors (grouped into shape (one descriptor), normality (one descriptor) and colour descriptors (four descriptors)) to form a feature space used to train a classifier for FP discrimination. Two classifiers, a three-layer neural network and an optimised SVM were considered in their work. Their experimental results showed that the three-layer neural network performed better than the SVM. The authors informed that the method would be implemented in smartphone devices in the near future.

6.2.2 Datasets 1-5 in the new GrapeCS-ML database

Datasets in an accessible form are required by researchers to make progress and advancements in computer vision, image processing and machine learning. A dataset is a collection of data, images or videos that can be used to evaluate techniques for specific applications. An evaluation of a suitable and unbiased dataset can validate a proposed technique or algorithm. Interestingly, the evolution of datasets can also reflect the progress of research in these fields. Researchers in computer vision gather datasets that are groomed to be within an attainable level of difficulty. Once the researchers have saturated performance on those datasets, they go in search of another more complicated dataset in order to design even better techniques.

It is also important to leverage multiple datasets because of the bias inherent in any single dataset. Viticultural databases include the European Vitis Database and the Vitis International Variety Catalogue VIVC. However, these databases were not designed for computer vision or machine learning research. For example, the VIVC currently has data for 23,000 cultivars. However, only one or few samples are available for each cultivar. This is in contrast to the

requirements for developing machine learning algorithms which require many samples from the same cultivar for training and evaluation.

Here we present a new database called GrapeCS-ML Database which has been specifically designed to progress computer vision and machine learning research for viticulture. A detailed explanation of the considerations and procedures in the database construction are also presented. The database consists of images of bunches from different grape varieties captured in three Australian vineyards and contains different datasets for evaluation. To the best of our knowledge, no such database is currently available for the research community in computer vision and machine learning for viticulture technology. The availability of such a database is important to researchers because data are required for machine training or learning and testing. We hope that the information contained in the database will help to spur extensive computer vision and machine learning research by providing significant training data for learning algorithms and image processing techniques.

The database consists of five datasets for 15 grape varieties taken at several stages of development and includes size and/or Macbeth colour references. Altogether, the database contains a total of 2,078 images. Some datasets also include the corresponding ground truth data (e.g. TSS, pH, etc.) obtained from chemical laboratory analysis. Table 1 shows a summary of the five datasets.

Table 1: Summary of five datasets collected for computer vision and machine learning.

Dataset 1	**Variety**	**Detail**
	Merlot (large scale)	- 7 subfolders contain the grape images taken in different rounds: Round 1 (16-19/1/17), Round 2 (22-19/1/17), Round 3 (6-9/2/17), Round 4 (16-19/2/17), Round 5 (27/2-4/3/17), Round 6 (20-22/3/17) and Round 7 (13/4/17) - Initial number of bunches: 242 - volume reference - dates
Dataset 2	**Variety**	**Detail**
		13 varieties - Varieties: Purple Cornichon, Merlot, Flame Seedless, Chardonnay, Cabernet Sauvignon, Saint Macaire, Viognier, Ruby Seedless, Riesling, Muscat Hamburg, Sultana and Sauvignon Blanc. - 13 subfolders. - Initial number of bunches: 1-5 bunches depending on variety. - volume reference - colour reference - dates
Dataset 3	**Variety**	**Detail**
A	Cabernet Sauvignon	- 14 subfolders contain the grape images taken on different dates. - Initial number of bunches: 4

		- volume reference - colour reference - dates
B	Shiraz	- 4 subfolders contain the grape images taken on different dates. - Initial number of bunches: 15 - volume reference - colour reference - dates
Dataset 4	**Variety**	**Detail**
A	Pinot Noir	- 11 subfolders contain the grape images taken on different dates. - Initial number of bunches: 12 - colour reference - dates
B	Merlot	- 7 subfolders contain the grape images taken on different dates. - Initial number of bunches: 12 - colour reference - dates
Dataset 5	**Variety**	**Detail**
	Sauvignon Blanc	- 3 subfolders contain the grape images taken on different dates. - Initial number of bunches: 10-12 bunches for each subfolder. - Segmented images - Corresponding laboratory data: TSS, berry weight, number of berries, volume, pH, dominant hue, etc. - dates

---

Dataset 1:

Dataset 1 contains images of Merlot bunches taken in seven rounds from the period Jan. to Apr. 2017. Figure 11 shows a typical growth curve. Initially after flowering, the grape berries increase in size rapidly but remain hard and green. This is followed by a lag phase, and then with onset of veraison, a second growth period occurs along with softening and colour development. This phase of grape berry growth is followed by a period of engustment when the aromas and flavours of the grape intensify (Coombe & McCarthy, 2000). The images in Dataset 1 allow for the construction of about 250 growth curves. These data can be used to perform the dynamic analysis to inform on the optimal berry harvest time based on berry size and colour. Figure 12 shows some sample images from Dataset1.

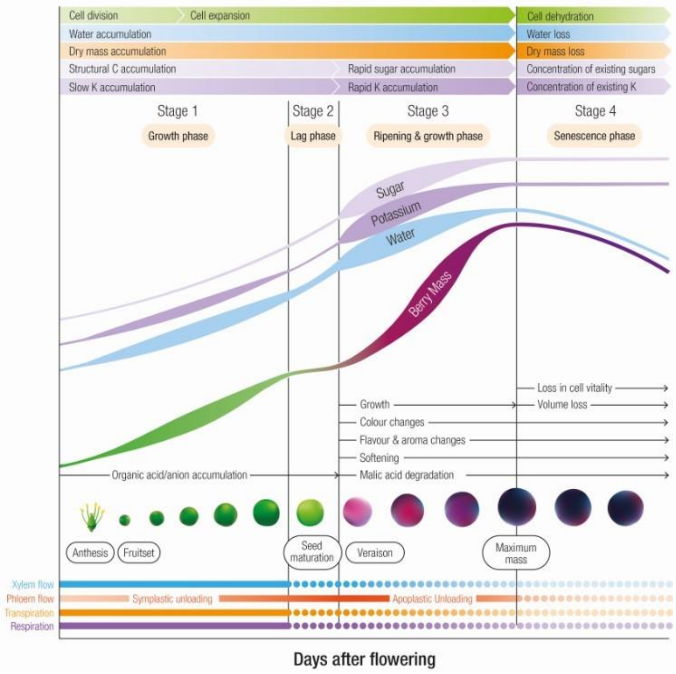


Figure 11: Shiraz berry growth and ripening curves. Image first published in (Rogiers et al., 2017).

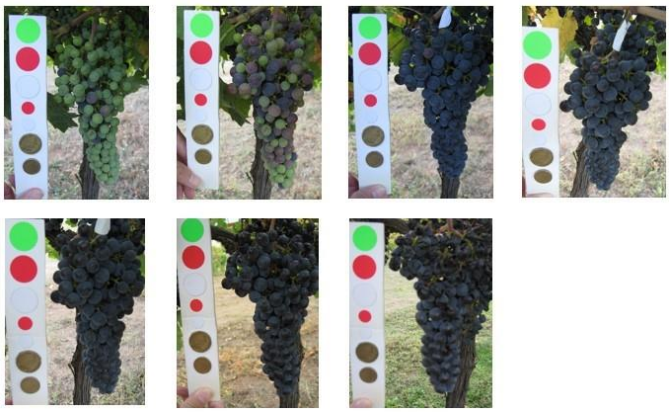


Figure 12: Dataset 1 – Sample images from dataset 1 at various stages of development.

Dataset 2:

Dataset 2 contains the subsets for 13 different varieties: Merlot, Cabernet Sauvignon (CS), Saint Macaire, Flame Seedless, Viognier, Ruby Seedless, Riesling, Muscat Hamburg, Purple Cornichon, Sultana, Sauvignon Blanc and Chardonnay. Each folder consists of images of bunches at several stages of development of the different varieties. Figure 13 and Figure 14 shows some samples from the dataset. This dataset is designed for research on berry and bunch volume and colour as the grapes mature.

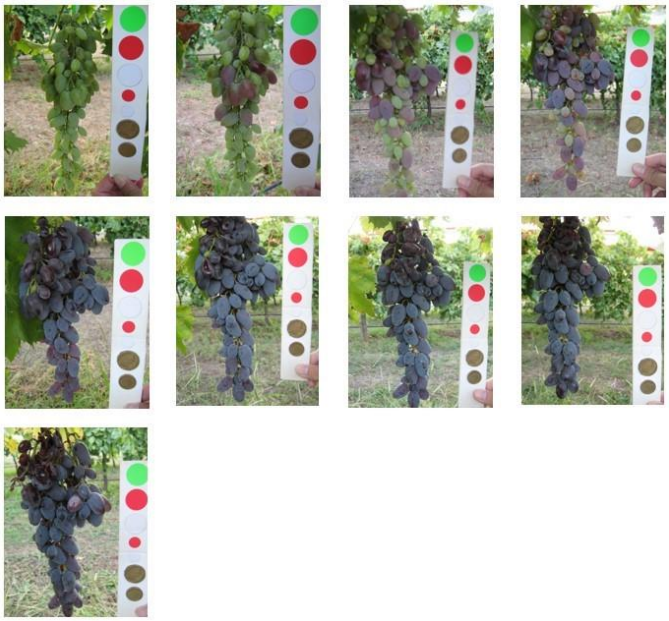


Figure 13: Dataset 2 – Sample images from dataset 2 including a volume reference.



Figure 14: Dataset 2 – Sample images from dataset 2 showing development following veraison and includes a colour reference.

Dataset 3:

Dataset 3 contains the subsets for two varieties (Cabernet Sauvignon and Shiraz) taken at dates close to maturity. Each image has been taken twice at the same time, once with the size reference and a second time with the colour reference. Thus, this dataset allows the relationship between size and colour transitions to be modelled at different stages of growth. Figure 15 and Figure 16 depicts sample images from the dataset.



Figure 15: Dataset 3 – Sample images from dataset 3 at various stages of bunch development.



Figure 16: Dataset 3 – Sample images from dataset 3 at various stages of bunch development.

Dataset 4:

Dataset 4 contains subsets of images for two varieties (Pinot Noir and Merlot) taken at dates close to maturity, with the focus on the colour changes with the onset of ripening. These images were taken almost daily and includes the colour reference. Thus, this dataset allows colour transitions to be modelled at different stages of development (Figure 17).



Figure 17: Dataset 4 – Sample images from dataset 4 at various stages of bunch development.

Dataset 5:

Dataset 5 contains the images of Sauvignon Blanc bunches taken on three different dates. Each image also contains a hand-segmented region defining the boundaries of the grape bunch to serve as the ground truth for evaluating computer vision techniques such as image segmentation. The grape bunches were also analysed in the laboratory for their basic composition including total soluble solids (TSS) and pH. Bunch weight, average berry fresh weight, number of berries per bunch, berry volume, dominant hue, etc. are also presented. This dataset can be used to relate the image data with the chemical composition of the bunches. Figure 18 provides an example of samples from the dataset.

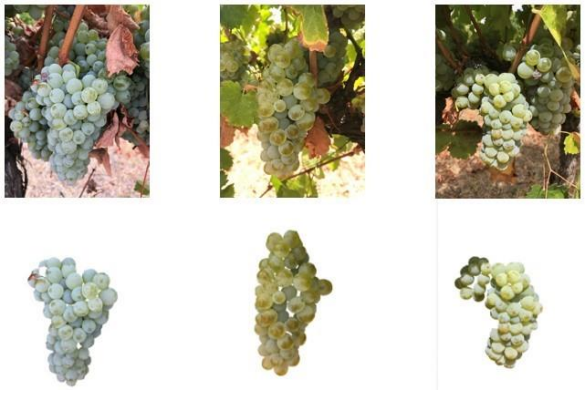


Figure 18: Dataset 5 – Images and corresponding segmented bunch regions.

6.3 Machine learning for app development

6.3.1 Pre-investigation and initial design of algorithms for app development

This section gives details on the initial design of algorithms for app development. Two separate designs were undertaken: (1) for white cultivars; and (2) for red cultivars. The designs utilised the berry images collected for the new GrapeCS-ML database described in Section 5.2. The initial design of the algorithms was performed to determine the feasibility of the image processing and machine learning flows before the selection of a final design for the implementation on the Android smartphone platform. This section gives a summary of the different approaches that were investigated and considered.

Figure 19 shows two initial algorithms that were designed for the image processing and machine learning flows for white grapes and cultivars. An important part of the investigation was to locate the grape berries in the image by modelling them as circular objects. The key idea in the algorithms flow is to perform this task using two stages: (1) The first stage uses information contained in the image to approximately identify potential grape berry locations. This is done using a colour filtering process where regions that have no possibility of containing the grape berries are removed from consideration; (2) The second stage focuses on applying circle detection algorithms to locate circular objects in the remaining regions. This was performed using the Circular Hough Transform (CHT), which is a well-established technique in machine learning for detecting circles. The two approaches in Figure 19 show the two algorithm design flows for Stages (1) and (2). Both designs were found to be effective for the purposes. However, the second design (bottom of Figure 19) had a lower complexity for implementation on smartphones, and we used a modification of the design together with a support vector machine (SVM) filter for the final implementation on the smartphone. The final design will be elaborated in Section 6 for the Android app development.

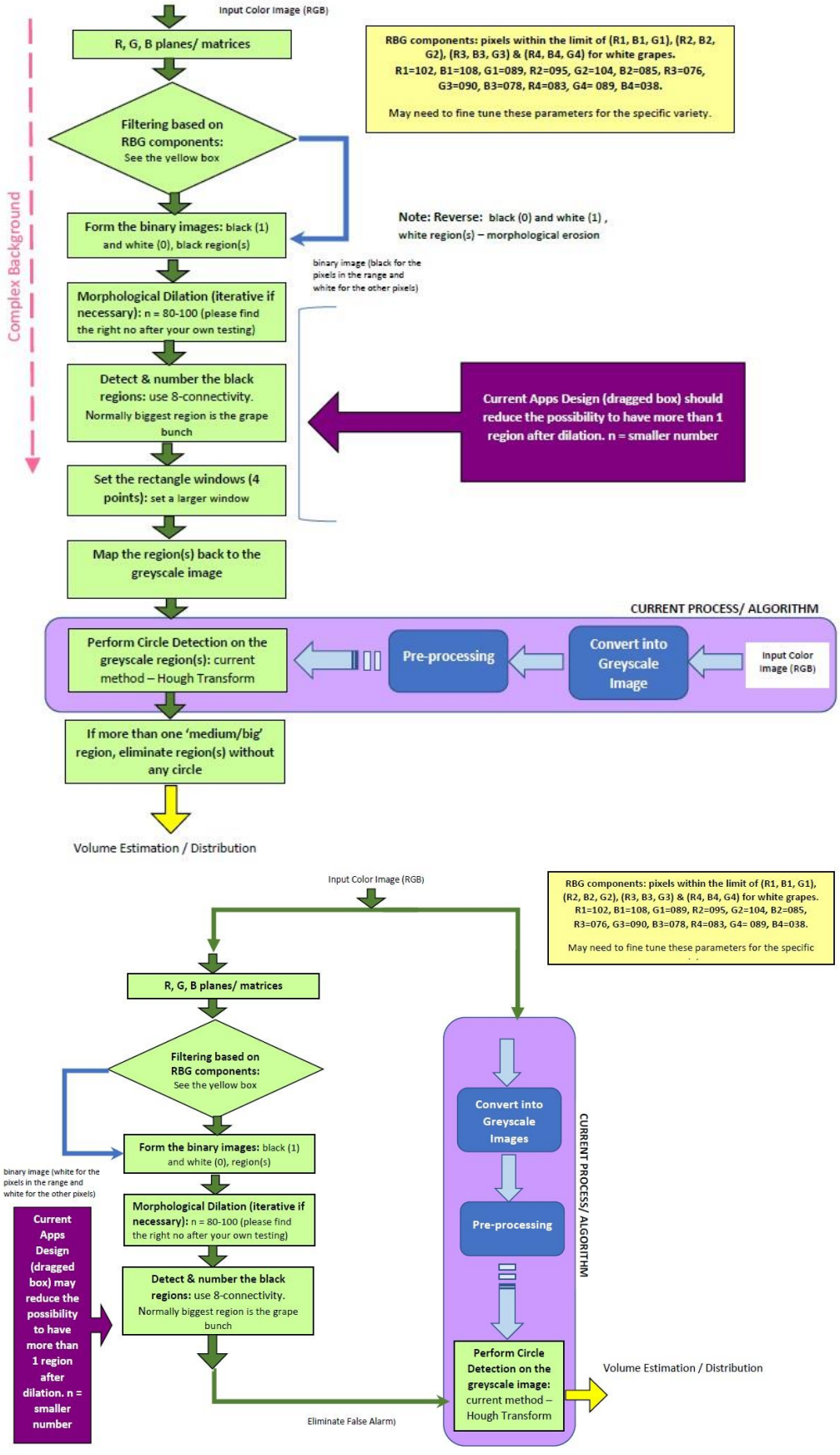


Figure 19: Image processing and machine learning algorithm flows for white cultivars.

Similarly, image processing and machine learning algorithm flows were designed for red berry cultivars. The algorithm designs for red berries were more challenging than for white berries. This was because the growth of red berries goes through three stages. In the early stage, the berries have a green colour, in the mid-stage the berries have a mixture of green and purple colours, and in the late stage the berries have a purple colour. Thus, unlike for green berry cultivars which have a consistent green colour (of different shades) throughout their growth, red berry cultivars could have different shades of green and purple depending on the growth stage. Figure 20 shows the algorithm flow design for red cultivars, with three separate paths.

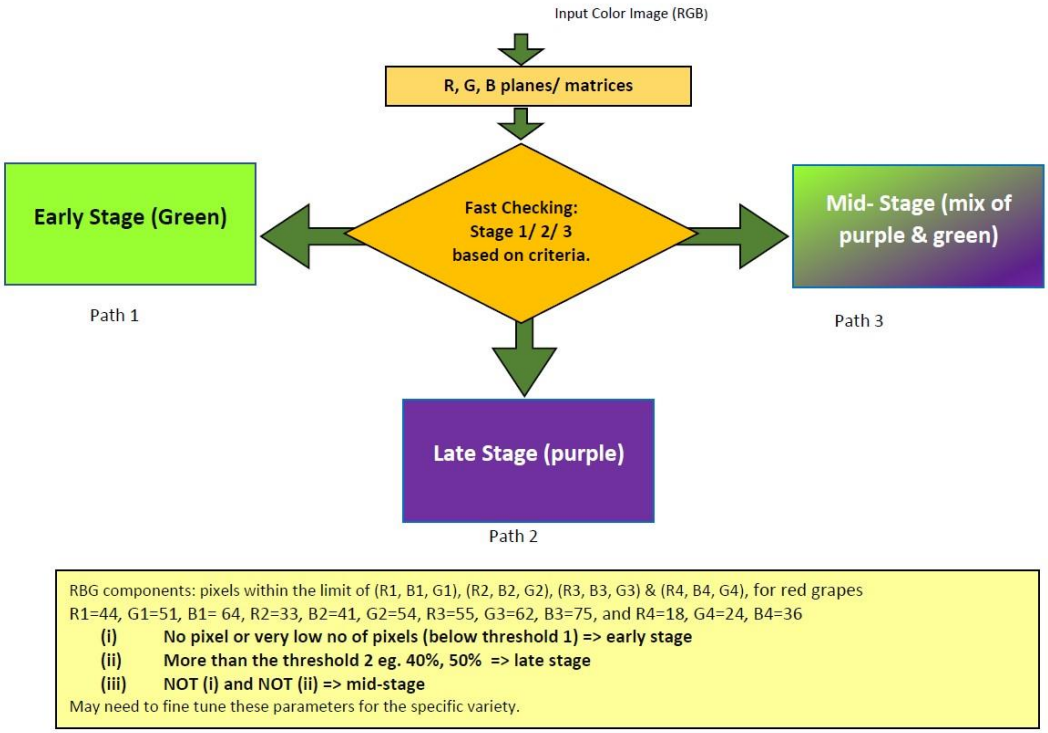


Figure 20: Image processing and machine learning algorithm flow for red cultivars.

The input into the algorithm flow is a colour image of the grape bunch and as shown in Figure 20, an initial check based on a set of criteria is utilised to classify the image into one of three stages (Early Stage, Mid-Stage, Late Stage). The algorithm then branches off into three different paths depending on this initial classification. Path 1 (shown in Figure 21) is used for early stage berry growth, Path 2 (shown in Figure 22) for middle stage berry growth and Path 3 (shown in Figure 23) for late stage berry growth.

Path 1:

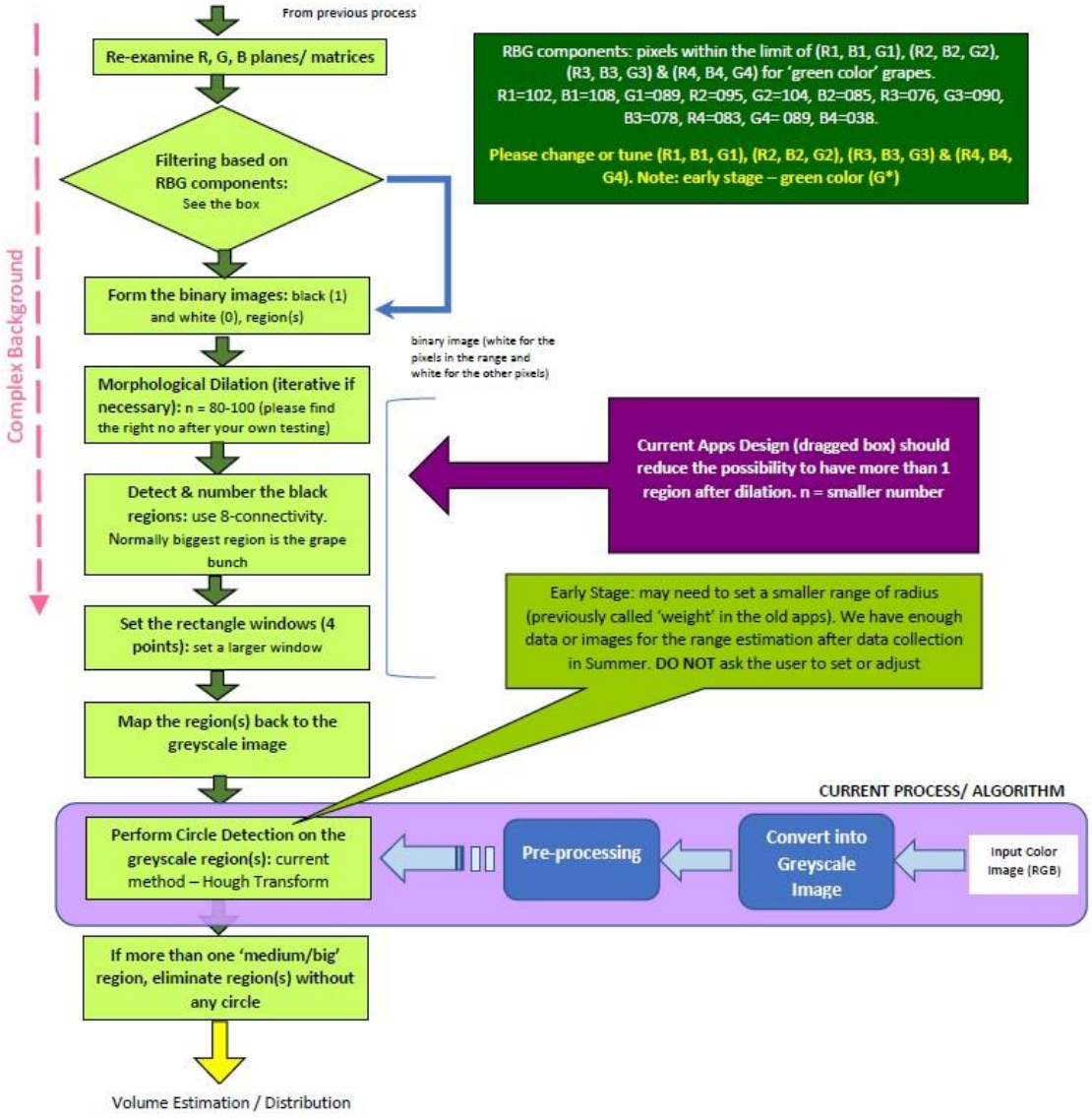


Figure 21: Path 1 – Early Stage image processing and machine learning flow for red cultivars.

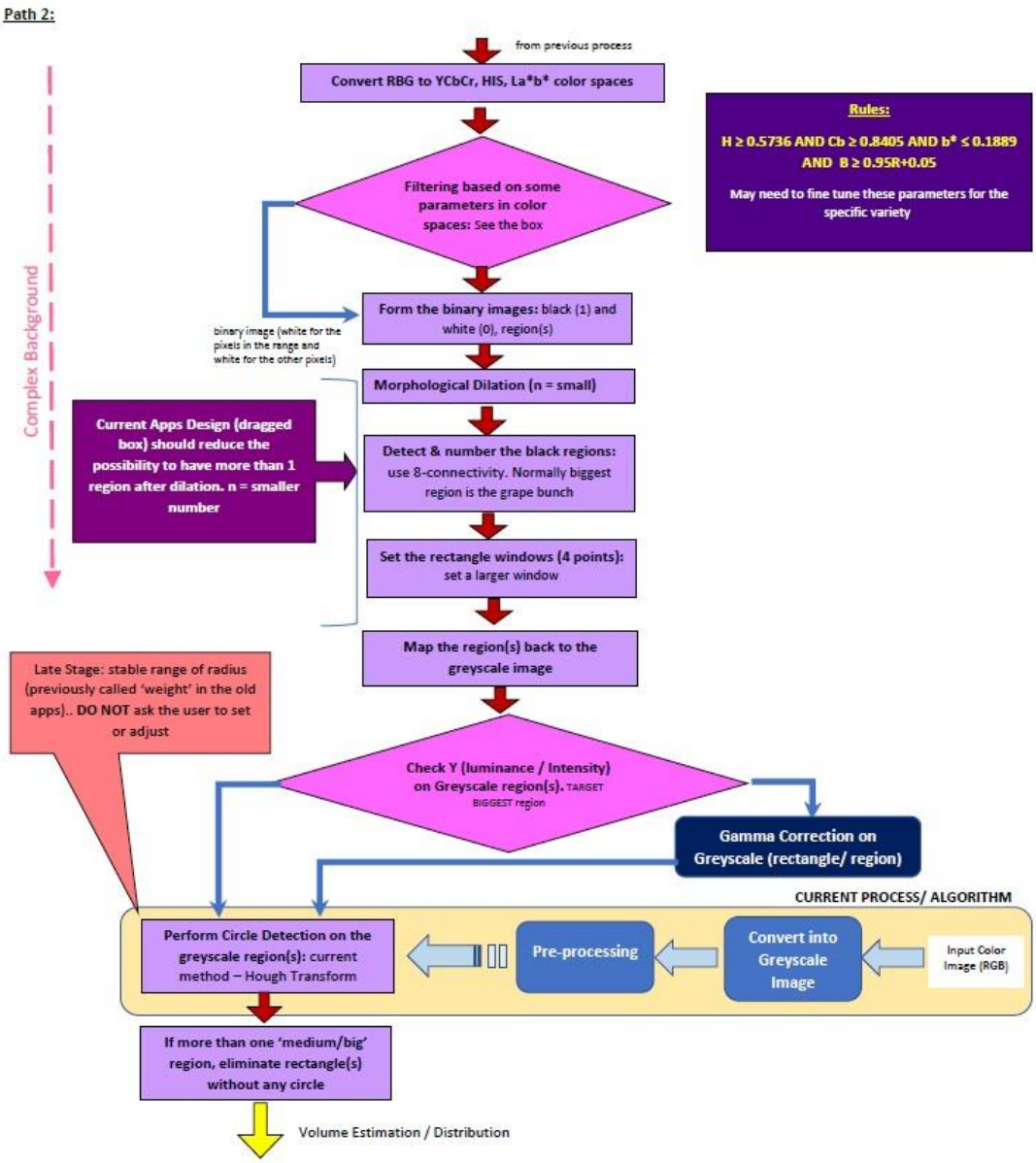


Figure 22: Path 2 – Middle Stage image processing and machine learning flow for red cultivars.

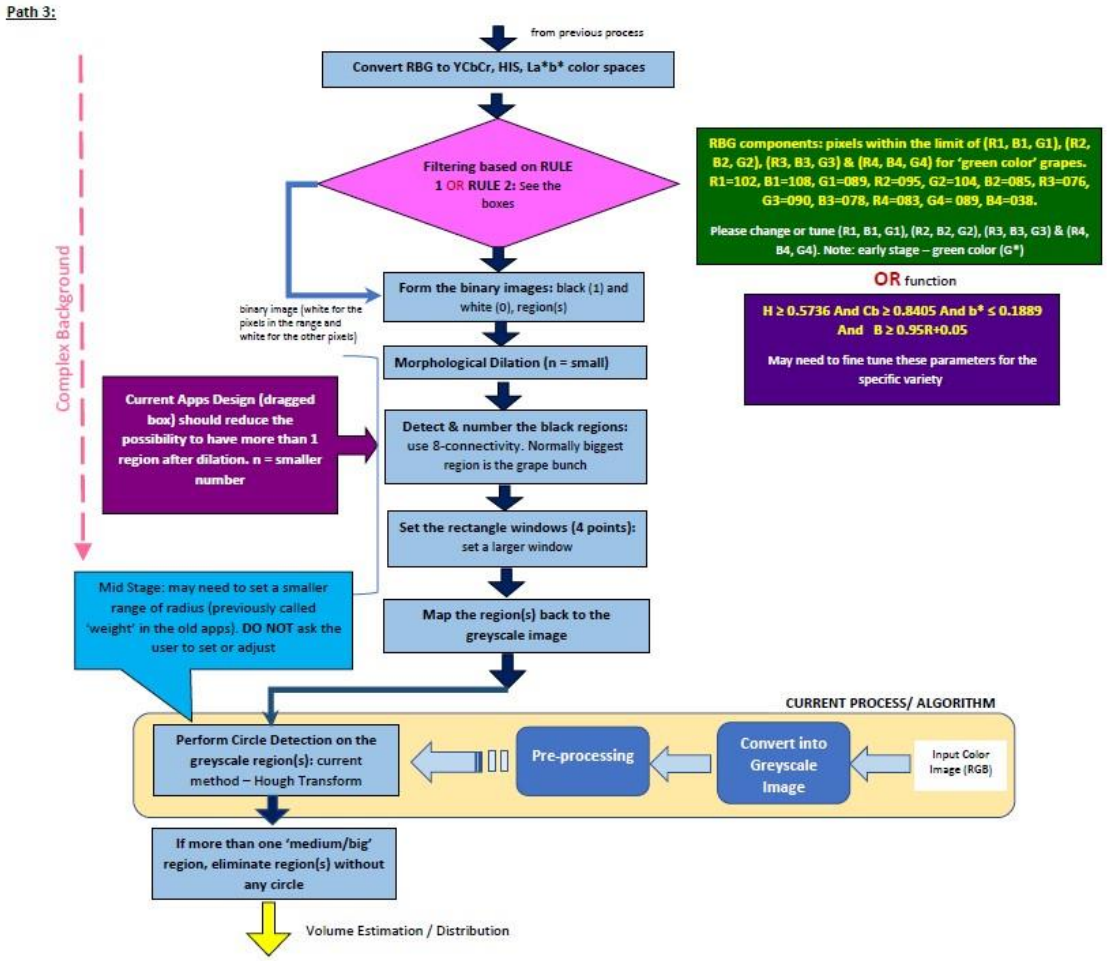


Figure 23: Path 3 – Late Stage image processing and machine learning flow for red cultivars.

6.3.2 Simulation results on machine learning

This section presents an illustration of the usefulness of the database and gives baseline comparisons for a colour-based berry detection application to detect berry pixels from the background using various machine learning approaches and colour spaces. The comparisons were performed for white and red berry cultivars from the images collected in the field. We performed a segmentation by hand to locate the grape bunch region from the background. These served as the ground truth images and are included in the GrapeCS-ML database for use by other researchers. We then transformed each bunch region into four colour spaces (RGB, YCbCr, HSV and Lab) and applied five machine learning classifiers (SVM, k-NN, logistic regression and boosted tree) towards the berry detection application. For our experiments, the SVM classifier used the Gaussian kernel, the value of k = 10 was used for the k-NN, whereas the Boosted tree used the Adaboost (Roe et al., 2005). Table 2 and Table 3 show the classification rates obtained for white and red berry cultivars respectively. Among the machine learning approaches, the SVM gave the highest performance among the classifiers followed by the k-NN.

This showed that the k-NN, with its advantages of lower computational requirements can be used, albeit with a slight decrease in classification performance. The logistic regression classifier gave the lowest performance. For the different colour spaces, the HSV gave the highest performance for white cultivars while the YCbCr gave the highest performance for red cultivars. The highest classification rate obtained for white cultivars was 84.4% and the highest classification rate obtained for red cultivars was 89.1%. The work in this section demonstrates the usefulness of the SVM for classifying white and red berry cultivars. The next section for the app development will use the SVM as a component in the machine learning app flow for berry detection and analysis.

Table 2: Classification rate (%) for white berry cultivars using various machine learning approaches and colour spaces.

	Colour space			
Classifier	RGB	YCbCr	HSV	Lab
SVM	82.8	84.3	84.4	84.4
k-NN	83.1	83.5	83.7	83.7
Logistic regression	78.1	78.1	78.9	77.9
Classification tree	78.1	80.1	80.4	79.9
Boosted tree	78.7	80.9	81.8	81.8

Table 3: Classification rate (%) for red berry cultivars using various machine learning approaches and colour spaces.

	Colour space			
Classifier	RGB	YCbCr	HSV	Lab
SVM	88.8	89.0	89.0	89.1
k-NN	88.5	88.8	88.6	88.7
Logistic regression	86.5	86.6	86.4	86.6
Classification tree	85.4	88.3	87.8	87.9
Boosted tree	87.6	88.7	88.4	88.4

6.4 Preliminary results on berry heterogeneity, spatial distribution and maturation within single bunches (cv. Shiraz)

This section presents a study to assess the spatial and temporal differences in individual fruit from single bunches at two developmental stages: veraison and ripening (cv. Shiraz, *Vitis Vinifera* L.) and of bunches from a warm and temperate climate of Australia (New South Wales). The preliminary results showed that berry position within bunches and branches did not influence the targeted physiological parameters. Strong interrelationships between berry seed number and sugar concentration, fresh and dry mass of the pericarp were found. The study

showed a correlation between the number of seeds per berry and skin colour at veraison, suggesting an important role of the seeds in the timing of ripening. No real differences between the two wine regions were observed.

6.4.1 Introduction to study

Berry morphology and composition, and heterogeneity within single bunches are important considerations with potential practical implications on vineyard management and wine making processes. The goal of this study was to assess the spatial and temporal differences in individual fruit from single bunches at two developmental stages: veraison and ripening (cv. Shiraz, *Vitis Vinifera* L.). This study therefore enables a better understanding of the berry variation within a single bunch of grapes and provides context for measuring grape variability using rapid methods of assessment. Wide ranging research has been reported during the last few years on berry size and sugar content, berry position and maturity, resource competition between berries during their development, and the effect of bunch heterogeneity on wine composition, however, this topic remains as a matter of debate. This research note presents some solid preliminary results that could contribute to the ongoing discussion, bringing new insights.

6.4.2 Materials and methods

The study compared bunches from hot-warm climate (Griffith) and cool-temperate climate (Orange) wine regions of Australia (New South Wales).

In Griffith, the vines use a sprawling training system, are mechanically pruned, double cordon and under irrigation. In Orange, the vines are trained in vertical shoot positioning, are hand pruned in a single cordon and irrigation is managed according to rainfall.

Bunch sampling was done at early veraison and ripening. The number of bunches studied was limited due to the huge amount of work required per bunch to analyse individual berries.

The following parameters were studied on a per berry basis:

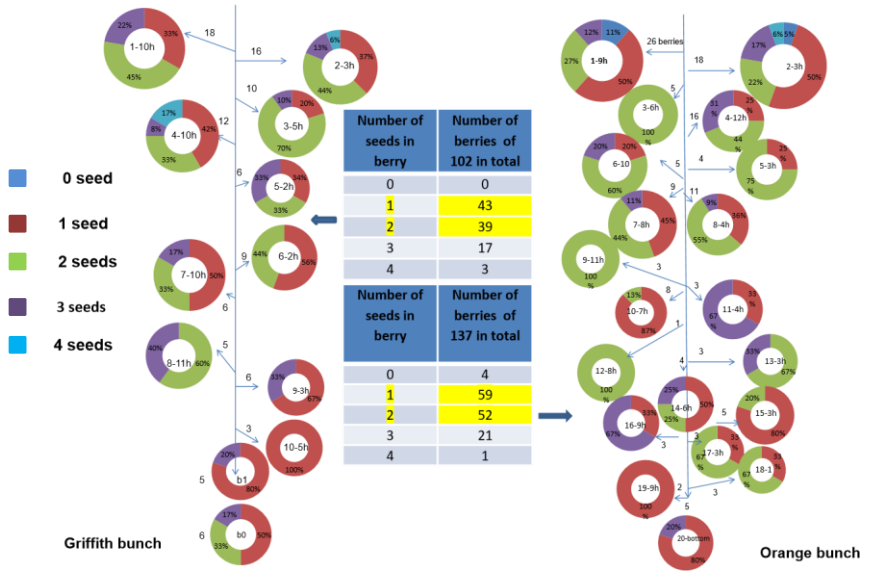
- Number-Position of the berry within single bunches
- Fresh mass of berry: seeds and pericarp
- Dry mass of berry: seeds and pericarp
- Seed number
- Skin colour
- Total Soluble Solids (Brix), sugar concentration per g of berry
- Water concentration
- Seed/berry ratio (SB)

In total, 607 berries from four different bunches sampled at veraison and mid ripening were analysed. Each single berry was removed from the stem according to the position on the rachis including ramification. Some results are presented according to clockwise position corresponding to the exposed and shadowed sides of a bunch.

6.4.3 Results

Spatial distribution of the berries on the primary side branches within the ripe bunches

A starting point for our study was the creation of a 'map' of berry spatial distribution. The arrows show the rachis and small branches with the counted number of berries on each. Circles are the groups of berries on each side branch regarding the number on the rachis and a clock position (Figure 24). The colours correspond to percentage of one-, two-, three- and four-seeded berries in the group. The majority of berries had one and two seeds randomly situated within the bunch. There was no gradient or apparent continuity in distribution and we did not find any influence of berry position on the physiological parameters studied. As no significant differences were observed between the warm and temperate climates of the two wine regions of Australia (NSW), it could be hypothesised that the flowering conditions were quite standard and did not affect ovules' fecundation.



Number of seeds in berry	Number of berries of 102 in total
0	0
1	43
2	39
3	17
4	3

Number of seeds in berry	Number of berries of 137 in total
0	4
1	59
2	52
3	21
4	1

Figure 24: Berry spatial distribution according to their seed number within a ripe bunch. The arrows show the rachis and small branches with the counted number of berries on each. Our results did not show differences between warm (a) and temperate (b) climates.

Studying berry heterogeneity within single bunches addresses the question of which parameters to study looking at berry development and composition. It has been showed that within the same bunch, each berry has its own dynamic of development and that could impact on individual berry composition. The histograms in Figure 25 show the berry distribution per class, based on seed number, within the bunch and how the seed content changes from small to large berries. Colour corresponds to the number of one-, two-, three- and four-seeded berries. These results are of interest and useful for grouping and sampling strategies as, for example, two major classes within the same cluster could be very different in Brix and seed content. This illustrates an asynchronous berry development starting at flowering and is linked to ovule fecundation by the pollen versus timing of fecundation and number of viable-normal seeds per berry. Proper ovule fecundation and therefore seed formation and number are certainly major factors that trigger the onset of berry cell multiplication and growth.

The berries of each bunch were classified from the lowest to highest pericarp fresh mass. The results (Figure 26) showed that the difference of almost 100% in fresh mass is correlated with a seed content but not with a water or carbon (dry weight) concentration. This observation is novel and may addresses the relation between berry volume and/or fresh mass and the associated complex interaction between cell number and enlargement. The determination of cell number is possible using an indirect analytical method such as DNA measurement, although further studies would be necessary to address this.

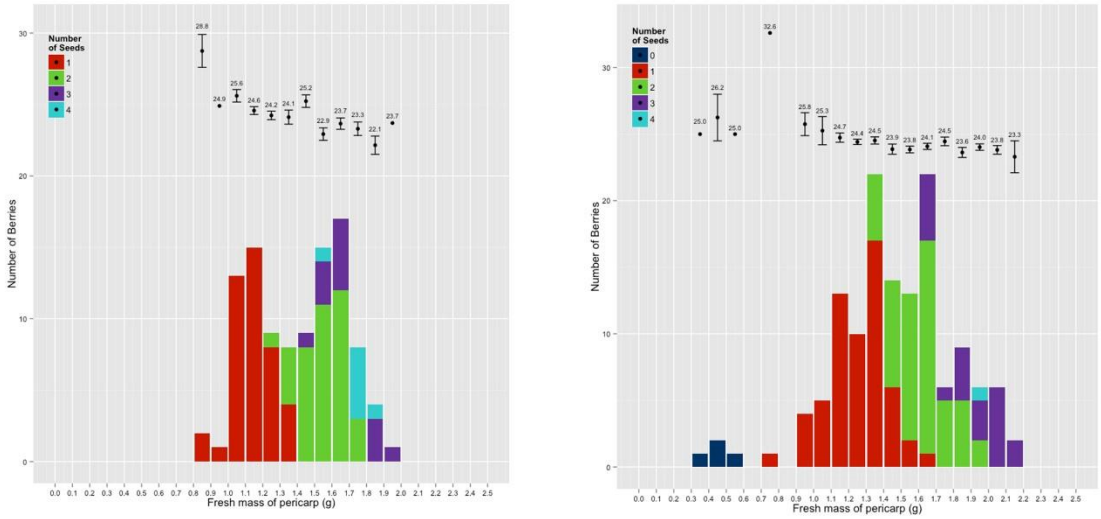
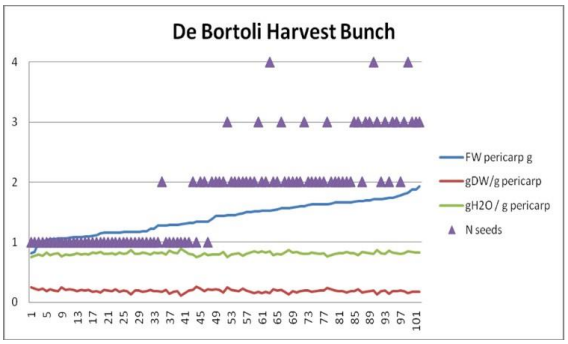
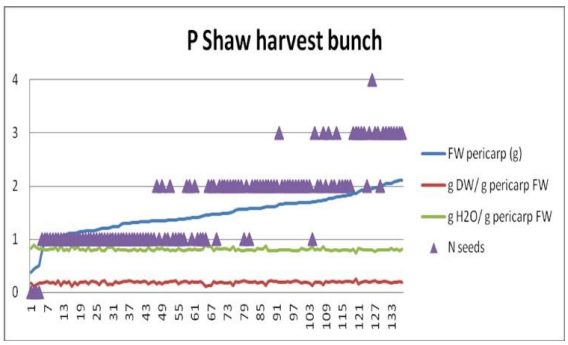


Figure 25: Berry number per class of pericarp fresh mass (g) and the associated seed number. The results show that berries from the same fresh mass could have a different seed number. No real differences are evident between warm (a) and temperate (b) climates.



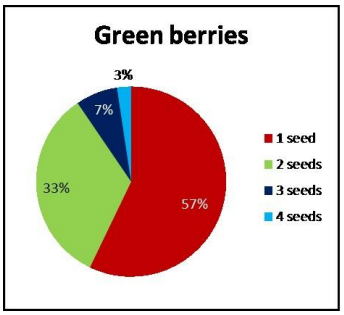


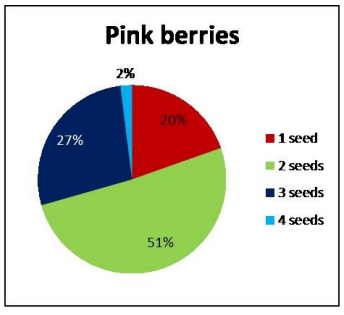
	Ave of 10% lowest FW (g) pericarp	Ave of 10% highest FW (g) pericarp	Difference %
FW pericarp g	1.0	1.8	+80
DWg [C] / pericarp FW g	0.212	0.174	-17.9
H2O %	79%	83%	+5.01
Brix	26.3	23.4	-11
Seed content N	1	2.9	+190

	Ave of 10% lowest FW(g) pericarp	Ave of 10% highest FW(g) pericarp	Difference %
FW pericarp g	1.02	2.03	+99
DWg [C] per g pericarp FW	0.180	0.199	+10.5
H2O %	82.1%	80.2%	-2.3
Brix	25.9	23.9	-7.7
Seed content N	1	3	+200

Figure 26: Selected berry composition parameters ordered for fresh weight. An apparent association between berry seed number (vertical axis) and berry mass is evident. No specific association between berry seed number and berry water content or dry weight mass is evident.

Seed content is well correlated with berry colour (biosynthesis of anthocyanins) and could play a major role in the timing of ripening (Figure 27). The majority of berries with one seed are green, two seeded berries are pink and red, three and four seeded berries are mostly red. This may be the result of seeds triggering the earlier onset of veraison, however this needs to be confirmed. This may infer that early veraison versus early berry softening will lead to an early berry sugar accumulation and biosynthesis of anthocyanins. In that regards, the difference between green, pink and red berries at veraison was significant for number of seeds, water and dry mass content in pericarp.





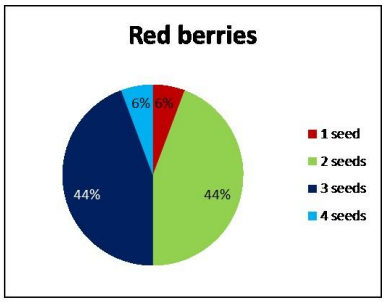


Figure 27: Seed content and berry colour at veraison: comparison between green, pink and red berries. The ripest berries in terms of anthocyanins biosynthesis (berry colour) had the highest seed content.

Principal Component Analysis (PCA) was conducted on berry composition. We found that the seeds could play an important role for other berry characteristics. These plots show well defined sample clusters for each group of berries with a different seed content (Figure 28 a, b). A clear association between berry seed number and measures of berry mass is evident and is not unexpected. Of interest is the lack of association between berry seed number and sugar concentration in the pericarp as evident by the proximity of the sugar g/g of pericarp variable to the origin for PC2.

The preliminary results showed that berry position within bunches and branches did not influence the targeted physiological parameters. Strong interrelationship between berry seed number and sugar concentration, fresh and dry mass of the pericarp were found. The study showed a correlation between the number of seeds per berry and skin colour at veraison, suggesting an important role of the seeds in the timing of ripening. We hypothesise that berry seed number influences berry size by alteration of cell numbers in the pericarp in the early stage of berry development. Flowering and the associated ovule fecundation will lead to berry seed number and viability. This could impact on berry cell multiplication and obviously on the onset of berry development and could help explain fruit asynchronous development and bunch heterogeneity.

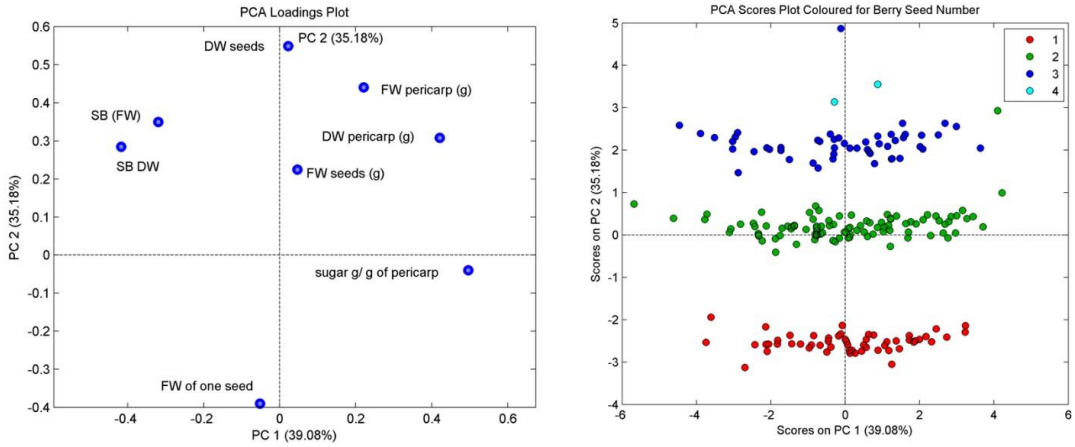


Figure 28 a, b: Principal Component Analysis loadings (a) and scores (b) plot of berry composition. PC2 shows a clear separation of samples according to berry seed number. Associated with berry seed number are highly loaded variables for pericarp mass and total dry weight of seeds. Of interest is the lack of position of sugar (g/g) in PC2 (near the origin) inferring a disassociation between berry sugar accumulation and seed number.

7 Android app development

This section gives details for the user interface and data workflow for the app. The smartphone application was developed on the Android platform. The development platform used was Android Studio with OpenCV for Android add-on library modules. The OpenCV (Open Source Computer Vision) is a well-established set of routines used by image processing and computer vision researchers. The final part of the section also gives details on a data management tool using the Excel Dashboard.

7.1 Code design and structure

Figure 29 shows a summary of the code design and structure for the app which has three major modules: (1) White cultivar module; (2) Red cultivar module; and (3) Berry Analysis Results. The modules for the white and red cultivars have a similar structure. They offer sub-modules to capture the grape image from the vineyard and store the image into a gallery for further analysis. The app also has a settings sub-module that allows the grower to enter the minimum and maximum berry width, probe width, and whether a probe is to be used or not. The Analysis Results module allows the grower to specify the vineyard, block and variety of the bunch to be analysed. The volume and colour information for the berries is displayed in the charts in the results page.

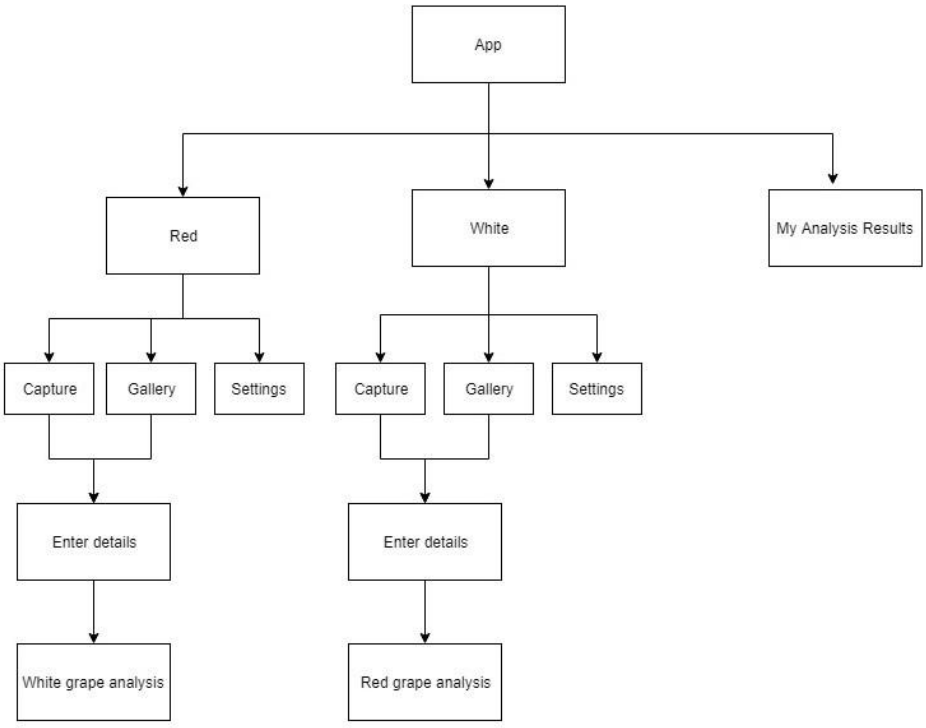


Figure 29: Code design and structure of app.

7.2 User interface and functionality

The graphical user interface (GUI) has been designed to be simple and robust to use. An Alpha version of the app was released to selected vineyard operators in early 2017 and using the feedback from that release, the user interface was redesigned and substantially improved. Figure 30 to Figure 35 shows the app user interface and functionalities. The initial screen that the grower would see on the smartphone application is shown in Figure 30. Figure 31 shows the image capture with the reference probe. During operation, the reference probe is inserted into the grape bunch to function as a size reference for volume estimation. The reference probe used had a diameter of 0.8mm.



Figure 30: NWGIC app screen.



Figure 31: Image capture with reference probe.

Figure 32 shows the data record screen to allow the grower to record the details of the captured grape bunch image, such as the date, vineyard, block and grape variety. Figure 33 and Figure 34 show the berry detection and sampling process and the resulting sampled berries for analysis respectively. There would be a target box that growers can drag to clip out the particular grape cluster to be analysed. Figure 35 shows the volume distribution calculated from the sampled

berries. The overall objective is to make the smartphone application easy for growers to use and the imaging settings would be automatically tuned or defaulted to work for the majority of image capture conditions without the need for growers to do the tuning themselves.

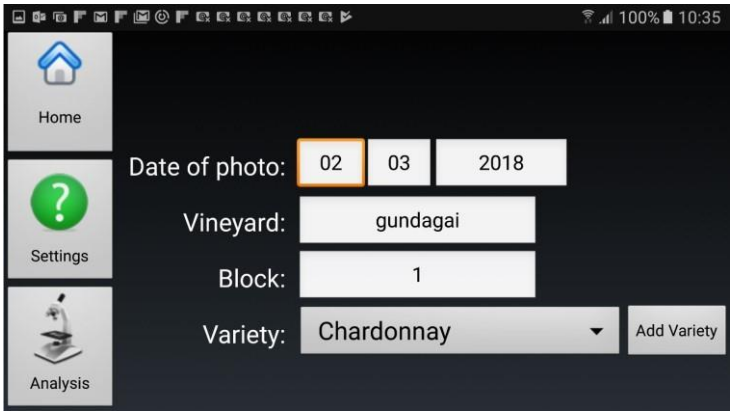


Figure 32: Data record.

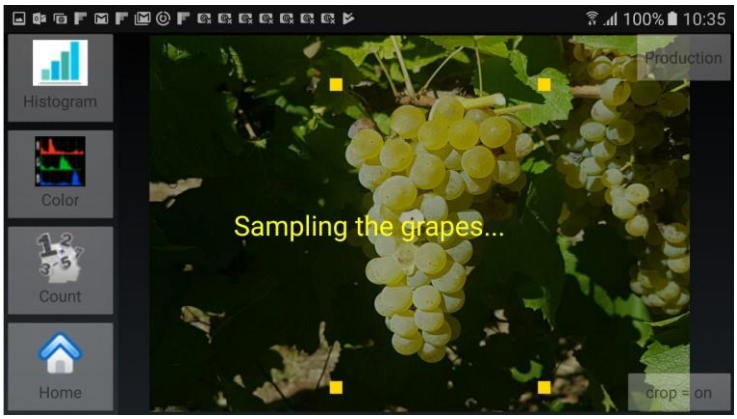


Figure 33: Berry detection and sampling.

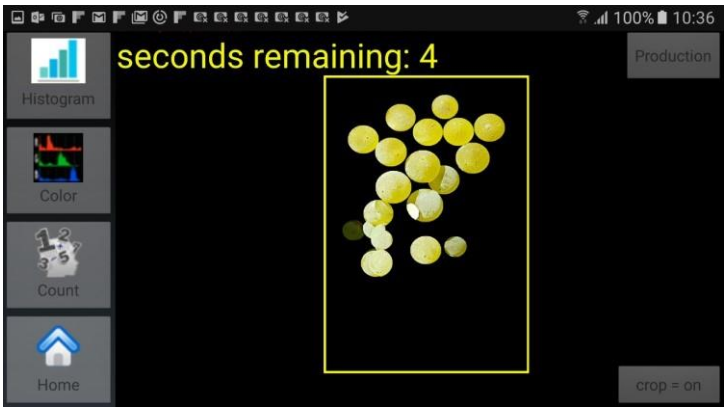


Figure 34: Sampled berries for analysis.



Figure 35: Distribution of berry volume.

7.3 Code and platform considerations

The app can be operated on Android Version 4.0.3 (Ice Cream Sandwich) or later versions of Android. The app requires a minimum storage space of 110MB although it is recommended that users have more than the required space as image analysis can be process intensive.

7.4 Circle detection and app flow

The detection and sampling of the berries from the grape bunch images is an important component for the app. Figure 36 shows the image processing and machine learning pipeline which was used for the berry detection. The pipeline consists of the following five stages:

1. Capture of a colour image with reference probe object
2. Conversion of colour image to grayscale
3. Histogram equalisation on grayscale image
4. Circle detection with Circular Hough Transform (CHT)
5. Berry detection filtering with support vector machine learning colour classifier.

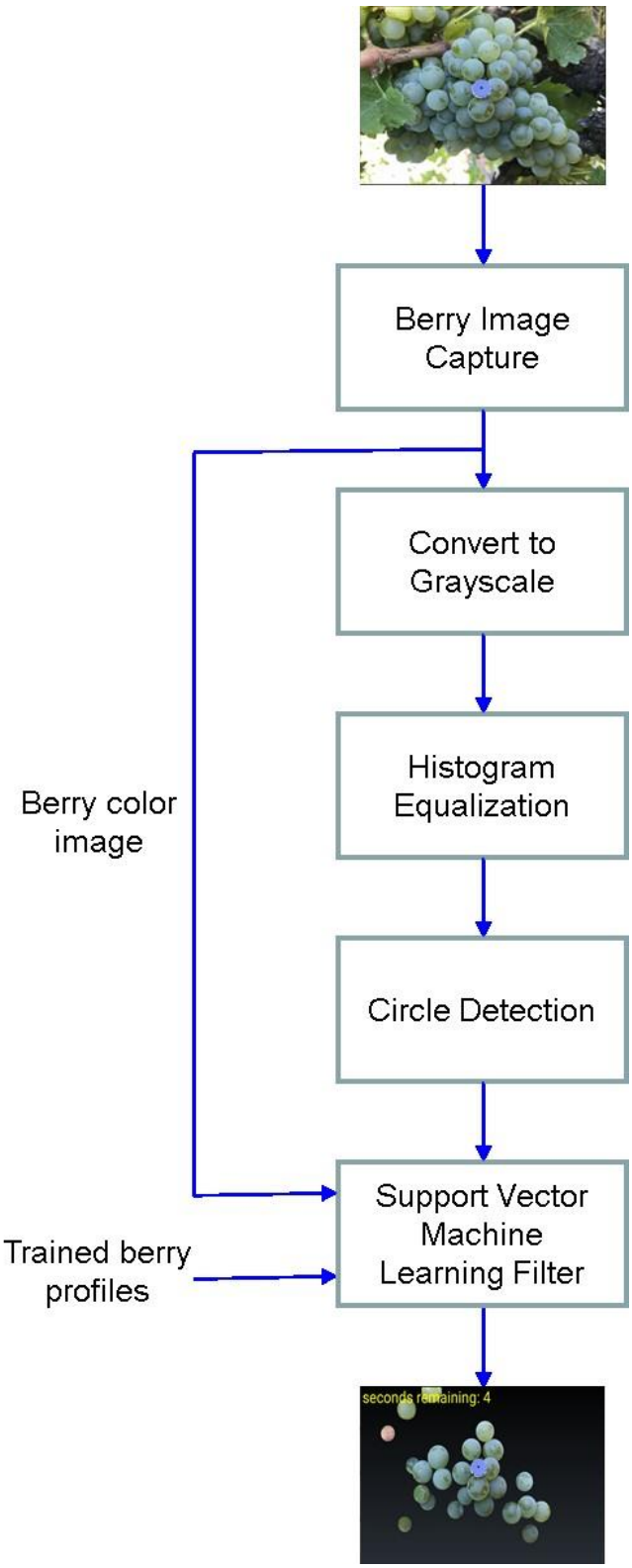


Figure 36: App berry detection image processing and machine learning pipeline.

The app flow begins by the grower taking a photo of the grape bunch in the field with a reference probe object. The circular part of the reference probe has a diameter of 0.8 cm for

berry size calibration. The app gives visual feedback to the grower on the probe detection. On successful detection of the probe, the app gives visual feedback to the user by highlighting the probe circumference on the screen display. This stage confirms that the probe has been successfully detected during the capture stage. If the probe cannot be detected, the grower is prompted to take another photo. Only photos with successful detection of the probe are saved for future analysis.

The second stage performs a conversion of the colour image to grayscale. The colour image contains three components (red, green and blue) or RGB. This stage converts the captured RGB image to grayscale. The conversion to grayscale is performed for two reasons: (1) To reduce the computational requirements of the app for implementation on the smartphone platform; and (2) To prepare the image for the subsequent stages of histogram equalisation and circle detection. The three colour components (RGB) are converted to a single luminance component (Y).
The third stage performs histogram equalisation on the luminance grayscale image. The objective of histogram equalisation is to adjust the contrast of an image by modifying the intensity distribution of the histogram. Since the app captures images from the field, the illumination varies depending on the time of day, weather and other environmental conditions. This stage performs pre-processing on the grayscale image for the subsequent stage of circle detection. The equalisation performs a mapping from the original distribution (the given histogram) to another distribution (a wider and more uniform distribution of intensity values) so the intensity values are spread over the whole range.

The app models grape berries as circular objects to be detected in the grayscale image. The detection of circles is a common task in image processing. There are various circle detection algorithms that have been proposed, such as the circular Hough transform (CHT) (Smereka & Dulba, 2008), EDCircles (Akinlar & Topal, 2013), and Ridge Ring Detector (Afik, 2015). The CHT was selected to be implemented in the app due to the following: (1) The algorithm is well established in the image processing and computer vision community; and (2) The OpenCV library for Android contained a module implementation of the CHT and the development did not require a custom circle detection technique to be re-implemented.

The CHT uses voting methods to detect circular shapes by finding the accumulated local maximum relating to circular objects. The two parameters used for circle detection are the berry centre and radius. The CHT module in OpenCV implements the Hough gradient method, which consists of two stages: (1) The first stage performs edge detection and finding the possible circle centres; and (2) The second stage locates the best radius for each candidate centre. Since the

CHT performs the circle detection task on grayscale images, the processing flow for white and red berries would be the same.

To achieve more accurate detection using the CHT, the app uses a two-stage detection scheme: (1) Dividing the circle detection range into five ranges corresponding to very small (VS), small (S), medium (M), large (L) and very large (VL) berries. The CHT was then applied for each berry range to produce a list of berry candidates for that range; and (2) The five lists of berry candidates for the different ranges were then merged to give a final list of circular candidates. During the merging stage, berry candidates which overlapped with other ranges were removed from the final list. Experiments with this approach of using the CHT with overlapping ranges gave more accurate detection compared to using the CHT with a single large range for detection of the different berry sizes.

The outcome from the fourth stage of circle detection is a list of potential circular candidates which may or may not be grape berries. This is due to the CHT which identifies potential circular objects in the grayscale image. To improve the berry detection task, the fifth stage uses the colour features from the captured RGB image to filter out circular objects which are not berries from the list. This is performed using two filtering stages: (1) A coarse filtering based on the hue values of the grape berries; and (2) A fine filtering using a support vector machine classifier.

The first stage performs a coarse filtering to broadly classify pixels that are too far out of the possible hues to be a grape berry. For example, with white grape berries, the app will consider hue pixel values that are below 30 or above 180 to be unlikely white grape pixels and will classify these as background. The second stage performs a fine filtering using a SVM classifier. The SVM is a well-established technique in machine learning for classification tasks. The SVM is first trained using a set of berry samples and taught to distinguish between berry pixels and background pixels from the colour features.

The SVM constructs what is termed a maximum margin hyperplane to classify the samples into berry pixels and non-berry (background) pixels. Two sets of training samples were used for the app. The first set trained an SVM classifier to distinguish pixels of white berries from the background, and the second set trained another SVM classifier to distinguish pixels of red berries from the background. In operation, depending on the task of detecting white or red berries, the respective SVM classifiers were used. The coarse and fine filters were used to classify pixels in potential circular objects. The object was classified as a grape berry if a 50% threshold of the pixels were detected as berry pixels. Otherwise, the object was removed from the detected berry list. The app uses the final detected berries, performs the sampling and calculates the estimated volume and hue distributions.

7.5 Berry size measurement

Before any volume calculations, the radius of sampled berries is converted from pixels into a physical unit of measurement (cm). The app uses the probe inserted into the bunch as a reference point to perform the conversion. The user can specify the size of the probe in the settings (by default the probe is 0.8 cm wide). The app detects the size of the probe in the image and performs the conversion from pixels to cm using the following formula:

$$R(cm) = r(pixels) \times \frac{p}{m}$$

where *R* is the calculated radius in cm, *r* is the measured radius in pixels, *p* is the probe width (in cm), and *m* is the measured probe width (in pixels).

To measure the size of the berries, the app calculates the radius of the detected berry (in cm), and then applies the volume (sphere) formula $\frac{4}{3} \times \pi r^3$ to give an approximation of the berry volume. The spherical volume is used in the app as an approximation for berry volume.

7.6 Tint measurement

For tint measurement, the app uses the colour information in the captured berry bunch image and converts to the HSI colour space. The medians of the hue colours for all of the sampled berries in a given image are then calculated. The overall hue for the bunch is then given by the median of the sampled berries.

7.7 File and data management

7.7.1 Data structure and analysis

Photographs

Photographs of grape bunches are taken in JPEG format. Any photo taken with or without the app will contain metadata in the JPEG file format containing information on when the photo was taken (called ‘date taken’), which is used to label and sort analysis results. A photo taken with the app will have a file name format of ‘yyyy-MM-dd-hh-mm-ss.jpg’ (time stamp), while a photo taken with the phone’s camera will save the file using that camera’s default file naming convention. All photos taken with the app are saved into the GrapeYield folder in the file manager. The JPEG image files generated by the app are a screenshot of the resulting berry detection from the app. These JPEG images contain information about the grape bunch in their

file names, including having the vineyard, block and variety so that users can see how the berry detection went with each analysis and reference them as they see fit. The file name for each generated image is 'yyyy-mm-dd_vy_<vineyard>_blk_<block>_var_<variety>.jpg'. All generated image files are saved in the GrapeAnalysisResults folder in the file manager.

App analysis results

The app analysis results are stored in three separate types of csv files:

- Global – the analysis results of every image analysed with the app. This csv file is required for the Excel Dashboard so that it has all the previously analysed images to reference. The file name is 'global.csv', and it contains the following fields:

Field	Description
Vineyard	The vineyard in which the image was taken
Block	The block in which the image was taken
Type (Variety)	The type/variety of the berries in the image
Date	The date the image was taken
Average Volume	The average volume of all of the detected berries
Volume Variance	The variance of the volumes of all the detected berries
Median Hue	The median hue of all of the detected berries
Decile 1	The 10^{th} percentile of the median hue
Decile 9	The 90^{th} percentile of the median hue
Dominant Hue	The dominant/mode hue of the detected berries
Hue Variance	The variance of the median hues of the detected berries
Berry Count	The number of berries detected

- All analysis results from a specific vineyard, block and variety – this contains all the analysis results from the specified vineyard, block and variety. This spreadsheet's file name contains the vineyard, block and variety so that it can be easily identified by both the app and by anyone looking through the csv files. This spreadsheet uses the same fields as the global.csv file and is named

  'vy_<vineyard>_blk_<block>_var_<variety>.csv'

- csv file for a specific analysed image – the filename contains the date, vineyard, block and variety. This csv file is useful if users would like to review analysis results for an image. The file name format is named

  'yyyy-mm-dd_vy_<vineyard>_blk_<block>_var_<variety>.csv',

and the spreadsheet contains the same fields as the global.csv, as well as the fields for individual berries:

Field	Description
Berry number	The ID of a detected berry
Volume	The volume of the detected berry
Average Hue	The average hue of the detected berry
Dominant Hue	The dominant/mode hue of the detected berry
Median Hue	The median hue of the detected berry

Dyostem system

There are many variables from the Dyostem results. The analysis results from the Dyostem system are displayed on the Dyostem system screen, as well as saved into a txt file. The variables that are useful for comparing the results to that of the app are listed below.

Field	Description
Berries found	The number of berries detected
Avg volume	The average volume of the detected berries
Volume std	The volume standard deviation of the detected berries
Hue 1 decile	The 10^{th} percentile of the hue of the detected berries
Hue 9 decile	The 90^{th} percentile of the hue of the detected berries
Hue median	The median hue of the detected berries

7.7.2 Data management - Dashboard

The analysis results are managed by internal processes within the app, which achieved its desired results when working with the app. However, it has become apparent that there will be a requirement to view and manage the app's analysis results data outside of the app too, primarily on PCs. To achieve this, we have developed an Excel spreadsheet that acts as a dashboard for displaying the analysis results and filters the results based on a given vineyard, variety, block and season. Figure 37 shows the dashboard that was developed to view analysis results from the app.

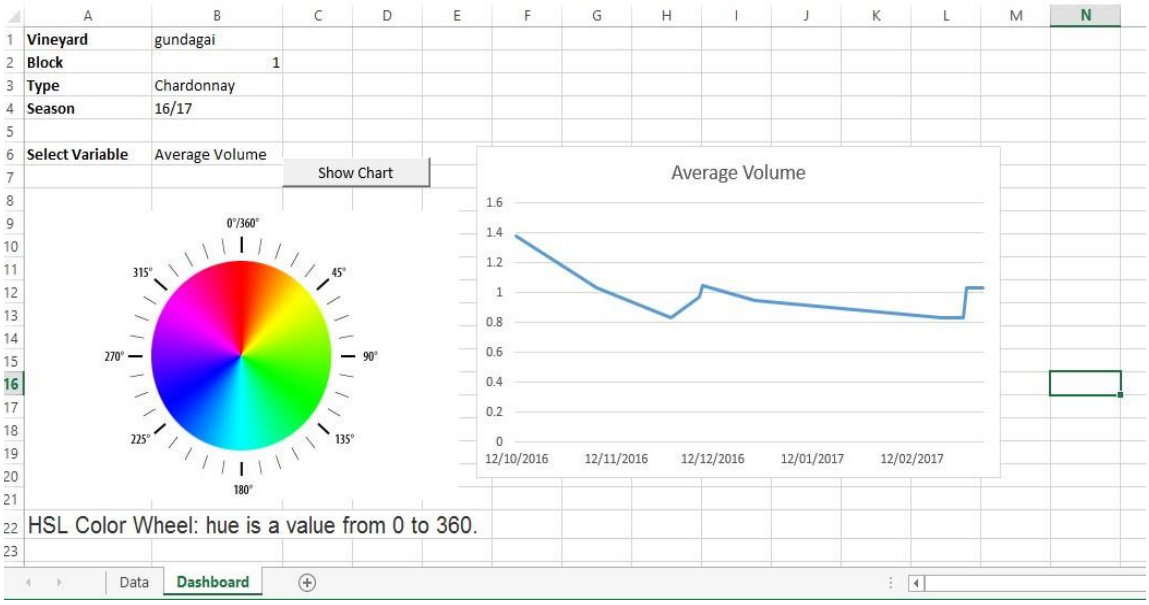


Figure 37: Dashboard on Excel spreadsheet for viewing app analysis results.

As shown in Figure 37, the dashboard allows the user to select four parameters (vineyard, vineyard block, cultivar type and season) and then a summary of the results is displayed to the user in the form of a chart for different dates contained in the app. The user can select to view the summary date for the average volume or the average hue colour. When the user clicks the 'Show Chart' button, the selected data will appear, generated by a VBA macro script connected to the 'Show Chart' button. The dashboard also contains an HSL colour wheel for a reference point when looking at the hue data. Figure 38 shows a sample from the global data spreadsheet tab. This tab is where the data is stored. The data from the global spreadsheet are derived from the global Excel .csv file so that the dashboard can use it as a reference

Block	Type(Variety)	Date	Average Volume	Volume Variance	Median Hue	Decile 1	Decile 9	Dominant Hue	Hue Variance	Berry Count	Date (for sorting purpo
1	Chardonnay	12/10/2016	1.38	0.23	66	57	70	69	220	12	201601012
1	Chardonnay	6/11/2016	1.03	0.41	103	28	201	70	4567	67	201601106
1	Chardonnay	29/11/2016	0.83	0.24	56	50	62	61	93	57	201601129
1	Chardonnay	8/12/2016	0.97	0.21	159	62	205	202	4698	28	201601208
1	Chardonnay	9/12/2016	1.05	0.37	180	57	186	180	4120	41	201601209
1	Chardonnay	25/12/2016	0.95	0.21	63.5	62	74	63	38	22	201601225
1	Chardonnay	21/02/2017	1.66	0.18	57	53	69	70	356	9	201700221
1	Chardonnay	21/02/2017	0.83	0.24	56	50	62	61	93	57	201700221
1	Chardonnay	22/02/2017	1.66	0.18	57	53	69	70	356	9	201700222
1	Chardonnay	22/02/2017	1.66	0.18	57	53	69	70	356	9	201700222
1	Chardonnay	28/02/2017	0.83	0.24	56	50	62	61	93	57	201700228
1	Chardonnay	1/03/2017	1.03	0.41	103	28	201	70	4567	67	201700301
14	Sauvignon Blanc	1/03/2017	1.66	0.16	153	100	181	168	1271	22	201700301
9	Sauvignon Blanc	1/03/2017	1.41	0.23	48	34	61	48	239	25	201700301
1	Chardonnay	6/03/2017	1.03	0.41	103	28	201	70	4567	67	201700306
1	Sauvignon Blanc	15/03/2017	1.56	0.07	74.5	65	190	70	4739	16	201700315
14	Sauvignon Blanc	15/03/2017	1.66	0.16	153	100	181	168	1271	22	201700315
14	Sauvignon Blanc	15/03/2017	1.66	0.16	153	100	181	168	1271	22	201700315
1	Sauvignon Blanc	16/03/2017	1.56	0.07	74.5	65	190	70	4739	16	201700316
1	Sauvignon Blanc	16/03/2017	1.56	0.07	74.5	65	190	70	4739	16	201700316
9	Sauvignon Blanc	19/03/2017	1.41	0.23	48	34	61	48	239	25	201700319
9	Sauvignon Blanc	19/03/2017	1.41	0.23	48	34	61	48	239	25	201700319

Data | Dashboard

Figure 38: Sample data from global spreadsheet used for the app analysis results.

8 Post-development analysis and testing

8.1 Apps analysis on images

Photographic images were collected for Chardonnay bunches from a vineyard in Gundagai (NSW) in February 2018. Two sets of images were collected: (1) Taken in natural daylight; and (2) Taken using an artificial shade to block the sunlight on the bunches. Figure 39 and Figure 40 show sample images for the Chardonnay grape bunches in daylight and with the artificial shade respectively. After photographing the bunches, they were removed for laboratory analysis with the Dyostem™. The phone app was used to analyse the bunches for hue and volume distributions and were compared with the Dyostem™ laboratory results as the reference.



Figure 39: Photographic images for Chardonnay grape bunches (2018 harvest) taken in daylight.



Figure 40: Photographic images for Chardonnay grape bunches (2018 harvest) taken in artificial shade.

8.1.1 Analysis and testing of app and Dyostem™ for berry hue

Figure 41 shows the comparison between the app and Dyostem for the bunch hue measurements taken in daylight. Figure 41(a) shows the scatter chart for the app plotted against Dyostem with the fitted line and the 95% mean confidence band. An observation of the scatter chart shows that the app measurement is consistently below the corresponding Dyostem measurement. Figure 41(b) and Figure 41(c) show the box plots for the app and Dyostem respectively. The overall statistics for the app and Dyostem are shown at the top of Figure 41(a). These give statistical measures for the mean, standard deviation (SD), minimum, median and maximum values. The statistical fit of the model is given by the coefficient of determination (R^2), correlation coefficient (R), root mean square error (RMSE), F value and p-value. The model of app hue in daylight has a coefficient of determination (R^2) of 0.731 indicating that 73.1% of the

variation is determined by the regression line. The model has a correlation coefficient of 0.85 which indicates a strong positive correlation between the app and Dyostem for hue measurements in daylight. The p-value (<0.0001) for the F-test gives sufficient evidence at the 5% significance level to conclude that the model fits the data better than the model with no independent variables. Overall, the results in Figure 41 show a strong relationship between the hue measurements from the app with the Dyostem reference for images taken in natural daylight. The app can be used in place of Dyostem to give comparable measurements at a convenient and cheaper cost.

Figure 42 shows the comparison between the app and Dyostem for the bunch hue measurements taken in artificial shade. The model of app hue in shade has a coefficient of determination (R^2) of 0.021 indicating that 2.1% of the variation is determined by the regression line. The model has a correlation coefficient of 0.14 which indicates a weak correlation between the app and Dyostem for hue measurements in the artificial shade. The p-value (0.6089) for the F-test provides insufficient evidence at the 5% significance level to conclude that the model fits the data better than the model with no independent variables. The scatter chart in Figure 42 show that the app gave six measurements where the hue values were higher than Dyostem and nine measurements where the hue values were lower than Dyostem. Overall, the results in Figure 42 show a weak relationship between the hue measurements from the app with the Dyostem reference for images taken in artificial shade. For further investigation, Figure 43 (a) and (b) shows a comparison of the same berry bunch taken in daylight and artificial shade with the corresponding app berry detections. For the bunch taken in daylight, the app gave a measured value of 60 whereas for the bunch taken in the artificial shade, the app gave a measured value of 82.

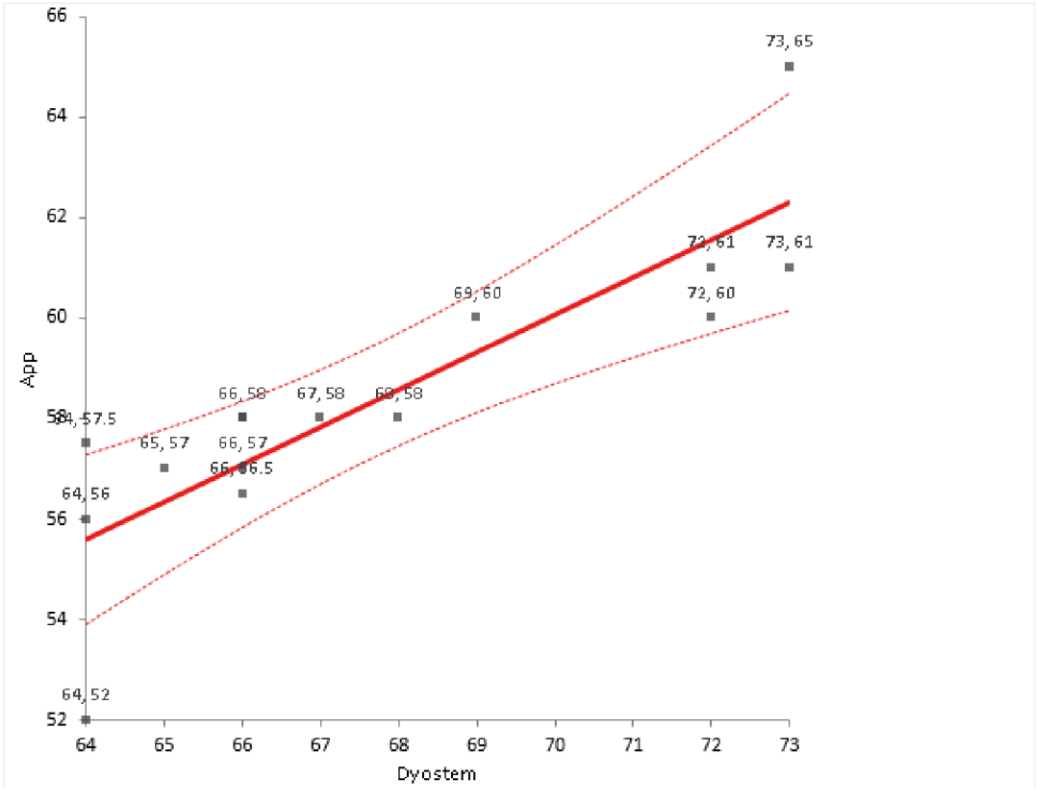
The following recommendations can be used to control and improve the colour hue measurements:

(1) For correct operation of the app, images should be captured in sufficient natural daylight conditions as shown in Figure 1 and Figure 43;

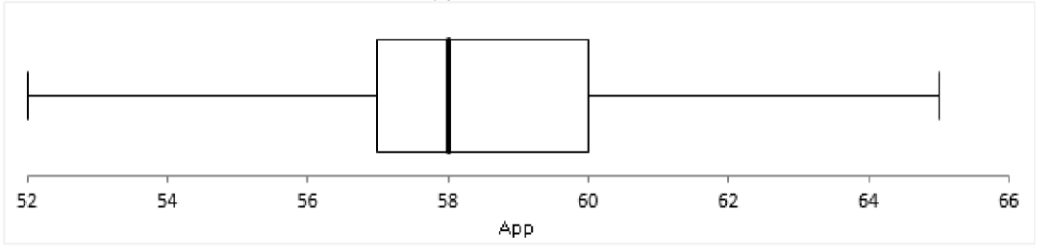
(2) A second recommendation is to investigate the incorporation of a colour reference on the probe for colour correction. This may allow images taken with insufficient sunlight to be corrected prior to analysis with the app.

	Mean	SD	Minimum	Median	Maximum
App	58.33	2.90	52.0	58.0	65.0
Dyostem	67.7	3.3	64.0	66.0	73.0

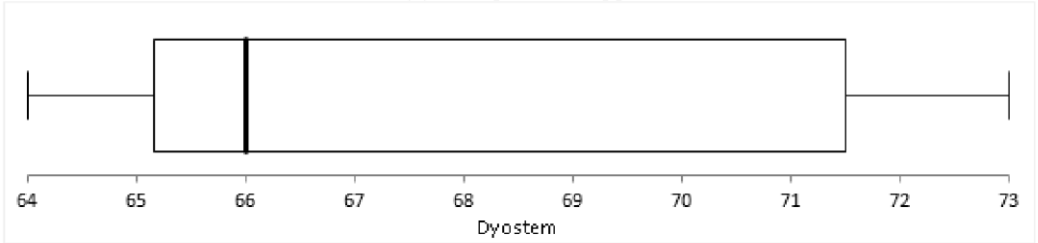
R2	R	RMSE	F	p-value
0.731	0.85	1.562	35.32	<0.0001



(a) Scatter chart.



(b) Box plot for App.

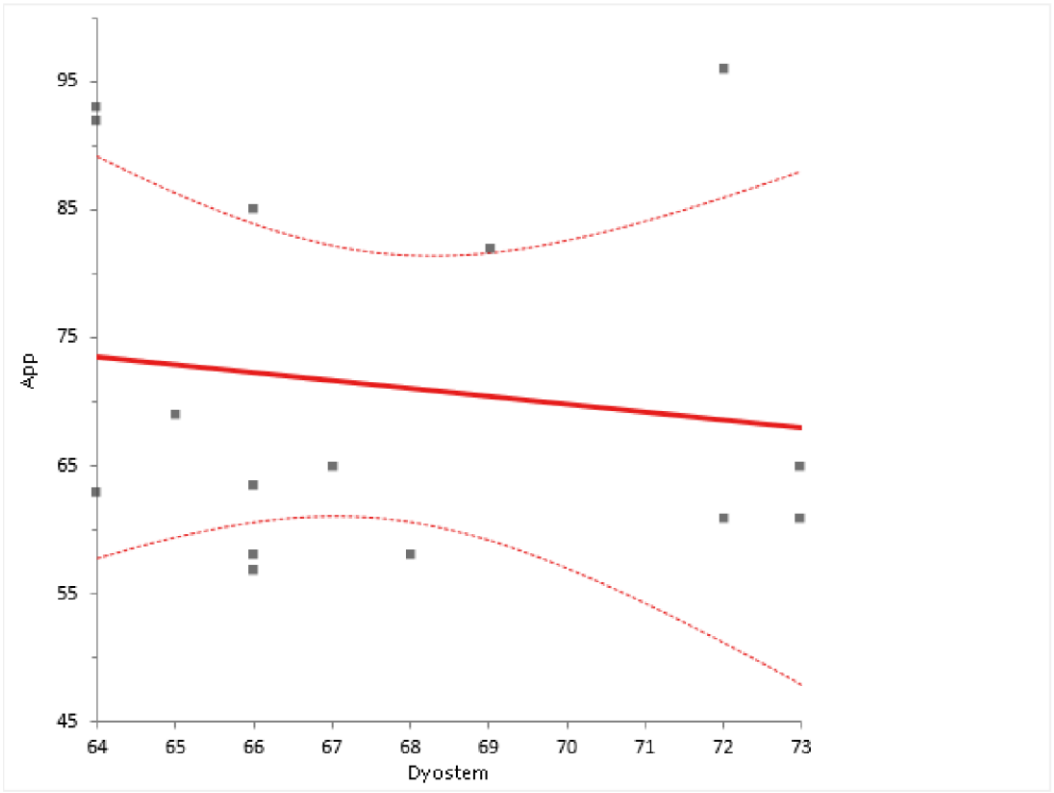


(c) Box plot for Dyostem.

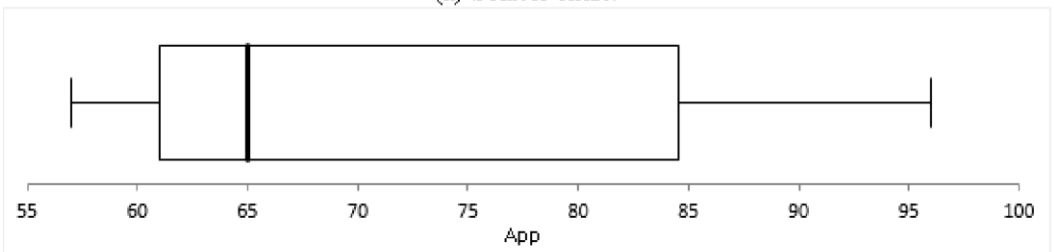
Figure 41: Comparison of phone app and Dyostem for Chardonnay bunch hue (2018 harvest) in daylight.

	Mean	SD	Minimum	Median	Maximum
App	71.23	14.13	57.0	65.0	96.0
Dyostem	67.7	3.3	64.0	66.0	73.0

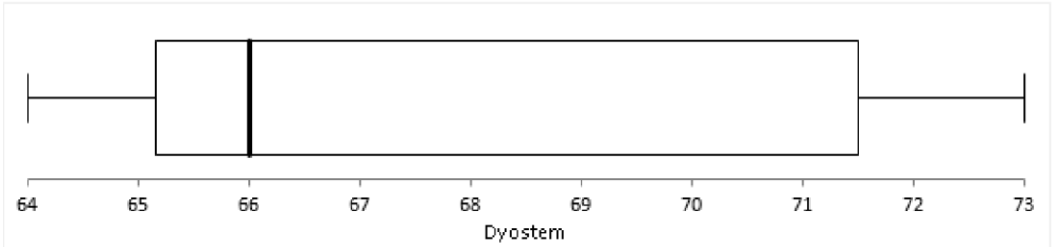
R^2	R	RMSE	F	p-value
0.021	0.14	14.514	0.27	0.6089



(a) Scatter chart.



(b) Box plot for App.



(c) Box plot for Dyostem.

Figure 42: Comparison of phone app and Dyostem for Chardonnay bunch hue (2018 harvest) in shade.



Figure 43: Sample bunch images taken in daylight and artificial shade with corresponding app berry detections. The measured hue values from the app are also shown.

8.1.2 Analysis and testing of app and Dyostem^{TM} for berry volume

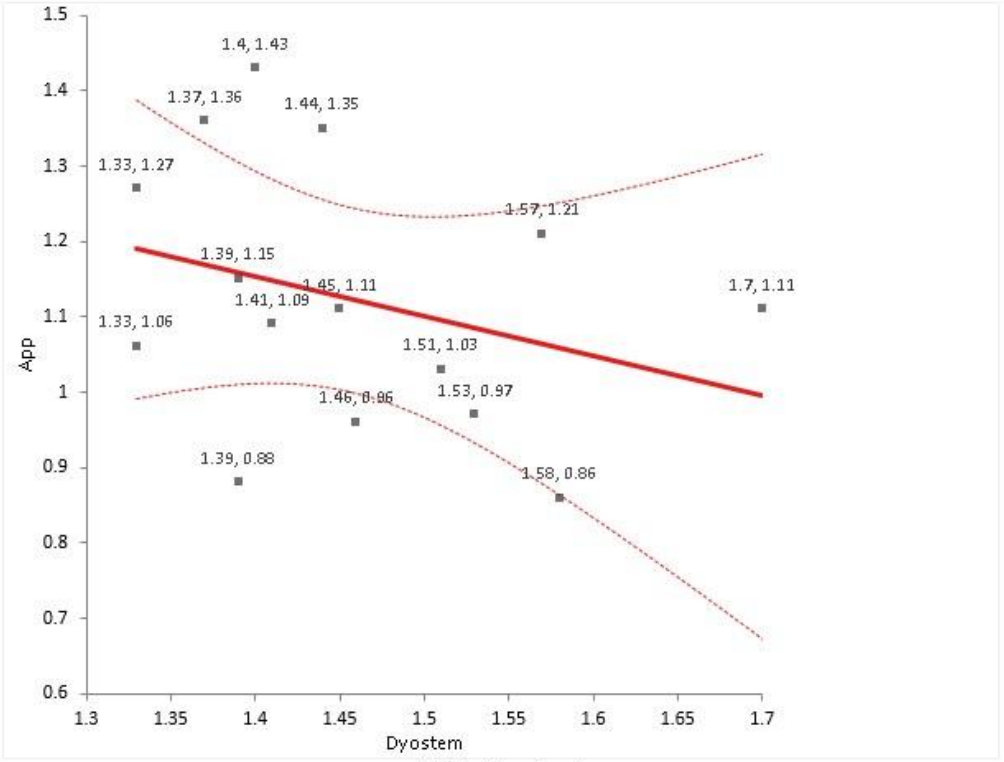
Figure 44 and Figure 45 show the comparisons between the app and Dyostem for the volume measurements taken in daylight and shade respectively. The model of app volume in daylight has a coefficient of determination (R^2) of 0.098. The correlation coefficient is 0.31 which indicates a poor correlation between the app and Dyostem measurements. The p-value (0.2564) for the F-test gives insufficient evidence at the 5% significance level to conclude that the model fits the data better than the model with no independent variables. The model of app volume in shade has a coefficient of determination (R^2) of 0.002. The correlation coefficient is 0.04 which indicates a very poor correlation between the app and Dyostem measurements. The p-value (0.8618) for the F-test gives insufficient evidence at the 5% significance level to conclude that the model fits the data better than the model with no independent variables. Overall, the results in Figure 44 and Figure 45 show a weak relationship between the volume measurements from the app with the Dyostem reference for images taken in natural daylight and artificial shade.

The following recommendations can be used to improve the volume measurements:

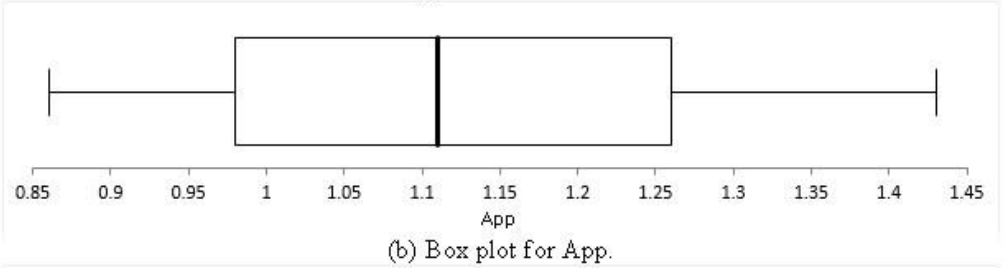
(1) The size of the reference probe can be increased. Currently, the reference probe has a diameter of 0.8 cm. Thus, a difference of one pixel in measurement would translate to a significant change in volume measurements. A larger probe diameter would reduce the sensitivity of the volume measurements towards the probe size. However, this has to be balanced because a larger probe size may cause occlusion of the berries on the bunch;

	Mean	SD	Minimum	Median	Maximum
App	1.123	0.174	0.86	1.110	1.43
Dyostem	1.457	0.103	1.33	1.440	1.70

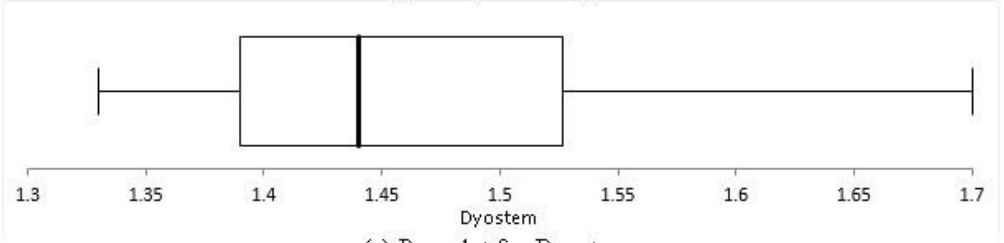
R^2	R	RMSE	F	p-value
0.098	0.31	0.1716	1.41	0.2564



(a) Scatter chart.



(b) Box plot for App.



(c) Box plot for Dyostem.

Figure 44: Comparison of phone app and Dyostem for Chardonnay volume (2018 harvest) in daylight.

	Mean	SD	Minimum	Median	Maximum
App	1.029	0.237	0.55	1.090	1.36

Dyostem	1.457	0.103	1.33	1.440	1.70

R^2	R	RMSE	F	p-value
0.002	0.04	0.2456	0.03	0.8618

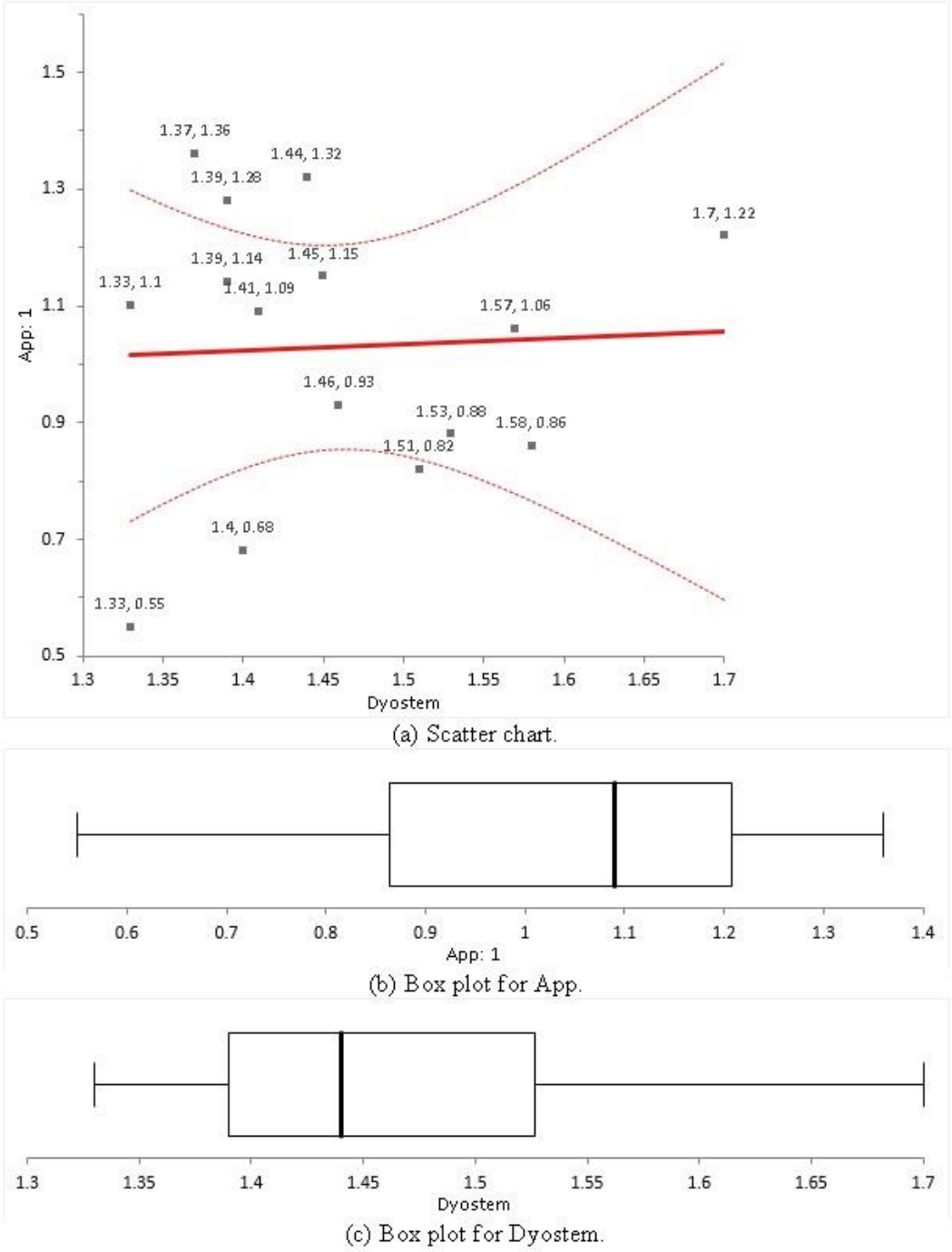


Figure 45: Comparison of phone app and Dyostem for Chardonnay volume (2018 harvest) in shade.

(2) One challenge is to position the probe within the bunch. The grape bunch occupies a three-dimensional space and the probe has to be placed within the bunch. The current practice is to position the probe to coincide with the closest surface berries to be detected.

However, positioning the probe is subject to human error. Another issue is that berries deeper within the bunch would be measured with a smaller diameter compared with berries at the surface of the bunch. This may be an explanation for the results in Figure 44 when the volume measured by Dyostem is consistently higher than the volume measured by the app.

8.2 Small scale vinification and grape berry analysis

8.2.1 Grape sampling for Dyostem™ and app calibrations

Grape bunches for imaging and sample collection for Dyostem™ analysis was conducted by randomly selecting bunches with a minimum distance of 10 metres from each row end. Bunches were selected from both sides of each row, positioned within the canopy with no more than two bunches selected from a single vine. For the purposes of imaging the vine, canes and leaves were removed to provide a clear field of vision.

Grape harvest for small lot winemaking

Replicates of 60 kg of grapes were harvested across the selected experimental vineyard plots established inside the commercial block. To minimise the effect of the variability between vines, grapes were hand harvested randomly across the experimental plot, picking only a few bunches per vine. Grapes were hand-picked, and sulfur added at 40 mg/kg of sulfur dioxide (SO_2) in the form of dissolved potassium metabisulfite and transported in crates to the NWGIC winery. Grapes were cooled at 4 °C overnight before further processing.

Vineyard locations

Grapes were sourced from a range of vineyards within the Orange and Riverina locations according to variety and maturity as shown in Table 4.

Table 4: Grape sampling for small lot wine making.

Vineyard	Cultivar	Grape Maturity	Year
Cumulus	Chardonnay	Early	2017
	Sauvignon Blanc	Early & Mature	2017
See Saw	Sauvignon Blanc	Early & Mature	2017
Gundagai	Chardonnay	Early & Mature	2017
Cumulus	Shiraz	Early	2017

Small-lot winemaking

All biological replicates were kept separate during grape processing. Grapes were destemmed, crushed and pressed to a maximum pressure of 1 Bar. Juice was transferred to 100 L stainless steel tanks and subsequently held for 24 hours at 4±1°C for clarification by cold settling. Juice

was racked and adjusted if necessary to approximately pH 3.6 with tartaric acid. The juice was inoculated with *Saccharomyces cerevisiae* yeast EC1118 (Lalvin) and fermentations were carried out at 15±1°C until a residual sugar of ≤0.5 g/L was achieved. For ferments with an initial TSS of less than 23.4 Brix, once alcoholic fermentation had caused a drop or 2 to 3 Baumé, the original yeast assimilable nitrogen (YAN) was adjusted to 200 mg/L with Fermaid K and diammonium phosphate (DAP). For ferments in excess of 23.4 Brix, the YAN was adjusted to 220 mg/L. Wines were cold stabilised for 21 days at 4°C, free SO_2 was adjusted to 30 mg/L prior to bottling and sensory analysis.

8.2.2 General analyses of grape maturity, yeast available nitrogen and basic wine parameters

Grape juice samples were collected after crushing for basic parameters of maturity. TSS expressed as Brix was analysed with a portable density meter (Anton Paar DMA 35N, Graz, Austria). Titratable acidity (TA) and pH were determined by sodium hydroxide titration to the end point pH 8.2 with an automatic titrator (Metrohm Fully Automated 59 Place Titrando System, Metrohm AG, Herisau, Switzerland). Ethanol was measured with an Anton Paar Alcolyser DMA 4500 density meter (Graz, Austria) whereas α-amino acids, ammonia and acetic acid in juice were measured by available enzymatic tests purposely designed and deployed on an Arena discrete analyser (ThermoFisher). Yeast assimilable nitrogen (YAN) was calculated from ammonium and free amino nitrogen (FAN) measurements (Illand et al., 2004).

Sensory analysis of wines

A panel of 12 assessors (six female, six male; 27–50 years) which regularly participates in wine sensory research was convened to evaluate the Chardonnay and Sauvignon Blanc wines using a consensus-based descriptive methodology (Blackman & Saliba, 2009). Panellists undertook 7 × 1h sensory training sessions. A sample of each treatment (n = 7) was provided over the first session, where panellists were asked to list the most dominant aromas in each wine. At each of the following three sessions, 10 descriptors and matching reference standards were presented. Panellists were asked whether or not they could detect each attribute in each of the seven wines. Terms that were detected by fewer than three of the panel were eliminated. As the training sessions continued, the list was gradually refined by consensus to a total of six descriptors (Table 5). Additionally, *sweetness, acidity*, *bitterness* and *alcohol* reference standards were presented, so that their rating could be practiced in a comparable manner as that described for aromas. Panellists practiced evaluation of intensity rating for all attributes. 'High' intensity standards were prepared using a 1:1 reference standard dilution in base wine (Berry Estates Traditional Dry White 5 L bag-in-box), while 'low' intensity standards were

obtained using a 1:3 reference standard dilution in water. During the training sessions, panellists encountered all replicates of each treatment on at least one occasion. Panel performance was assessed using PanelCheck® (ver. 1.4.2; Nofima Mat, Norway) while evaluating a subset of the wines in duplicate (Tomic et al., 2010). Since all panellists were found to perform to an acceptable level (minimal wine-by-panellist interactions, with a reasonable reliability and discrimination) the formal sensory evaluation of the wines commenced. During the formal assessment, the samples (25 mL) were presented to panellists in 215 mL ISO/INAO covered clear wine glasses, labelled with a three-digit random number generated in Excel™. Testing was performed in individual booths at 22 ± 1°C under red lighting to prevent colour bias. The same five or six samples were presented to the judges in a randomised order generated in Excel, with a total of 21 samples (seven treatments in triplicates) presented during four sessions over two days. The panellists familiarised themselves with the reference standards before entering the booths. Filtered water, plain breadsticks and containers for expectoration were provided. The intensity of each descriptor was rated using an unstructured 90 mm line scale anchored by 'absent' and 'high intensity'. Results were recorded using ballot charts and pencils on a continuum from 0 to 9 with scores transferred to Excel worksheets for analysis using Senpaq (Qi Statistics).

Table 5: Reference standards for sensory descriptive analysis

Attribute	Reference standard*
Tropical fruit	5 g fresh banana + 5 g fresh papaya + 5 g fresh mango + 5 g fresh passion fruit
Pear/apple	10 g fresh pear + 10 g fresh apple
Apricot/peach	10 g fresh apricot + 10 g fresh peach
Grassy	One-quarter of a cup of fresh grass
Floral	5 µL rosewater (Queen Fine Foods Pty Ltd., Alderley, Australia)
Citrus	10 g fresh grapefruit + 10 g fresh lime
Sweetness	15 g/L D-fructose (Sigma–Aldrich) dissolved in standard solution
Acidity	1.5 g/L tartaric acid (Univar, Tarent Point, Australia) dissolved in standard solution
Bitterness	0.2 g/L quinine sulfate (Univar) dissolved in standard solution
Alcohol	20 mL 68% v/v grape spirit (Tarac Technologies, Nuriootpa, Australia) in standard solution

For the purpose of reporting results for grape maturity data, wine production and sensory profiling will be discussed for each grape cultivar.

Chardonnay wines - Vintage 2017

Grape maturity data for Cumulus and Gundagai vineyards are presented in Figure 46 and Figure 47 respectively. Due to excessive powdery mildew incidence at the Cumulus vineyard, only a single harvest for winemaking was considered useful for winemaking. Overall trends for berry maturity parameters are broadly consistent between vineyards: Increasing berry maturity with rising Brix is accompanied by a decreased mean berry hue, diminished titratable acidity and higher pH. Chardonnay grape berry volume does not show any consistent trends during the sampling times for the two vineyard locations but noteworthy is the large variance associated with berry volume during sampling period. Berry volume heterogeneity is consistently between 25-30% of the grape berry volume. A decrease is berry hue is particularly noteworthy for grapes in the Gundagai vineyard between sampling dates with hue decreasing from 80 to around 65; the decrease in hue is not as evident for the Cumulus vineyard samples (74 to 72) and this may be associated with a lower level of sugar accumulation in these samples.

Chardonnay grape analysis at harvest and finished wine analysis data are presented in Table 6. A second Chardonnay grape harvest from the Cumulus vineyard was not undertaken as the grapes remaining after the commercial harvest were excessively impacted by powdery mildew. Powdery mildew was evident in the first harvest from Cumulus, however, with careful bunch selection the overall level of infection for harvested grapes was considered acceptable.

A clear difference in the finished wine alcohol levels is evident for the two wines from the Gundagai vineyards. Sensory descriptive analysis of these wines (Figure 48; Table 7) shows changes in the grassy (decrease) and apricot/pear (increase) ratings as berries mature and these observations correspond to the change in berry hue angle decrease. A PCA biplot of the mean sensory ratings for the Chardonnay wines is shown in Figure 49. Clearly separated along PC1 are the Gundagai first and second harvest wines; with PC2 separating the Cumulus wines from Gundagai. The associated loadings for PC1 demonstrate the association of grassy and acidity attributes for the Gundagai first harvest wines; with more mature apricot/peach attributes associated with the second harvest. The Cumulus Chardonnay wine is also associated with mature grape sensory attributes but has also some pear/apple characters along with notable perception of bitterness. Powdery mildew affected grapes are noted to result in wine with increased phenolic extraction and bitterness, and the decision to not harvest a second crop of grapes from the Cumulus vineyard appears to be sound.

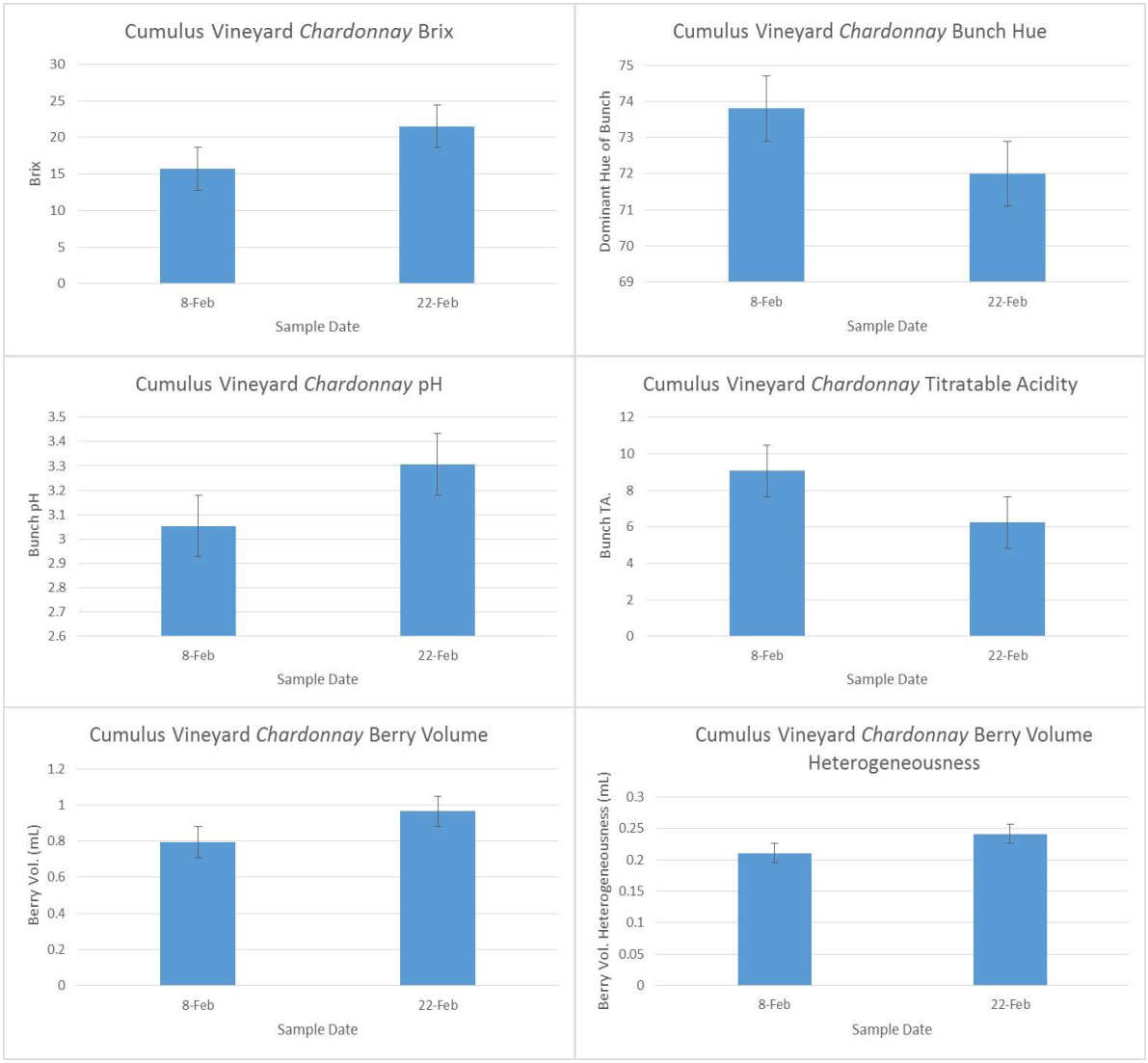


Figure 46: Chardonnay grape berry maturation data for the Cumulus vineyard - Vintage 2017.

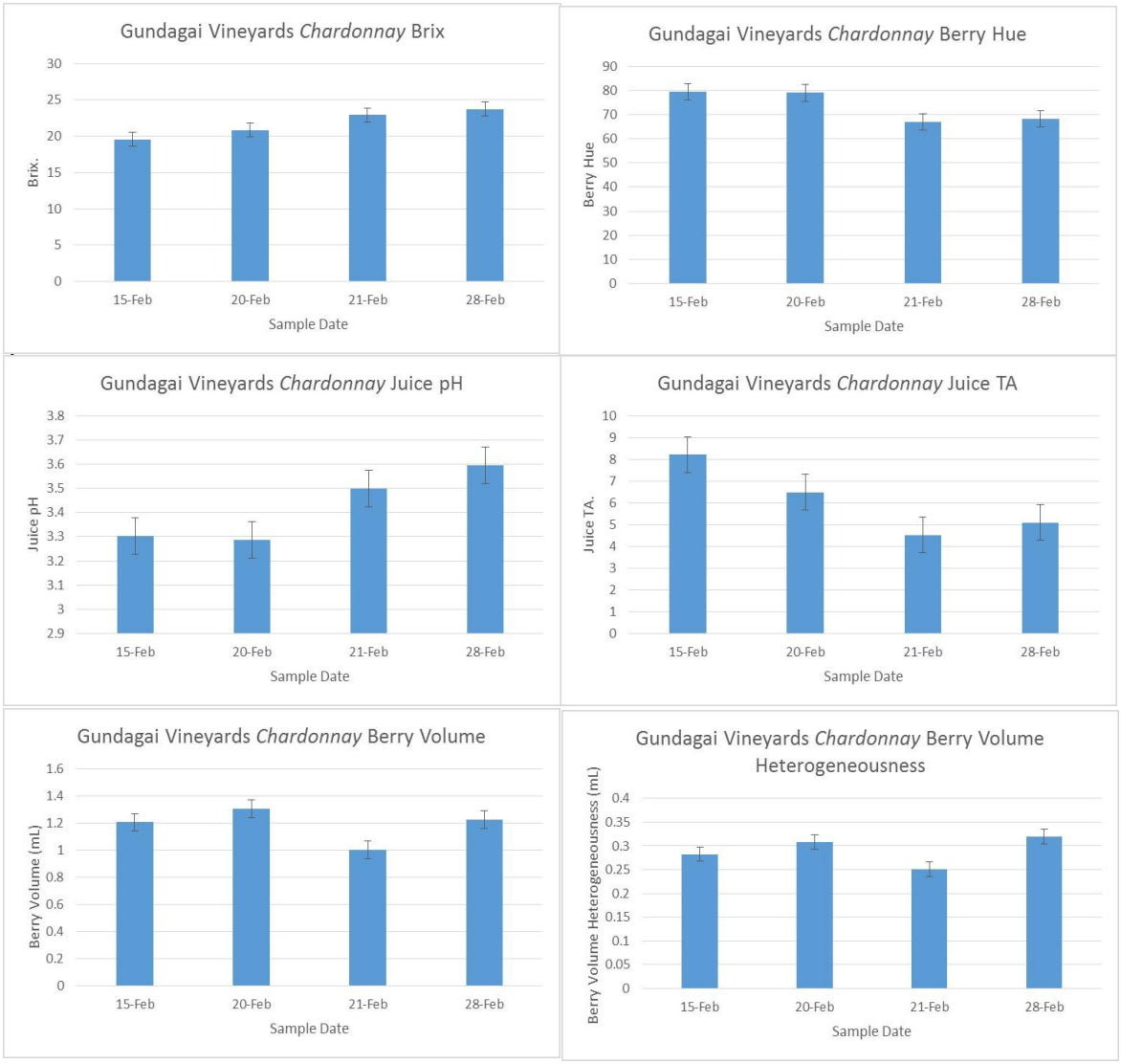


Figure 47: Chardonnay grape berry maturation data for the Gundagai vineyard - Vintage 2017. Samples from 15 and 20 February are from early maturation blocks; 21 and 28 February samples from mature blocks.

Table 6: Chardonnay grape analysis at harvest and finished wine data.

	Cumulus Vineyard		Gundagai Vineyard	
	Grape analysis at harvest			
	Harvest 1	Harvest 2[†]	Early	Mature
pH	3.31 ± 0.07		3.5 ± 0.06	3.6 ± 0.07
Titratable Acidity	6.24 ± 0.60		4.52 ± 0.29	5.1 ± 0.53
Brix	21.5 ± 0.9		22.9 ± 0.3	23.7 ± 1.3
	Finished Wine Analysis			
pH	3.28		3.3	3.27
Titratable Acidity	5.4		6.0	6.5
Free SO_2 (mg/L)	32		31	34

Total SO_2 (mg/L)	105	102	174
Molecular SO_2 (mg/L)	1.03	0.95	1.11
Alcohol (%v/v)	13.3	12.1	14.3
Acetic acid (g/L)	0.12	0.12	0.27
Residual sugar (g/L)	0.86	0.68	1.46
L-malic acid (g/L)	1.70	2.82	2.52

† Harvest 2 was not conducted due to excessive powdery mildew incidence.

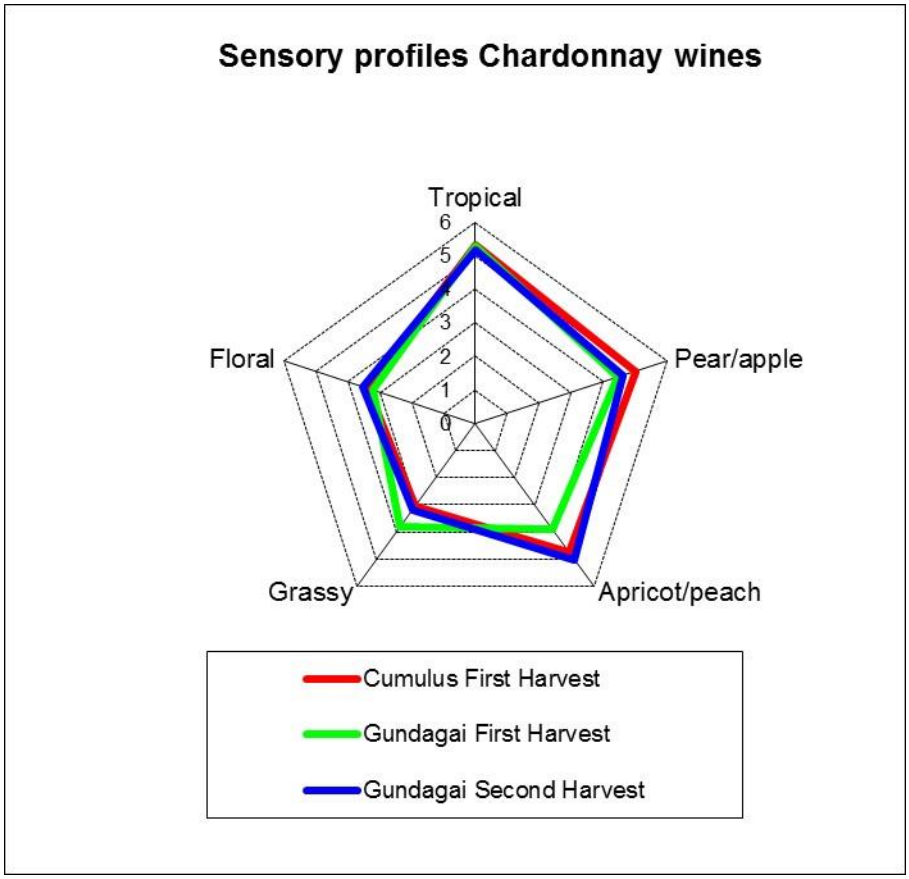


Figure 48: Sensory descriptive ratings for Chardonnay wines - Vintage 2017.

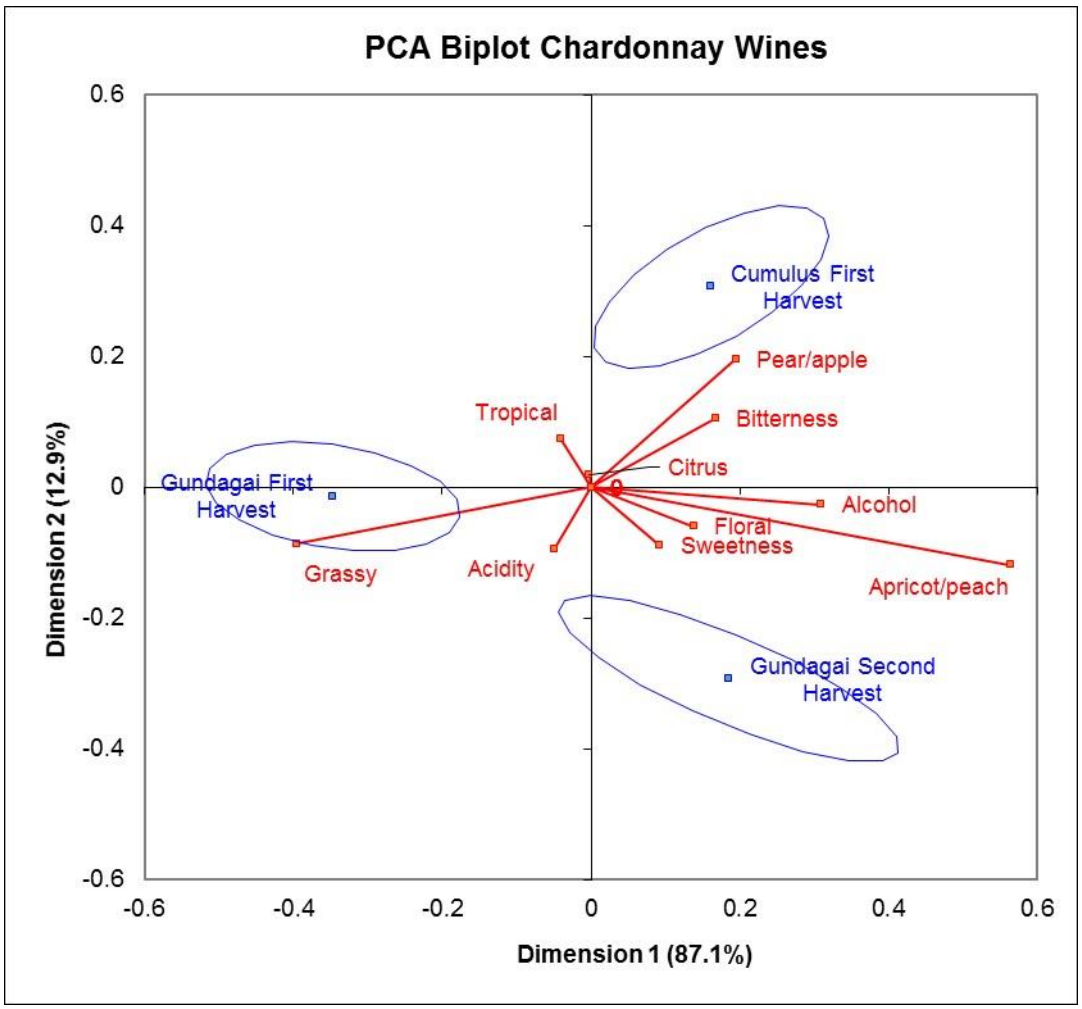


Figure 49: Principal Component Analysis biplot of sensory descriptive ratings for Chardonnay wines.

Table 7: Sensory descriptive analysis mean ratings for Chardonnay wines. Letters in each row indicate significant differences between wines.

	Cumulus First Harvest		Gundagai First Harvest		Gundagai Second Harvest	
Tropical	5.3	a	5.3	a	5.2	a
Pear/apple	5.0	a	4.5	a	4.6	a
Apricot/peach	4.7	a	3.9	b	5.0	a
Grassy	3.1	a	3.8	a	3.2	a
Floral	3.4	a	3.2	a	3.5	a
Citrus	4.1	a	4.1	a	4.0	a

Sweetness	3.7	a	3.6	a	3.9	a
Acidity	3.9	a	4.0	a	4.0	a
Bitterness	4.2	a	3.8	a	4.0	a
Alcohol	4.9	a	4.5	a	5.0	a

Sauvignon Blanc wines - Vintage 2017

Grape maturity data for the Cumulus and See Saw vineyards are presented in Figure 50 and Figure 51 respectively. Overall trends for berry maturity parameters are broadly consistent between vineyards: For the Cumulus vineyard an increasing berry Brix is accompanied by increased mean berry hue; diminished titratable acidity and higher pH. Sauvignon Blanc grape berry volume does not show any consistent trends during the sampling times for the two vineyard locations; berry volume is rising in the Cumulus vineyard, but the reverse appears at See Saw. It is noted that a large variance associated with berry volume during the sampling period is evident from both vineyard locations. These observations may be explained by site selection of the See Saw blocks rather than the continuous sampling approach of a single block used for monitoring the Cumulus vineyard.

Grape analysis at harvest and finished wine analysis for the Sauvignon Blanc wines are presented in Table 8. Of interest is the similarity of Brix measurements for Harvest 1 (Cumulus) and Early & Mature Harvests from See Saw. Consecutive harvests from See Saw were not possible to arrange due to commercial decisions for harvesting and consequently grapes representing a 'mature' stage of ripening were obtained from an alternative block, thereby providing an 'early' and 'mature' profile as advised by the vineyard proprietor.

Sensory descriptive analysis of the resulting wines is presented in Figure 52, a PCA biplot of the mean sensory ratings in Figure 53 and Table 9 presents the mean sensory ratings. A clear and significant change in the sensory descriptions of the Sauvignon Blanc wines is evident as grapes ripen from 'early' to 'mature'. Sensory attributes of 'grassy' and 'pear/apple' diminish while 'tropical', 'floral' and 'apricot/peach' increase with maturity. The PCA biplot of the wine sensory attributes shows very clear separation along PC1 for grape maturity level at harvest. Wines from both vineyard 'mature' harvests are projected into the right side of the PCA along with the 'floral', 'tropical', 'apricot/peach', 'alcohol' and 'sweetness' attributes. The proximity of alcohol with sweetness is expected as higher ethanol concentrations are often perceived as a contributing factor to increased mouthfeel and sweet sensations. The earlier harvested grapes resulted in wines perceived as grassy, high in pear/apple and with higher levels of acidity.

Overall the of changes in grape berry colour appear to be well correlated with the changes in the sensory features of the Sauvignon Blanc wines. The association between berry colour changes and resulting wine sensory features are more readily apparent when the vineyard block is continuously monitored during the growing season, rather than discrete measures at and immediately prior to grape harvest. These observations support the requirement for reliable, rapid, simple to implement measures of berry colour that are linked to temporal and spatial data management systems.

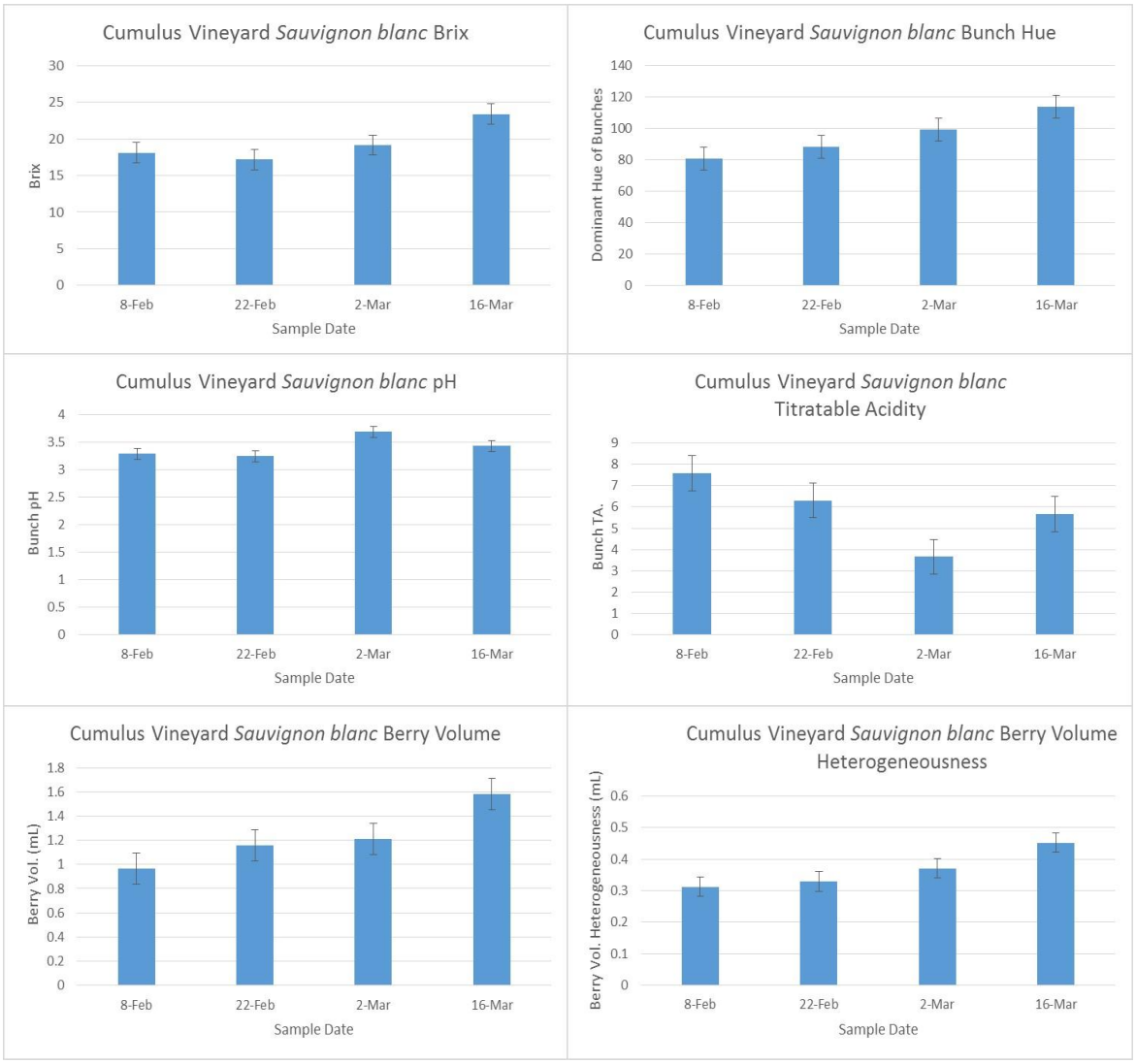


Figure 50: Cumulus vineyards Sauvignon Blanc maturity data - Vintage 2017.

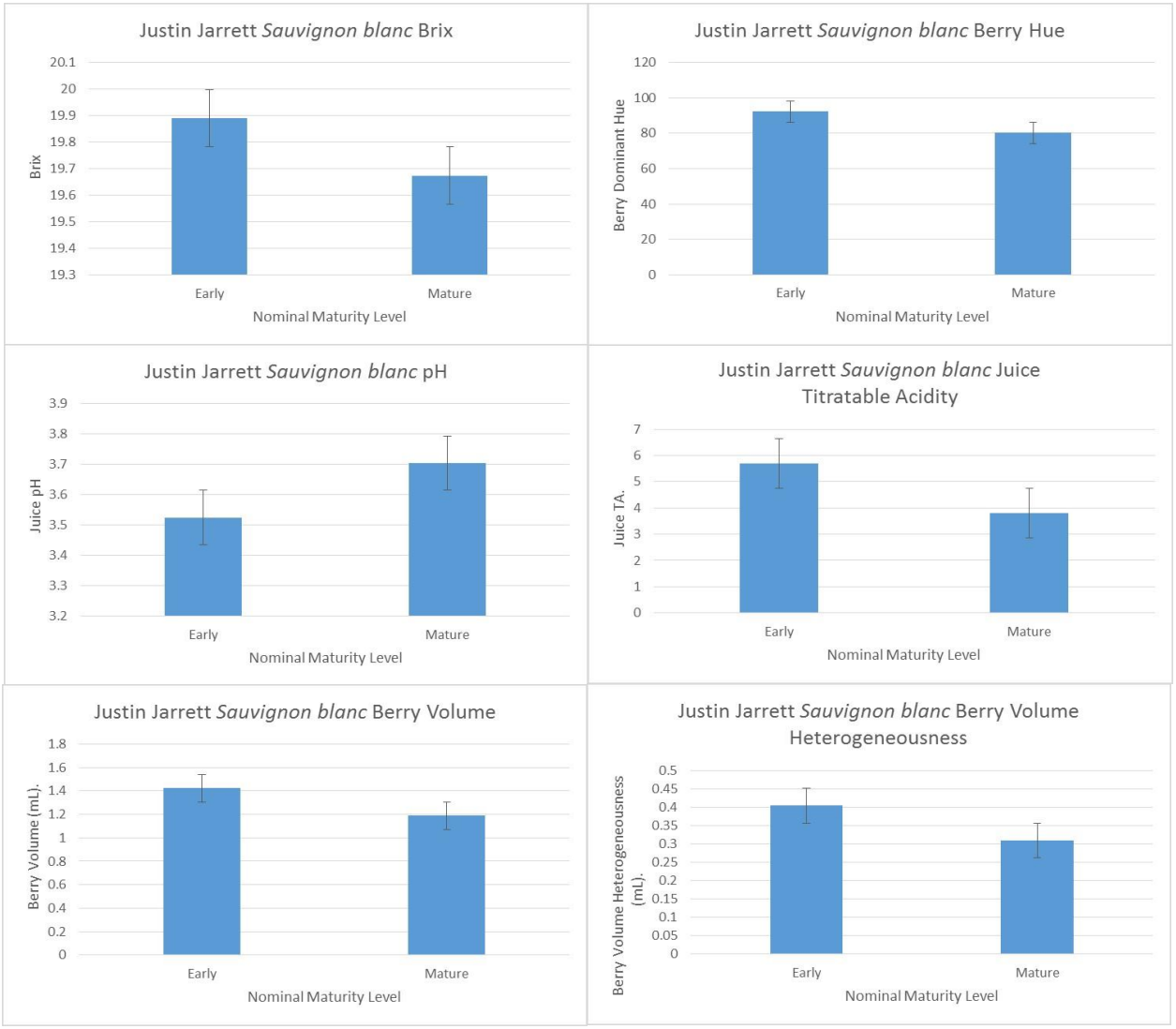


Figure 51: See Saw vineyards Sauvignon Blanc maturity data - Vintage 2017.

Table 8: Sauvignon Blanc grape analysis at harvest and finished wine data.

	Cumulus Vineyard		See Saw Vineyard	
	Grape analysis at Harvest			
	Harvest 1	Harvest 2	Early	Mature
pH	3.69 ± 0.09	3.44 ± 0.05	3.53 ± 0.1	3.70 ± 0.07
Titratable Acidity	3.66 ± 0.31	5.66 ± 0.89	5.70 ± 0.72	3.81 ± 0.17
Brix	19.1 ± 2.4	23.4 ± 0.9	19.9 ± 1.8	19.7 ± 1.3
	Finished Wine Analysis			
pH	3.00	3.11	2.92	3.23
Titratable Acidity	6.2	7.0	7.5	5.0
Free SO_2 (mg/L)	24	24	22	30
Total SO_2 (mg/L)	104	111	88	123

Molecular SO_2 (mg/L)	1.42	1.12	1.55	1.07
Alcohol (%v/v)	11.5	14.3	11.1	12.1
Acetic acid (g/L)	0.16	0.37	0.08	0.10
Residual sugar (g/L)	0.41	0.23	0.29	0.08
L-malic acid (g/L)	1.2	1.95	1.84	1.16

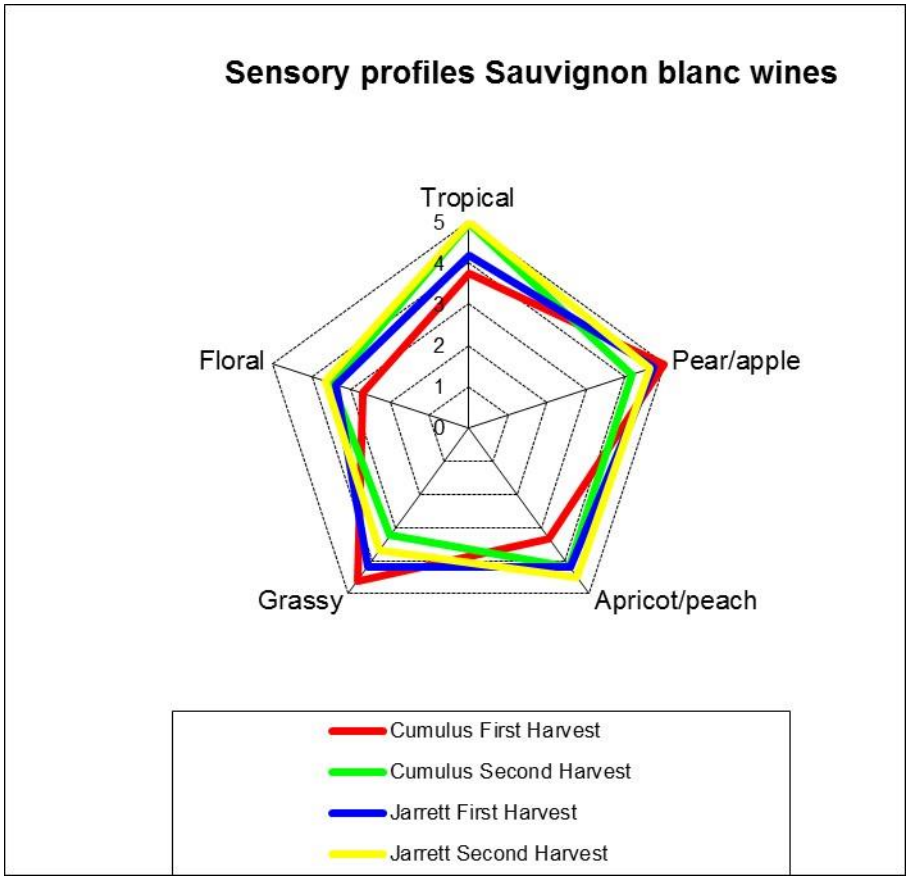


Figure 52: Descriptive sensory analysis of Sauvignon Blanc wines harvested at early and mature levels of grape maturation at two vineyards - Vintage 2017.

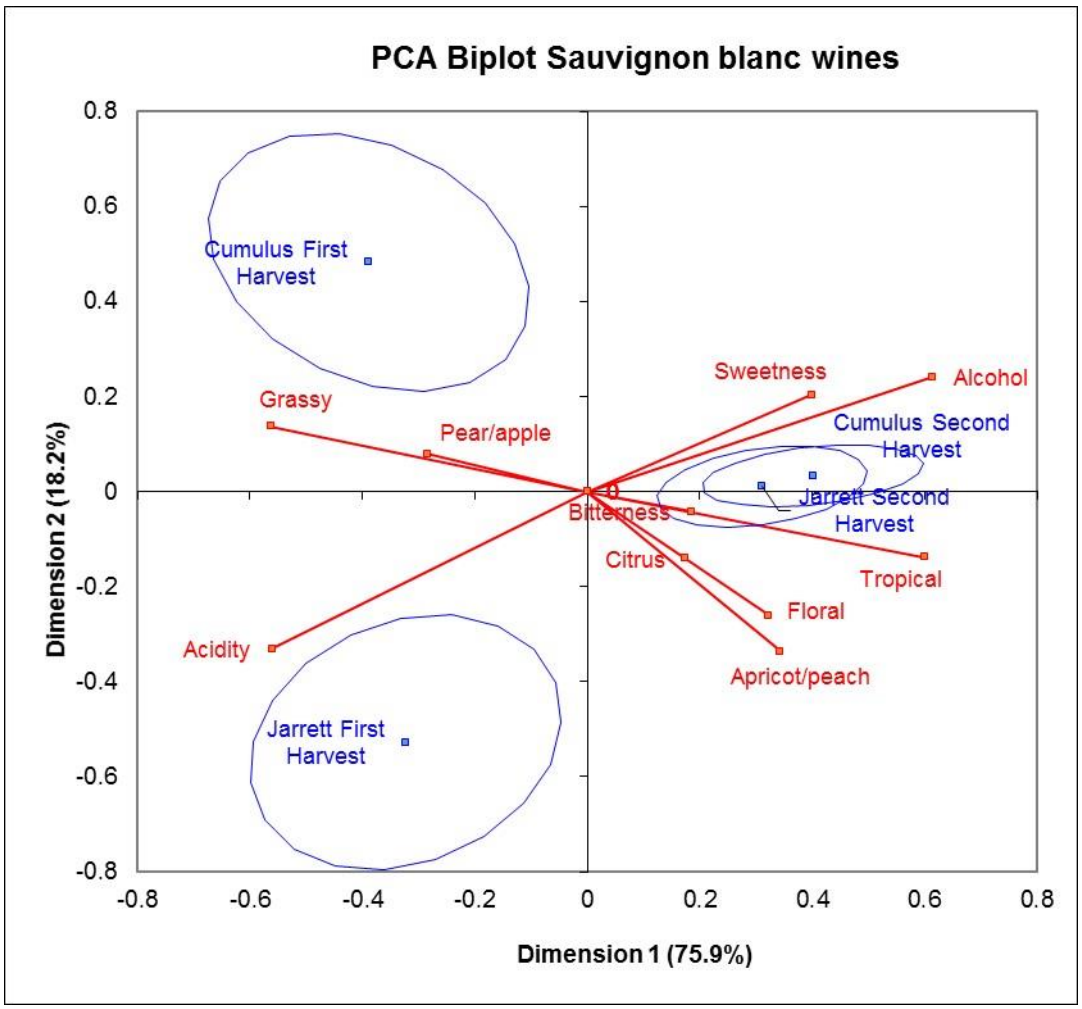


Figure 53: Principal Component Analysis biplot of sensory descriptive ratings for Sauvignon Blanc wines.

Table 9: Mean sensory ratings for Sauvignon Blanc wines. Different letters infer a significant difference.

	Cumulus First Harvest		Cumulus Second Harvest		See Saw First Harvest		See Saw Second Harvest	
Tropical	3.7	b	5.0	a	4.2	ab	5.0	a
Pear/apple	5.0	a	4.2	b	4.7	ab	4.7	ab
Apricot/peach	3.3	b	4.2	ab	4.2	ab	4.5	a
Grassy	4.6	a	3.2	b	4.2	ab	3.7	ab
Floral	2.7	b	3.5	ab	3.4	ab	3.7	a

Citrus	3.8	b	4.4	a	4.2	ab	4.1	ab
Sweetness	2.5	ab	2.9	a	2.1	b	3.1	a
Acidity	5.4	ab	4.8	b	6.1	a	4.6	b
Bitterness	3.7	a	4.1	a	3.8	a	3.9	a
Alcohol	4.0	bc	5.0	a	3.5	c	4.6	ab

Shiraz wines - Vintage 2017

Grape maturity data for the Gundagai and Cumulus Shiraz vineyards are presented in Figure 54 and Figure 55 respectively. Rising berry Brix measures are associated with increasing berry pH and decreasing titratable acidity for both vineyards. These results are expected. Of interest is the berry volume measures that indicate a gradual reduction in mean berry volume during the course of berry maturation. A reduction in berry volume is especially noted for the Cumulus vineyard with grapes reducing from a mean volume of 1.45 mL to 1.05 mL between 20 February and the harvest date of 23 March. Such observations represent a reduction in the order of 27% of total berry volume and while berry flavour development must be considered for commercial harvest decisions, this order of berry weight loss represents a significant reduction in crop load across the vineyard. Interestingly, measures of berry volume heterogeneity reduce marginally for the corresponding period. A greater consistency in berry volume at or close to harvest decisions may indicate the potential to develop novel measures of berry ripening based upon volume variance rather than total berry volumes, Brix, pH and titratable acidity.

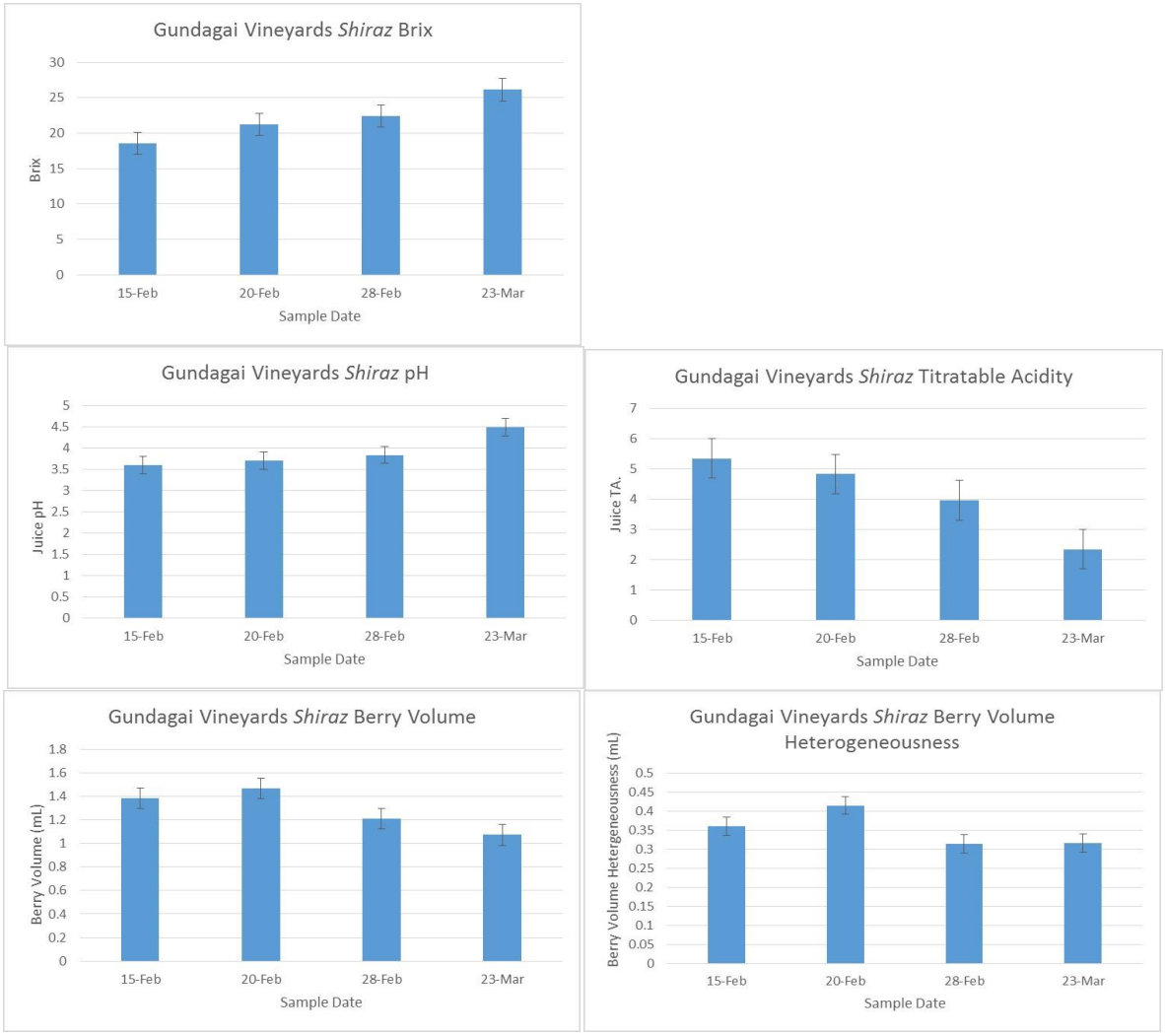


Figure 54: Gundagai vineyard Shiraz grape maturity data - Vintage 2017.

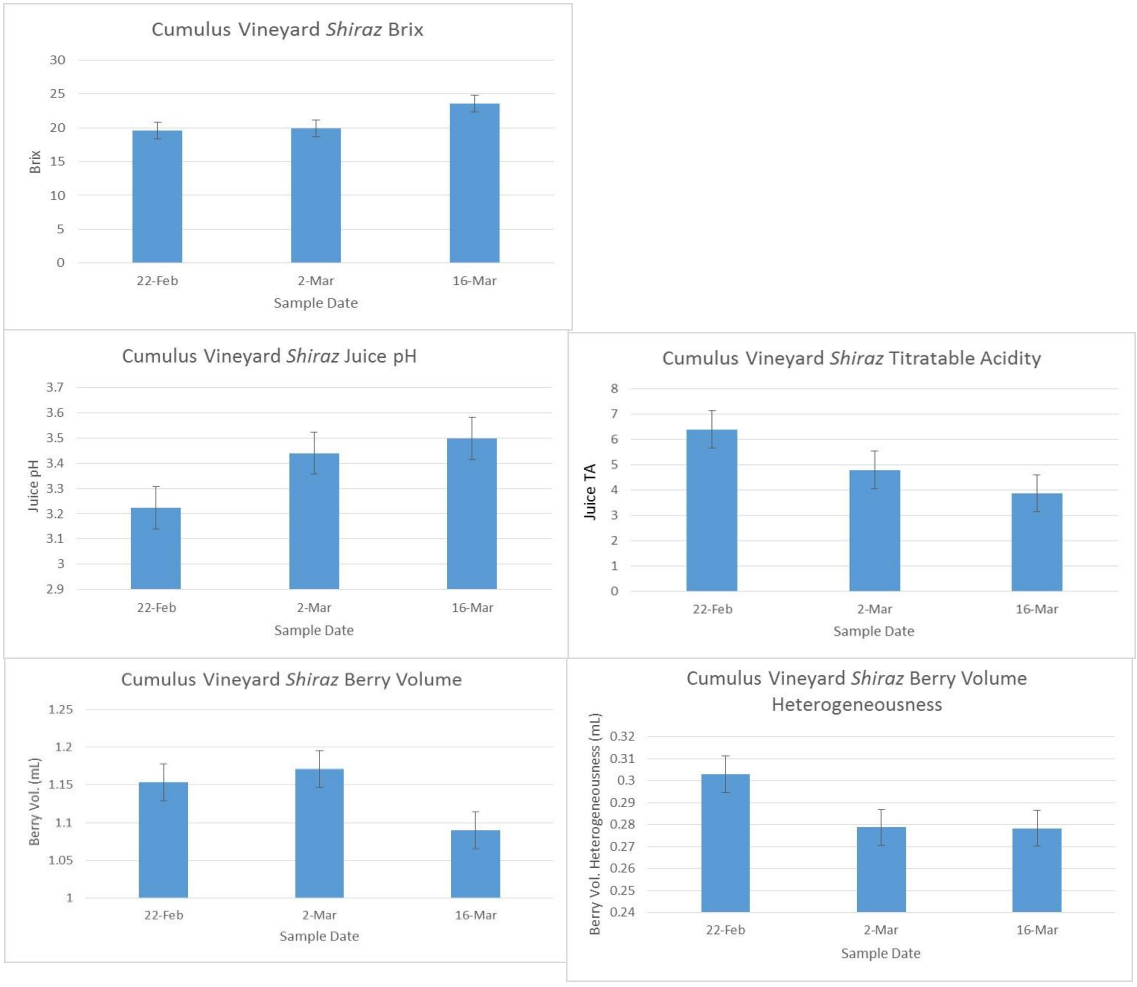


Figure 55: Cumulus Vineyards Shiraz maturity data - Vintage 2017.

9 Outcomes and conclusions

This investigation was undertaken as a proof of concept project to demonstrate the feasibility of using smartphone apps for detection and quantification of grape berry size and colour in real time within vineyards. Considerable progress towards implementation of machine learning algorithms embedded into an Android platform have been accomplished. Linking the outputs of the app to a desktop dashboard within the Excel environment has created a means for spatial and temporal data management and interpretation across growing seasons and vineyard blocks. This aspect of data management is relatively simple in design and is deserving of greater attention but was not the immediate or highest priority of the project.

The Android platform **WineOZ SmartGrape** can be downloaded from the App store:

https://play.google.com/store/apps/details?id=com.nwgic.grapeyield

The dashboard with instructions is available from the NWGIC website:

https://www.csu.edu.au/nwgic/research/wineoz-smartgrape-mobile-application

Significant investigation into image capture parameters and data manipulation for berry detection have been undertaken and results for berry colour estimations are well correlated with an industry standard approach of measurement when images are taken in full sunlight. These results were achieved without colour cast correction in the app and demonstrates a significant achievement for the computing resources of a smartphone, compared to a desktop platform.

The positioning of a reference probe within the bunch allowed a more consistent calibration of depth of field and estimation of berry size, with results expressed in centimetres. This aspect of image analysis requires some refinement as the selected calibration probe proved to be too small for consistent measurements and can be improved by enlargement in size. The reference probe could also incorporate a colour swatch on the surface to enable image colour correction. Berry colour in white grapes could be correlated to wine sensory outcomes when grapes were harvested at two different levels of maturity and demonstrates the value of incorporating measures of berry colour distribution and flux for harvest decision for specific wine styles. Refinement of the app to improve berry size estimations, image analysis and incorporation of vineyard management features such as geofencing, vineyard block and varietal information linked to GPS coordinates is warranted. Such improvements will enable a more informed link to be established between berry colour measures and wine styles. The link between grape berry colour and white wine styles has been established with a limited number of trials within this report and is deserving of a greater level of investigation.

10 Recommendations

Measures of berry composition pertaining to size for red cultivars, and size and colour for white cultivars are important metrics providing information and context about vineyard management, irrigation, water availability, evapotranspiration losses, berry maturation and potential resulting wine styles. Development of in-field devices that facilitate the collation and curation of these data will become important decision support tools for vineyard managers. The goal of this project was to demonstrate a proof of concept smartphone app for berry measures. Improvements to the app can be easily achieved with a carefully selected larger reference probe incorporating colour correction swatches, guidance for image collection and berry detection algorithm improvements. Data curation within an Excel dashboard can be extended to a whole

of vineyard plan and incorporation of improved vineyard and block definitions linked to GPS coordinates will simplify the user experience. These aspects of the user interface will be incorporated into the next generation of smartphone app for release to vineyard managers.

11 Appendices

Appendix 1: Communications

11.1 Publications in international peer review journals:

Šuklje, K., Zhang, X., Antalick, G., Clark, A., Deloire, A.; Schmidtke, L. M. (2016). Berry shriveling significantly alters Shiraz (vitis vinifera L.) grape and wine chemical composition. *J. Agric Food Chem. 64*, 870–880.

11.2 Book Chapters (Conference Proceedings):

Ang, L.-M., K.P. Seng, A. Oczkowski, A. Deloire, and L.M. Schmidtke Development of a smartphone app for berry quality assessment. In Proceedings of the Oenoviti 7th International Symposium. P.-L. Teissedre and L. Martinez (eds.), pp. 79-85. Oenoviti International Network.

11.3 Oral communications at conferences:

Ang, L.-M., K.P. Seng, A. Oczkowski, A. Deloire, and L.M. Schmidtke Development of a smartphone app for berry quality assessment. In Proceedings of the Oenoviti 7th International Symposium. P.-L. Teissedre and L. Martinez (eds.), pp. 79-85. Oenoviti International Network.

11.4 Reports for the industry

N/A

11.5 Oral communications for the industry

Beta app version release and feedback with Vineyard growers in Orange, Drs Schmidtke, Ang, Pailthorpe and Lu, February 2017.

11.6 Posters:

Kraeva-Deloire, E, Deloire, A., and Schmidtke, L. M. 2016. Berry heterogeneity, spatial distribution and maturation within single bunches (cv. Shiraz). Australian Wine Industry Technical Conference, Adelaide, 24-28 July 2016.

Pailthorpe, B., Kraeva-Deloire, E., Bordes, N., Šuklje, K., Schmidtke, L. & Deloire, A. 2016. Smartphone imaging tool to assess grapevine berry and bunch characteristics. Australian Wine Industry Technical Conference, Adelaide, 24-28 July 2016.

Berry heterogeneity, spatial distribution and maturation within single bunches (CV. Shiraz)

Elena KRAEVA-DELOIRE[a], Alain DELOIRE[a], Leigh M. SCHMIDTKE[a,b]

[a] National Wine and Grape Industry Centre, Charles Sturt University, Locked Bag 588, Wagga Wagga, NSW 2678, Australia.
[b] School of Agricultural and Wine Sciences, Charles Sturt University, Locked Bag 588, Wagga Wagga, NSW 2678, Australia.



Karl Briullov. The Italian midday. 1827.

Introduction

Berry growth and morphology are characterised by asynchrony between berries within a single bunch posing an important research question with potential practical implications for vineyard management and wine making processes. The goal of this study is to assess the spatial and temporal differences in individual fruit from single bunches at two developmental stages: veraison and mid ripening (CV Shiraz, *Vitis Vinifera* L.). Wide ranging research has been reported during the last few years on berry size and sugar content, berry position and maturity, resource competition between berries during their development, the effect of bunch heterogeneity on wine composition, etc. [1,2,3,4,5,6]. But still, this topic remains as a matter of debate.

Materials and Methods

The study was done in Griffith and Orange regions NSW, Australia; very different in climate and cultural practices.

Mechanical pruning
Number of shoots: 92
Double cordon, open sprawling canopy
Yield/vine 18.6 kg
Flowering conditions: From the 15th of Oct to the 1st of Nov
Temperature min ave 10.9 °C
Temperature max ave 30.3 °C
Rain 0 mm



Griffith

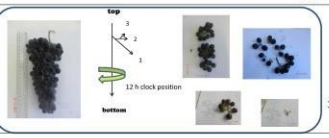


Orange



Manual pruning
Number of shoots: 21
Double cordon, VSP
Yield/vine 4.3 kg
Flowering conditions: From the 15th of Nov to the 1st of Dec
Temperature min ave 12.1 °C
Temperature max ave 28.3 °C
Rain 14.6 mm

607 berries from 4 different bunches sampled at veraison and mid ripening harvest were analysed. Each single berry was removed from the stem according to the position on the rachis including ramification. Clock wise position corresponds to the exposed and shadowed sides.



Twenty parameters, for each single berry were measured and calculated.

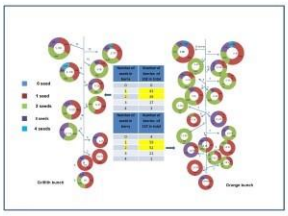
11533 values in total...



- Number-Position
- Fresh mass berry, seeds, pericarp
- Dry mass berry, seeds, pericarp
- Seed content and seed weight
- Colour
- Total Soluble solids (Brix),sugar concentration per g of berry
- Water concentration
- Seed/berry ratio (SB) [7]
- Others

Results

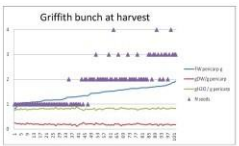
A " map" of spatial distribution of the berries on the primary side branches within the bunch at harvest.

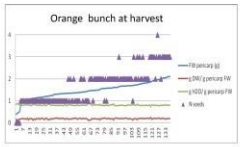


The arrows show the rachis and small branches with the number of berries on each. Circles are the groups of berries on each side branch regarding the number on the rachis and a clock position. The colours correspond to percentage of one, two, three and four seeded berries in the group.

The majority of berries have one and two seeds randomly situated within the bunch. There is no gradient or apparent continuity in distribution. We didn't find any influence of berry position on the physiological parameters studied.

How different are the berries within the bunch?



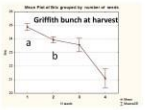


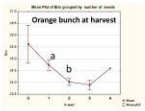
	Ave of 10% lowest FW (g) pericarp	Ave of 10% highest FW (g) pericarp	Difference %
FW pericarp g	1.0	1.8	+80
DWg (C) / pericarp FW g	0.212	0.174	-17.9
H2O %	79%	83%	+5.01
Brix	26.3	23.4	-11
Seed content N	1	2.9	+190

	Ave of 10% lowest FW(g) pericarp	Ave of 10% highest FW(g) pericarp	Difference %
FW pericarp g	1.02	2.03	+99
DWg (C) per g pericarp FW	0.180	0.199	+10.5
H2O %	82.1%	80.2%	-2.3
Brix	25.9	23.9	-7.7
Seed content N	1	3	+200

The berries of each bunch were classified from the lowest to highest pericarp fresh mass. We found that the difference of almost 100% in fresh mass is correlated with a seed content but not with a water or carbon (dry weight) concentration.

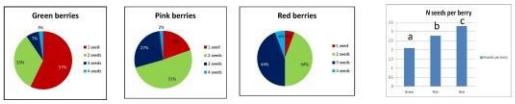
Seed content and sugar (Brix, g sugar per berry, g sugar per g pericarp)





A significant difference in sugar concentration was up to 0.7 Brix = 7 g/L (0.3-0.4 % alc) between one and two seeded berries, which were the major classes within the bunch.

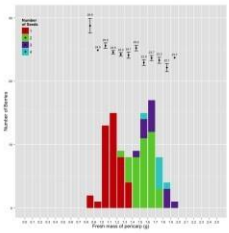
Seed content and berry colour at Veraison. Orange bunch. The most ripe berries had the highest seed content.



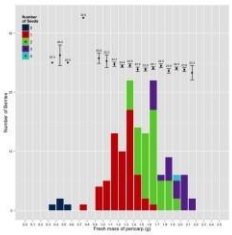
Seed content was well correlated with berry colour and could play a major role in the timing of ripening. The majority of berries with one seed were green, two seeded berries were pink or red, three and four seeded berries were mostly red. This may be the result of seeds triggering the earlier onset of veraison, however this needs to be confirmed.

Heterogeneity of berry pericarp fresh mass within single bunch.

Griffith bunch at harvest

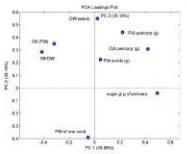


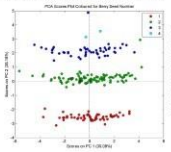
Orange bunch at harvest



The histograms show the berry distribution per class within the bunch and how the seed content changes from small to large berries. Colour corresponds to the number of one, two, three and four seeded berries within each class. This could be interesting and useful for grouping and sampling strategies. For example, two major classes within the same cluster are very different in Brix and seed content, which can have an important consequences for final wine style.

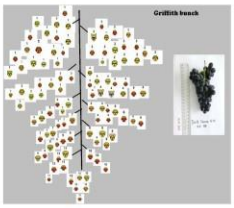
Principal component analysis.





PCA was conducted on berry composition. We found that the seeds could play an important role for other berry characteristics. These plots shows well defined sample clusters for each group of berries with a different seed content.

Conclusion



Single bunch represented with Cheroff faces. Each face is one single berry. Each face characteristic corresponds to one of the berry parameters. Face color is an average of sets of variables.

Results showed that berry position within bunches and branches did not influence the targeted physiological parameters. Strong interrelationship between berry seed number and sugar concentration, fresh and dry mass of the pericarp were found. The study showed a correlation between the number of seeds per berry and skin colour at veraison, suggesting an important role of seeds in the timing of ripening. We hypothesize that berry seed number influences berry size by alteration of cell number in the pericarp at early stage of berry development. Flowering and early berry development stages could be partly responsible for bunch heterogeneity and this is discussed in the light of our original results.

[1]. Matthews M and Nuzzo V. (2007) Acta Hort. 415-435. [2]. Ferrer M. et al., (2014) S. Afr. J. Enol Vitic, vol 35, No 1, 101-113.[3]. Dai ZW et al., (2009). Journal of Agricultural and Food Chemistry. [4]. Friend et al., (2009) Australian Journal of Grape and Wine research 15, 168-174 [5]. Torchio et al., (2014) S. Afr J. Enol Vitic,Vol 35, No 1. [6].Friend et al., (2016) Australian Journal of Grape and Wine research [7]. Gouthu S and Deluc L (2015). BMC Plant Biology 15:46.

This project was partly funded by NWGIC and the Australian Grape and Wine Authority, with matching funding from the Australian federal Government.

Smartphone imaging tool to assess grapevine berry and bunch characteristics

B. PAILTHORPE[1], E. KRAEVA-DELOIRE[2], N. BORDES[1], K. SUKLJE[2], L. SCHMIDTKE[3], A. DELOIRE[2]

[1] CM3, Charles Sturt University, Panoram Avenue, Bathurst, NSW 2795, Australia.
[2] National Wine and Grape Industry Centre, Charles Sturt University, Locked Bag 588, Wagga Wagga, NSW 2678, Australia.
[3] School of Agricultural and Wine Sciences, Charles Sturt University, Locked Bag 588, Wagga Wagga, NSW 2678, Australia,

Introduction

Grape growers are facing challenges optimizing irrigation and harvest dates due to hotter, drier seasons compressing harvests.
Knowing quantitatively in the vineyard:

- Berry volume and homogeneity,
- Berry dehydration (yield loss),
- Bunch and vineyard homogeneity, and
- White grape berry skin colour to decide on optimal harvest window,

will help growers and winemakers to make better decisions

We are developing a smartphone based imaging tool that will help growers to make decisions related to irrigation and harvest in real-time.

Materials and Methods

The study was done in Orange at the Cumulus and See Saw (JJ) vineyards.
The grapes studied were chardonnay and Sauvignon Blanc.
Six grape bunches were tagged and photographed over a period of four weeks to follow berry size and colour.
At each visit, three grape bunches were photographed and then cut from the vine to be analysed. The size and weight of the berries were measured; the berry skin colour was determined using the Dyostem imaging device (vivelys.fr).

Image analysis was done using the Matlab image processing toolbox. A prototype smartphone app was also developed.

Results

Image Analysis: Automatic Detection of Berries



Fig. 1: chardonnay berries detected using Matlab imfindcircle algorithm.

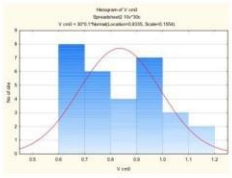


Fig. 2 a: volume distribution measured for a chardonnay grape.

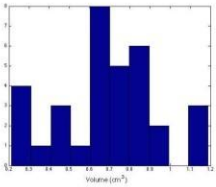


Fig. 2 b: volume distribution calculated by the algorithm for the same grape.

The volume distribution shows two peaks near 0.65 and 0.8-0.9 cm^3 for both the measured and calculated berry volumes.
So far we are only sampling about 60% the berries presented at the bunch surface.

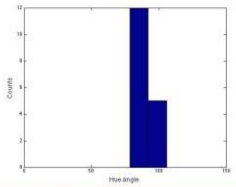


Fig. 2 c: hue tint angle distribution calculated for the chardonnay grape.

The tint angle is in the 90-100 range suggesting that the grape are not ripe. The Dyostem measured tint angle was 82-100.

Colour Calibration



Fig. 4 a



Fig. 4 b



Fig. 4 c

Fig. 4 a: photograph of grape taken in the vineyards
Fig. 4 b: colour-balanced photograph using the colour checker card.
Fig. 4 c: colour-balanced photograph ready for analysis.

Light incidence, time of the day, lighting conditions introduce a colour cast to digital photographs. In order to be able to measure the colour of the berries precisely, this colour cast must be eliminated. This is done by using a calibrated colour card.
A picture of the colour card is taken under the same lighting conditions as the grape. Colour correction can then be done based on the known RGB values of the colour card. Squares on the card can be used to calibrate distance.



Fig. 5: prototype app running on android phone.

Future Work

- Testing of compact codes for Android phones.
- Generation of calibration procedures to accommodate varying light intensities, illumination conditions, background colours and viewing angles, to ensure colour accuracy;
- Accuracy of image analysis, by comparison with lab analysis of grape samples;
- Use of machine learning (ie. statistical techniques) to correct for varying conditions, measurement bias;
- User experiences with the system, to ensure simple and robust operation.

Acknowledgments
We would like to thank Marty Gransden from Cumulus Wine and Justin Jarrett from See Saw for giving us access to the vineyards.
This project was funded by the Australian Grape and Wine Authority with matching funding from NWGIC and CM3 at CSU.

Appendix 2: Intellectual property

The compiled version of the smartphone app is released to growers. Intellectual property pertaining to the smartphone app source code remains within the NWGIC on behalf of the funding body in accordance with the project contract.

Appendix 3: References

Afik, E. (2015). Ridge Ring Detector. Scientific Reports, 5, 1-9.

Akinlar, C., & Topal, C. (2013). EDCircles: A Real-time Circle Detector with a False Detection Control. Pattern Recognition, 46, 725-740.

Antalick, G., Šuklje, K., Blackman, J. W., Meeks, C., Deloire, A., & Schmidtke, L. M. (2015). Influence of Grape Composition on Red Wine Ester Profile: Comparison between Cabernet Sauvignon and Shiraz Cultivars from Australian Warm Climate. Journal of Agricultural and Food Chemistry, 63(18), 4664-4672. doi: 10.1021/acs.jafc.5b00966.

Aquino, A., Millan, B., Gaston, D., Diago, M.-P., & Tardaguila, J. (2015). vitisFlower(®): Development and Testing of a Novel Android-Smartphone Application for Assessing the Number of Grapevine Flowers per Inflorescence Using Artificial Vision Techniques. Sensors (Basel, Switzerland), 15(9), 21204-21218. doi: 10.3390/s150921204.

Aquino, A., Diago, Maria P., Millan, Borja & Aguila, Javier Tard (2017). A new methodology for estimating the grapevine berry number per cluster using image analysis. Biosystems Engineering, 156, 80-95.

Battany, M. (2008). A Practical Method for Counting Berries based on Image Analysis. 2nd Annual National Viticulture Research Conference, University of California, Davis, USA, 4-5, July 9-11.

Benkwitz, F., Nicolau, L., Lund, C., Beresford, M., Wohlers, M., & Kilmartin, P. A. (2012). Evaluation of Key Odorants in Sauvignon Blanc Wines Using Three Different Methodologies. Journal of Agricultural and Food Chemistry, 60(25), 6293-6302. doi: 10.1021/jf300914n.

Bindon, K., Varela, C., Kennedy, J., Holt, H., & Herderich, M. (2013). Relationships between harvest time and wine composition in Vitis vinifera L. cv. Cabernet Sauvignon 1. Grape and wine chemistry. Food Chemistry, 138(2-3), 1696-1705. doi: 10.1016/j.foodchem.2012.09.146.

Birchmore, W., Scott, E., Zanker, T., Emmett, B., & Wade, P. (2015). Smart-phone app field assessment of powdery mildew. Australian and New Zealand Grapegrower and Winemaker, 622(Nov), 46-47.

Blackman, J., and A. Saliba (2009). Sensory characterization of Hunter Valley Semillon using descriptive analysis. Flavour and Fragrance Journal 24:238-244.

Brittany K. & Michelle M. (2017). Vineyard Yield Estimation, Washington State University, http://cru.cahe.wsu.edu/CEPublications/EM086E/EM086E.pdf. Accessed August 3, 2017.

Calderon-Orellana, A., Matthews, M. A., Drayton, W. M., & Shackel, K. A. (2014). Uniformity of Ripeness and Size in Cabernet Sauvignon Berries from Vineyards with Contrasting Crop Price. American Journal of Enology and Viticulture, 65(1), 81-88. doi: 10.5344/ajev.2013.13084.

Casser, V. (2016). Using Feedforward Neural Networks for Color Based Grape Detection in Field Images. http://cscubs.cs.uni-bonn.de/2016/proceedings/paper-02.pdf. Accessed August 3, 2017.

Chamelat, R., Rosso, E., Choksuriwong, A., Rosenberger, C., Laurent, H., Bro, P. (2006). Grape Detection by Image Processing. Proceedings of IEEE 32nd Annual Conference on Industrial Electronics (IECON 2006), Paris, France. 3697–3702.

Coombe, B.G.; McCarthy, M.G. (2000). Dynamics of grape berry growth and physiology of ripening. Aust. J. Grape Wine Res., 6, pp. 131–135.

Crupi, P., Coletta, A., & Antonacci, D. (2010). Analysis of Carotenoids in Grapes to Predict

Norisoprenoid Varietal Aroma of Wines from Apulia. Journal of Agricultural and Food Chemistry, 58(17), 9647-9656. doi: 10.1021/jf100564v.

De Bei, R., Fuentes, S., Gilliham, M., Tyerman, S., Edwards, E., Bianchini, N., et al. (2016). VitiCanopy: A Free Computer App to Estimate Canopy Vigor and Porosity for Grapevine. Sensors, 16(4), 585.

Deloire, A. (2013). New method to determine optimal ripeness for white wine styles. Practical Winery and Vineyard Journal, Winter, 1-4.

Deloire, A. (2014). Physiological Indicators to Predict Harvest Date and Wine Style. Paper presented at the 15th Australian Wine Industry Technical Conference, Sydney.

Diiago, Mario-Paz, Crhistian Correa, Boria Millan, Pilar. B, Constantino V., Javier T. (2012). Grapevine yield and leaf area estimation using supervised classification methodology in RBG images taken under field conditions, Sensors, 12(12), 16988-17006.

Dunn, G. M., & Martin, S. R. (2004). Yield prediction from digital image analysis: a technique with potential for vineyard assessments prior to harvest. Australian Journal of Grape and Wine Research, 10, 196-198.

Drumm, J., White, N., Sweigers, M., & Davey, M. (2017). Smart everything, everywhere Mobile Consumer Survey 2017 The Australian cut. Sydney, Australia: Deolitte Touche Tohmatsu Limited.

Etchebarne, F., Ojeda, H., & Hunter, J. J. (2010). Leaf:Fruit Ratio and Vine Water Status Effects on Grenache Noir (Vitis vinifera L.) Berry Composition: Water, Sugar, Organic Acids and Cations. [Article]. South African Journal of Enology and Viticulture, 31(2), 106-115.

Farias, C. Correa, C. Valero Ubierna, and P. Barreiro Elorza (2012). Characterization of vineyard's canopy through fuzzy clustering and svm over color images. 3rd CIGR Int. Conf. of Agricultural Engineering (CIGR-AgEng2012).

Font, D., Tresanchez, M., Martínez, D., Moreno, J., Clotet, E., & Palacín, J. (2015). Vineyard Yield Estimation Based on the Analysis of High Resolution Images Obtained with Artificial Illumination at Night. Sensors, 15(4), 8284-8301.

Greer, D. H., Rogiers, S. Y., & Steel, C. C. (2006). Susceptibility of Chardonnay grapes to sunburn. Vitis, 46(3), 147-148.

Hill, G. N., Evans, K. J., Beresford, R. M., & Dambergs, R. G. (2014). Comparison of methods for the quantification of botrytis bunch rot in white wine grapes. Australian Journal of Grape and Wine Research, 20(3), 432-441. doi: doi:10.1111/ajgw.12101.

Illand et al (2004) Iland, P., N. Bruer, G. Edwards, S. Weeks, and E. Wilkes (2004). *Chemical analysis of grapes and wine: techniques and concepts*. Patrick Iland Wine Promotions Pty Ltd, Campbelltown.

Kalua, C. M., & Boss, P. K. (2009). Evolution of volatile compounds during the development of cabernet sauvignon grapes (Vitis vinifera L.). Journal of Agricultural and Food Chemistry, 57(9), 3818-3830. doi: 10.1021/jf803471n.

Kicherer, A., Herzog, K., Pflanz, M., Wieland, M., Rüger, P., Kecke, S., et al. (2015). An Automated Field Phenotyping Pipeline for Application in Grapevine Research. Sensors, 15(3), 4823.

Kwasniewski, M. T., Vanden Heuvel, J. E., Pan, B. S., & Sacks, G. L. (2010). Timing of Cluster Light Environment Manipulation during Grape Development Affects C13 Norisoprenoid and Carotenoid Concentrations in Riesling. Journal of Agricultural and Food Chemistry, 58(11), 68416849. doi: 10.1021/jf904555p.

Liu, S., Marden, S., & Whitty, M. (2013). Towards Automated Yield Estimation in Viticulture. Paper presented at the Proceedings of Australasian Conference on Robotics and Automation, Sydney.

Liu, S., S. Marden, & M. Whitty (2013). Towards Automated Yield Estimation in Viticulture. Proceedings of Australasian Conference on Robotics and Automation, 24, UNSW, Sydney, Australia.

Liu, S., M. Whitty, & S. Cossell (2015a). A lightweight method for grape berry counting based on automated 3D bunch reconstruction from a single image. Proceeding of the Workshop on Robotics in Agriculture, Seattle, USA.

Liu S., Whitty M., & Cossell S. (2015b). Automatic grape bunch detection in vineyards for precise yield estimation. In Machine Vision Applications (MVA), 14th IAPR International Conference, May 18, 238-241.

Luo, L., Zou, X., Yang, Z., Li, G., Song, X., & Zhang, C. (2015). Grape image fast segmentation based on improved artificial bee colony and fuzzy clustering. Trans. CSAM, 46, 23-28.

Luo, Lufeng, Yunchao Tang, Xiangjun Zou, Chenglin Wang, Po Zhang, Wenxian Feng (2016). Robust Grape Cluster Detection in a Vineyard by Combining the AdaBoost Framework and Multiple Color Components. Sensors, 16(12), 2098.

Millan, B., Aquino, A., Diago, M. P., & Tardaguila, J. (2017). Image analysis-based modelling for flower number estimation in grapevine. Journal of the Science of Food and Agriculture, 97(3), 784-792. doi: 10.1002/jsfa.7797.

Murillo-Bracamontes E.A., Martínez-Rosas, M.E., Miranda-Velasco, M.M., Martínez-Reyes, H.L., Martínez – Sandoval, J.R., Carvantes-de-Avila, H. (2012). Implementation of Hough transform for fruit image segmentation. Procedia Engineering, 35, 230-239.

Nuske, S., Achar, S., Bates, T., Narasimhan, S., and Singh, S. (2011). Yield Estimation in Vineyards by Visual Grape Detection. IEEE/RSJ Int. Conf. on Intelligent Robots and Systems (IROS), San Francisco, CA, USA, 2352–2358.

Nuske, S., Gupta, K., Narasimhan, S., and Singh, S. (2012)., Modeling and Calibrating Visual Yield Estimates in Vineyards, 8th Int. Conf. on Field and Service Robotics, Miyagi, Japan, 16-19 July, pp.343-355, 2012.

Nuske, S., K. Gupta, S. Narasimhan, S. Singh (2014a). Modeling and calibrating visual yield estimates in vineyards Field and Service Robotics. 343-356, 2014.

Stephen Nuske, Kyle Wilshusen, Supreeth Achar, Luke Yoder, Srinivasa Narasimhan, Sanjiv Singh (2014b). Automated Visual Yield Estimation in Vineyards", Journal of Field Robotics, 837-860.

Ojeda, H., Andary, C., Kraeva, E., Carbonneau, A., & Deloire, A. (2002). Influence of Pre- and Postveraison Water Deficit on Synthesis and Concentration of Skin Phenolic Compounds during Berry Growth of Vitis vinifera cv. Shiraz. American Journal of Enology and Viticulture, 53(4), 261-267.

Pongnumkul, S., Chaovalit, P., & Surasvadi, N. (2015). Applications of Smartphone-Based Sensors in Agriculture: A Systematic Review of Research. Journal of Sensors, 2015, 18. doi: 10.1155/2015/195308.

Rabatel, G., & Guizard, C. (2007). Grape berry calibration by computer vision using elliptical model fitting. 6th European Conference on Precision Agriculture (ECPA 2007), Skiathos, Greece. 581-587.

Ries, M.C., Morais, R., Pereira, C., Soares, S., Valente, A., Baptista, J., Ferreira, J.S.G., and Cruz, J.B. (2011). Automatic Detection of White Grapes Using Image Processing. Soft Computing in Industrial and Environmental Applications, 87, 19-27.

Reis, M.J.C.S., R. Moraisb, E. Peresc, C. Pereirad, O. Contentee, S. Soaresa, A. Valentea, J. Baptistad, P.J.S.G. Ferreiraf, & J. Bulas Cruzd (2012). Automatic detection of bunches of grapes in natural environment from color images. Journal of Applied Logic, 10 (4), 285-290, 2012.

Roe, B., H. Yang, & J. Zhu (2005). Boosted decision trees, a powerful event classifier. Proc. Statistical Problems in Particle Physics, Astrophysics and Cosmology.

Rogiers, S.Y., Coetzee Z.A, Walker R.R., Deloire, A., & Tyerman, S.D. (2017). Potassium in the grape (Vitis vinifera L.) berry: transport and function, Front. Plant Sci, 8(1629).

Rogiers, S. Y., & Holzapfel, B. P. (2015). The plasticity of berry shrivelling in 'Shiraz': A vineyard survey. Vitis, 54(1), 1-8.

Sabbatini, P, I. Dami, & G. S. Howell (2017). Predicting Harvest Yield in Juice and Wine Grape Vineyards (E3186) http://msue.anr.msu.edu/uploads/resources/pdfs/ Predicting_Harvest_Yield _in_Juice_and_Wine_Grape_Vineyards_%28E3186%29.pdf. Accessed August 3, 2017.

Smereka, M., & Dulba, I. (2008). Circular Object Detection using a Modified Hough Transform. International Journal of Applied Mathematics and Computer Science, 18(1), 85–91.

Šuklje, K., Antalick, G., Meeks, C., Blackman, J. W., Deloire, A., & Schmidtke, L. M. (2017). Grapes to wine: the nexus between berry ripening, composition and wine style.

Šuklje, K., Lisjak, K., Baša Česnik, H., Janeš, L., Du Toit, W., Coetzee, Z., et al. (2012). Classification of Grape Berries According to Diameter and Total Soluble Solids to Study the Effect of Light and Temperature on Methoxypyrazine, Glutathione, and Hydroxycinnamate Evolution during Ripening of Sauvignon Blanc (Vitis vinifera L.). Journal of Agricultural and Food Chemistry, 60(37), 9454-9461. doi: 10.1021/jf3020766.

Šuklje, K., Zhang, X., Antalick, G., Clark, A. C., Deloire, A., & Schmidtke, L. M. (2016). Berry Shriveling Significantly Alters Shiraz (Vitis vinifera L.) Grape and Wine Chemical Composition. Journal of Agricultural and Food Chemistry, 64(4), 870-880. doi: 10.1021/acs.jafc.5b05158.

Tardaguila, J., Diago, M.P., Millán, B., Blasco, J., Cubero, S. García-Navarrete, O.L., Aleixos, N. (2012). Automatic estimation of the size and weight of grapevine berries by image analysis. CIGR- AgEng., 2012. http://wcigr.ageng2012.org/images/fotosg/tabla_137_C1735.pdf.

Tomic, O., G. Luciano, A. Nilsen, G. Hyldig, K. Lorensen, and T. Næs (2009). Analysing sensory panel performance in a proficiency test using the PanelCheck software. European Food Research and Technology 230: 497.

Appendix 4: Staff

Prof Alain Deloire
Project Supervisor and Chief Investigator January 2016 to September 2016, Charles Sturt University, National Wine and Grape Industry Centre

Dr Leigh Schmidtke
Investigator, January 2016 to September 2016; Chief Investigator September 2016 to June 2018. Charles Sturt University, National Wine and Grape Industry Centre.

Dr Li-Minn (Ken) Ang
School of Computing and Mathematics and CM3, Charles Sturt University, April 2016 to June 2018.

Dr Nicole Bordes
Business Manager, CM3, Faculty of Business, Justice and Behavioural Studies, Charles Sturt University. January 2016 to June 2018.

Professor Junbin Gao
Investigator Machine Learning, January 2016 to April 2016, School of Computing and Mathematics and CM3, Charles Sturt University.

Dr Elena Kraeva-Deloire
Researcher, January 2016 to September 2016, National Wine and Grape Industry Centre, Charles Sturt University.

Dr Feng Lu
Programmer, National Wine and Grape Industry Centre, January 2016 to July 2017.

Professor Bernard Pailthorpe
Head CM3, Faculty of Business, Justice and Behavioural Studies, Charles Sturt University. January 2016 to June 2018.

Dr Kah Phooi Seng (Jasmine)
School of Computing and Mathematics and CM3, Charles Sturt University, August 2016 to June 2018.

Dr Katja Šuklje
Viticulturist, National Wine and Grape Industry Centre, January 2016 to August 2016.

Mr Alex Oczkowski
Programmer, National Wine and Grape Industry Centre, September 2017 to June 2018.

Appendix 5: MATLAB codes for desktop

Listing of the MATLAB code (mathworks.com) described in Section 5.4 and used for desktop computer analysis. Note that '%' indicates a comment and '%%' indicates a separate computational cell.

```
% Analyse grape pictures:  bap (Aug-2015 - Apr-2018)
% Use circle detection - using marlab's Image Proc toolbox
%   cf Help menu:
http://au.mathworks.com/help/images/examples/detectand-measure-circular-
objects-in-an-image.html
%   Uses Cell mode - to compartmentalise calc. : execute, #1,[2 if
needed?], then 3, etc
% V3  (24/121/15) : Built from tests in GrapePic2.m (Sept'15) wine
grapes ~ more circle-like
% V4  (27/1/16)   : adds extra for Elena K-D (Wagga): info on samples
% V5  (16/6/16)   : use NB's Lightroom indexing of GrapePics %
And add Fenglu's Brightness etc functions
%
% this code:
% 1) imports image from file [typically .jpg]
%    - nb. imfinfo can find facts about image (metadata)
% 2) User crops image tight to grape bunch, to eliminate or reduce
sky/light & leaves
%    2.1) User manipulates imdistline tool on image, to get typical
cicle diam.
%          - yields radius range for imfindcircle code
% 3) ** finds circles (grape berries) in gray pic, via dark & bright
object polarity
%    - need to play with radius range & Sensitivity [~ 0.95-0.98] in
imfindcircle, to min. false finds
%    - typically finds about half the circular objects present
%    - radii in pixels: needs 1cm calibration scale: eg in
ColourChecker square: 0.95cm
%    + lists radii of numbered grape berries
%   3.1 & 3.2) find radius (& vol) distribution & stats, for Bright &
Dark   circles
%   3.3 convert to cm scale:  needs object to measure scale
% 4) mask ea. circle, to get per-berry colours: then hue angle stats &
```

```
distr'n
% 5) ColourChecker card - for colour calibration & 1-cm dist scale % 6)
& White Balance the Image - against B/W squares on ColourChecker card

%% 1. Setup;  specify path to file locations;  read files close
all; clear all
fprintf('\n >> Grape pictures V5: analyse circles, radii, Colour, Hue
angle \n')
% specifiy paths for files, codes: modify to suit
%addpath('/bap_working/MatLabfiles/MachineLearning/pics'); % for images
etc - on Desktop
%addpath('/bap_working/MatLabfiles/MatlabFiles/GrapeProject/pics'); %
on Laptop  % for test images etc
%addpath(genpath('/bap_working/MatLabfiles/MatlabFiles/GrapeProject/pic
s')); % include sub-directories
% 2016

%addpath('/bap_working/MatLabfiles/MatlabFiles/GrapeProject/2016GrapePi
cs/chardonnay_cumulus/chardonnay_b'); % Log p52; & p14 (for 3rd visit)
addpath('/bap_working/MatLabfiles/MatlabFiles/GrapeProject/2016GrapePic
s/chardonnay_cumulus/chardonnay_c'); %   & Log p50

%addpath('/bap_working/MatLabfiles/MatlabFiles/GrapeProject/2016GrapePi
cs/chardonnay_cumulus/chardonnay_test_elena');
%addpath('/bap_working/MatLabfiles/MatlabFiles/GrapeProject/2016GrapePi
cs/sauvignon_blanc_cumulus/sauvignon_blanc_a'); % Log,p38

%addpath('/bap_working/MatLabfiles/MatlabFiles/GrapeProject/2016GrapePi
cs/chardonnay_see_saw/chardonnay_b');

%addpath('/bap_working/MatLabfiles/MatlabFiles/GrapeProject/2016GrapePi
cs/chardonnay_see_saw/chardonnay_test_elena');

% 2017
%addpath('/bap_working/MatLabfiles/MatlabFiles/GrapeProject/20170116Cum
ulus/Chard'); % 1st visit (16/1/17)
%addpath('/bap_working/MatLabfiles/MatlabFiles/GrapeProject/201700228JJ
'); % 1st visit (28/2/17)
```

```
addpath('/bap_working/MatLabfiles/MatlabFiles/GrapeProject/CodesFunctio
ns'); % for fenglu's codes

% 2016 pics of Ch. at Cumulus (6/1/16) - 1st, 2nd, 3rd visits
fprintf('\n >> Cumulus_Chdy: 06,14, 21/1/16, row C - pics \n')
 %fprintf('\n >> Cumulus_Chdy: 06,14, 21/1/16, Elena tests - pics \n')
   %fprintf('\n >> Cumulus_Chdy: 21/1/16, sample III - pics \n')
 %fprintf('\n >> Cumulus_SauvBlanc: 21/1/16, row A - pics \n')
%fprintf('\n >> SeeSaw(JJ)_Chdy: 21/1/16, row b - pics \n')
% 2017
% fprintf('\n >> Cumulus_Chdy: 16/1/2017, C1 - pics \n')
  %grapepic=imread('20170116_100022.jpg'); % Row 5, 25th vine:  "C1"
%grapepic=imread('20170116_101140.jpg'); % Row 5 across, 25th vine:
"C2"
%fprintf('\n >> SeeSaw(JJ)_Chdy: 28/2/17, row F - pics \n')

% pics at Cumulus (21/1/16)
 %grapepic1a=imread('20160121_chardonnay_cumulus_elena_I_0004.jpg');
%Elena sample
 %grapepic1a=imread('20160121_chardonnay_cumulus_elena_I_0003.jpg'); %
with Colour Checker card: Sq : 214px
 %grapepic=imread('20160106_chardonnay_cumulus_elena_I_0001.jpg'); %
  %grapepic1a=imread('20160106_chardonnay_cumulus_elena_III_0003.jpg');
% with Colour Checker card: Sq : 167 px
  % & note woody stem has diam:  120 px
%grapepic=imread('20160114_chardonnay_cumulus_b_0001.jpg'); % same
bunch: 3 dates
%grapepic=imread('20160121_chardonnay_cumulus_a_0001.jpg'); % same
bunch: 3 dates
%grapepic=imread('20160106_chardonnay_cumulus_b_0001.jpg'); % same
bunch: 2 dates with C/card
grapepic=imread('20160106_chardonnay_cumulus_c_0003.jpg'); % w C/card:
good eg.

%grapepic=imread('20160121_chardonnay_cumulus_d_0002.jpg'); % same
bunch: 2 dates + C/card
%grapepic=imread('20160106_chardonnay_cumulus_e_0003.jpg');  % probably
same bunch: 2 dates + C/card
%grapepic=imread('20160121_chardonnay_cumulus_e_0002.jpg');    % & 2
wks later
```

```
%grapepic=imread('20160114_chardonnay_cumulus_a_0001.jpg'); %  only
this one for 3 x visits
%grapepic=imread('20160121_sauvignon_blanc_cumulus_a_0002.jpg'); % w
C/card
  % Elena Samples
    %grapepic=imread('20160121_chardonnay_cumulus_elena_III_0003.jpg');
% with C/Card, samples marked
    %grapepic=imread('20160121_chardonnay_cumulus_elena_II_0003.jpg');
%grapepic=imread('20160121_chardonnay_cumulus_elena_II_0003.jpg'); %
good pic

% JJ_SeeSaw, Jan 21 2016
%grapepic=imread('20160121_chardonnay_see_saw_a_0004.jpg'); %     #4
darker; #1 bright
%grapepic=imread('20160121_chardonnay_see_saw_b_0002.jpg'); % #2 C/Card
is better aligned
% JJ_SeeSaw, Feb 19 2016 (#2 visit)
 %grapepic=imread('20160219_chardonnay_see_saw_b_0002.jpg');     %     #2
C/Card is better aligned
  % Elena Samples
%grapepic=imread('20160121_chardonnay_seesaw_elena_I_0003.jpg'); % with
C/Card, pic is dark/shaded
%grapepic=imread('20160121_chardonnay_xxxx_elena_III_0005.jpg'); % with
C/Card, samples marked

% JJ 28/02/17
%grapepic=imread('20170228_141929.jpg'); % 4k x 3k

% Gundagai, Feb 14 2017
%fprintf('\n >> Gundagai_Chdy: 14/2/2017 - pics \n')
%addpath('/bap_working/MatLabfiles/MatlabFiles/GrapeProject/20170214Gun
d'); % Leigh: 1st visit (14/2/17)
%grapepic=imread('CHARD_1_GUNDAGAI_HIGH_BLOCK_20170214_110520.jpg');
%poor, a little out of focus
%grapepic=imread('CHARD_1_GUNDAGAI_LOW_BLOCK_120170214_112018.jpg'); % p

%% 2. manually CROP the image: tight onto the bunch of grapes/berries
figure; grape_crop=imcrop(grapepic);  % GUI: drag'n'drop, then dblclick
figure; h=imshow(grape_crop);    % now 772 x 1096 / 886 x 122/ 936 x
1270 px {x 3}
```

```
[imgdata,flag] = getimage(h); % get the image data {CData} - into an
array [3 deep: R,G,B]
 % flag =4: ie  R,G,B image  % size(imgdata)  % data is 1536 x 2048
array {x 3 channels}  & file was ~700 KB
  % need this array for later analysis of the circles, as found
  %hold on
 % tighter is better: less bright background light & leaves d =
imdistline; % shows range of diam:  113-120 / 88-100 /  68-72 / 91-
98
     % ie. almost spr. gray_image = rgb2gray(grape_crop);
% get grey-scale image figure; imshow(gray_image); %
check it
 % save the cropped image
 %imwrite(grape_crop, 'GrapeBunch545_crop2.jpg'); % now 130 KB

% test check the image histogram
%fprintf('\n >> Grape picture: perform Histogram Equalization of image
\n')
figure; imhist(gray_image,64); grayh=histeq(gray_image);
figure; imhist(grayh,64);  %figure; imshow(grayh);

 %% 2.1 Optional:  Auto brighten the image:  this may, or may not,
help??
IMG1=double(grape_crop);
IMG2(:,:,1) = 1.5 * IMG1(:,:,1);  %RED Channel
IMG2(:,:,2) = 1.5 * IMG1(:,:,2);  %GREEN Channel IMG2(:,:,3)
= 1.5 * IMG1(:,:,3);  %BLUE Channel
if IMG2(:,:,1) > 255, IMG2(:,:,1) = 255, end; % adjust for out-of-range
if IMG2(:,:,2) > 255, IMG2(:,:,2) = 255, end; if IMG2(:,:,3) > 255,
IMG2(:,:,3) = 255, end;
 % figure; hist(double(IMG2(:,:,1)))  % check that it works ok :
preserves hist ok
IMG2 = uint8(IMG2); %conversion from double to unit8
figure; subplot(1,2,1);
imshow(grape_crop);  title('Original RGB Picture'); subplot(1,2,2);
imshow(IMG2); title('Brightened Image'); clear
IMG1
gray_image =rgb2gray(IMG2); % now analyse the brightened image
clear IMG2
```

```
 % ... and/or ....
%% 2.2  check the image histogram [equalise?] fprintf('\n
>> histogram equalise gray scale ... \n')
  %figure; imhist(gray_image,64);
grayh=histeq(gray_image);
%figure; imhist(grayh,64); figure;
subplot(1,2,1);
imhist(gray_image,64);  title('Original Gray Hist'); subplot(1,2,2);
imhist(grayh,64); title('Hist Eq: new Hist');

% compare the pics figure;
subplot(1,2,1);
imshow(gray_image);  title('Original Gray Picture'); subplot(1,2,2);
imshow(grayh); title('Hist Eq Picture'); figure;
imhist(gray_image,64);

% Decide?   maybe ? use the cropped & Hist Eq image - in the circle
finder at #3
gray_image = grayh; %clear grayh

%% 3.  find circles - Hough transform method
% it uses grayscale anyway;  default method is 'PhaseCode'
% params tested in v2. % smaller r range  & use output metric, to
filter out false finds
% get typical diam from imdistline; then "guess" range of radii, to
search
% need to scan sensitivity >0.95 :: & check for min. false finds

fprintf('\n >> Grape pictures; find circles: Bright/ Dark polarity \n')
fprintf('\n  > radii range for grape pic [r1 r2], Sensitivity 0.98,
EdgThr 0.1  \n')
% 3.1 BRIGHT:  find the "bright-find" circles
r1= 86; r2= 138; % range (pixels) - est from imdist tool on picture
[r1 r2]
[centers,   radii,      metric]     =     imfindcircles(gray_image,[r1
r2],'ObjectPolarity','bright', ...
    'Sensitivity',0.98, 'EdgeThreshold', 0.1);  % us hi Sensitivity %
low edge gradient - to find more
Nbright=length(radii)
```

```
Avradius=mean(radii)
StdRadii=std(radii)
ratio=StdRadii/Avradius  clear
Avradius StdRadii ratio

% highlight bright-find circles, as found
  %figure; imshow(grapepic); hold on  % Full pic - as taken figure;
imshow(grape_crop); hold on  % Cropped pic - tight on bunch
title('Cumulus          2016          Chard          C:          find
circles','FontSize',14,'FontWeight','bold')
%title('Cumulus         2016         SauvBlanc         A:         find
circles','FontSize',14,'FontWeight','bold')
 %d = imdistline; % for scale length; % get the 1-cm scale: squares are
0.95 cm
% draw bright (red) circle, to highlight circles found
viscircles(centers, radii);  % overlay the found circles %
number (ID) the circle: on the graphic and list them for
i=1:Nbright
  text((centers(i,1)+1),(centers(i,2)+1),num2str(i),      'FontSize',20,
'Colour', 'r');
end
list= (1:Nbright)';  %radii=round(radii); % approx to nearest integer
%[list, radii] % in pixels
% convert to cm scale:  needs imdistline on ColourChecker card : 0.95cm
squares
%rcm=radii*1.33/300.3;
%[list, rcm]

% 3.2 DARK:  now find the "dark-find" circles
[centersd,  radiid,     metric]     =     imfindcircles(gray_image,[r1
r2],'ObjectPolarity','dark', ...
    'Sensitivity',0.98, 'EdgeThreshold', 0.1);
Ndark=length(radiid)
Avradius=mean(radiid)
StdRadii=std(radiid)
ratio=StdRadii/Avradius  clear
Avradius StdRadii ratio

% draw dark (blue) found circles
%figure; hist(radiid)
```

```
viscircles(centersd, radiid, 'EdgeColour','b'); %
number (ID) the circle: on the graphic and list them
for i=1:Ndark
  text((centersd(i,1)+1),(centersd(i,2)+1),num2str(i), 'FontSize',20,
'Colour', 'b');
end hold off
list= (1:Ndark)';  %radii=round(radii); % approx to nearest integer
 %[list, radii]; % in pixels
% nb. for cropped image:
    % ??purge 'false' cicles: eg containing bright sunlisht / Plot Hist
radii
% merge lists of bright + Dark finds
%centers=vertcat(centers, centersd); % merge the (column) lists
%radii= vertcat(radii, radiid);
clear radiid centersd figure;
hist(radii); hold on
title('Cumulus            06Jan2016            Chard:            Radius
distribution','FontSize',14,'FontWeight','bold') xlabel('radius
(pixels)','FontSize',14); hold off

%% 3.3 convert to cm scale:  needs object to measure scale %
Calibrate:  use imdistline on ColourChecker card : 0.95-cm squares
rcm=radii*0.95/219.2; % Colour Card square is 0.95cm
 %[list, rdcm] figure;
hist(rcm); hold on
title('Cumulus    SauvBlanc   A,    21Jan16:    Radius      -
distribution','FontSize',14,'FontWeight','bold') xlabel('radius
(cm)','FontSize',14); hold off
%
Avradius=mean(rcm)
StdRadii=std(rcm)  %
Volume
vol=(4*pi/3)*rcm.^3;
figure; hist(vol); hold on
title('Cumulus    SauvBlanc   A,    21Jan16:    Berry       volume
distribution','FontSize',14,'FontWeight','bold') xlabel('Volume
(cm^3)','FontSize',14); hold off
AvVols=mean(vol)   StdVol=std(vol)
```

```
% Export Vol Hist to Excel %
set range (cm)
r1cm=floor(min(rcm)); % round down r2cm=ceil(max(rcm));
% round up
binrange=linspace(r1cm,r2cm,15); % get Vol range from hist plot already
bincounts=histc(vol,binrange);
 %figure; bar(binrange, bincounts,'histc') % check radius pic
%[binrange', bincounts]  % get both as col vec
VolHistData=[binrange', bincounts];
 %csvwrite('20170106_time_ChyC_VolHist.csv',VolHistData);  % save
radius data
  %  or  % csvwrite('20160121_sample#_Chy2_VolHist.csv',VolHistData);

% >     >   >   >   Colour detection
%% 4. Hue calc.  Mask to crop circles from orig image  % R,G,B or H,S,V
% get colour per grape-berry
fprintf('\n  >>  Grape  pictures;  mask  circles:  find  Hue  \n')
h=imshow(grape_crop);   % now 772 x 1096 pixels / 886 x 122/ 936 x 1270
px {x 3}
[imgdata,flag] = getimage(h); % get the image data {CData} - into an
array [3 deep: R,G,B]
imgsize=size(imgdata); % down, then across
imgarea=imgsize(1)*imgsize(2)
cropedimgAll=uint8(zeros(imgsize)); % set up 3D array (for all cicles)
hueg=zeros(length(radii),1); % array to hold hue angle (average) for ea.
grape berry figure; hold on
% cycle through each disc found:
for i=1:length(radii)
cropedimg=uint8(zeros(imgsize)); % set up array (for this cicle)
% set up mask, for 1st disc, then try #2
     %[xx, yy]= ndgrid((1:imgsize(1))-centers(2,1),
(1:imgsize(2))centers(2,2));
[xx,  yy]= ndgrid((1:imgsize(1))-centers(i,2),
(1:imgsize(2))centers(i,1)); % may need to switch x,y axes, to match
i,j indexing in image
 %[xx, yy]= ndgrid((1:imgsize(1))-centers(1,2),
(1:imgsize(2))centers(1,1)); % circle #1
mask=uint8((xx.^2 +yy.^2) < radii(i)^2 ); for
j=1:3
```

```
cropedimg(:,:,j)=imgdata(:,:,j).*mask; % need
to filter each R,G,B layer end
cropedimgAll=cropedimgAll + cropedimg; % add in the new cicle
imshow(cropedimgAll);
% get Hue of this circle, so need HSV:
cropedimghsv=rgb2hsv(cropedimg);
 cropedimgh=cropedimghsv(:,:,1); cropedimgh=cropedimgh*360; % get Hue,
in degrees
 npix=length(find(cropedimgh(:)>0)); % get # pixels in this circle
HueAv1=mean(cropedimgh(:))*imgarea/npix;  % Av hue of this circle: need
to rescale by # non-0 elements
 HueStd1= std(cropedimgh(:));
%HueStats = [i npix HueAv1 HueStd1] % Testing: print out result for
each circle
 %figure; stem(cropedimgh(:,:,1))
hueg(i)=HueAv1; % accumulate the Hue angles
%pause % examine each circle (testing)  clear
cropedimg mask cropedimghsv cropedimgh end
title('grape: circles found'); hold off

figure; hist(hueg); hold on
title('Cumulus SauvBlanc A, Jan21: Hue angle (raw)
distribution','FontSize',14,'FontWeight','bold')
xlabel('Hue angle','FontSize',14); ylabel('Counts','FontSize',14);
axis([50 75 0 10])  % elim outlier at ~200-250deg - ie. C/C card whiteish
square  hold off
HueAvAll=mean(hueg) HueStdAll=
std(hueg)

% handle Outliers, if needed? (eg fingers, white sq, bright background,
leaves etc)
fprintf('\n >> Grape pictures; eliminate outlier Hue \n')
list=find(hueg<=130); % eliminate outliers
hueg1=hueg(list);   figure; hist(hueg1) % check them
 title('Cumulus Chard C, Jan06: Hue tint angle
distribution','FontSize',14,'FontWeight','bold');
 xlabel('Hue angle','FontSize',14); ylabel('Counts','FontSize',14); hold
off   mean(hueg1)   std(hueg1)  clear list
```

```
%% 5. test ColourChecker reference card - of colour squares  (27/12/15)
: use Samsung G4


%addpath('/bap_working/MatLabfiles/MatlabFiles/GrapeProject/ColourChecker'); % on Laptop  % for test images etc
 %imfinfo('ColourChecker/ColourChecker_IMG_0177.jpg') % iPhone pic.  4k x 3k
 %cardpic=imread('SamsungColourChecker20151227_120412.jpg'); %  Samsung G4 pics - of Colour card
 %cardpicCM=imread('SamsungColourChecker20160102_075546_cm.jpg'); % includes 1cm mark - for scale
 %figure; imshow(cardpic)

%cardpic=imread('20160121_114752.jpg');  % Samples: Elena JJ Chy01  % _ has ColourCard
cardpic=imread('20160121_113721.jpg');   %   JJ Chy pos'n #1   % _ has ColourCard figure; imshow(cardpic)
d = imdistline; % get the pixel-cm scale: squares are 0.95 cm
   % convert to cm scale:  needs imdistline on ColourChecker card : 0.95-cm squares
   %(0.95/128)*212

%card_crop=imcrop(cardpic);  % GUI: drag'n'drop, then dbl-click
%figure; imshow(card_crop);
%impixelinfo  % get per-pixel
%imtool(card_crop); % then hover over areas - for (x, y), (r, g, b)  %d = imdistline; % get the 1-cm scale: 322 (LHS) & 316( RHS) pixels per cm - 1st image #546
      % nb. varies with croping!!   % and 289, 298 pix on 2nd image (#610)
 % overall fairly good: ~10% diff.

%% 5.1 ColourChecker at CUMULUS - reference card of colour squares (6/1/16) : Samsung G4
 % fairly good: ~10% diff.
%addpath('/bap_working/MatLabfiles/MatlabFiles/GrapeProject/ColourChecker'); % on Laptop  % for images etc
%imfinfo('ColourChecker/ColourChecker_IMG_0177.jpg') % iPhone pic.  4k x 3k
```

```
%cardpic=imread('SamsungColourChecker20151227_120412.jpg'); %  Samsung G4 pics - of Colour card
%cardpicCM=imread('SamsungColourChecker20160102_075546_cm.jpg');  % includes 1cm mark - for scale
 %figure; imshow(cardpic)

% GUI: drag'n'drop, then dbl-click
 %figure; imshow(card_crop);
 %impixelinfo  % get per-pixel
 %imtool(card_crop); % then hover over areas - for (x, y), (r, g, b)

% grab the ColourChecker from in-field photo - by hand!!;  % then get black sq; then wht. card_black=imcrop(grapepic);  % GUI: drag'n'drop, then dbl-click to get file
  figure; imshow(card_black);
card_white=imcrop(grapepic);         figure;    imshow(card_white);
imtool(card_black); % then hover over areas - for (x, y), (r, g, b)
imtool(card_white);
 %d = imdistline; % get the 1-cm scale: 322 (LHS) & 316( RHS) pixels per cm - 1st image #546
 % nb. varies with croping!!   % and 289, 298 pix on 2nd image (#610)

 % get av RGB for ea square:
 rgb_black=mean(mean(card_black(:,:,1:3)))
rgb_white=mean(mean(card_white(:,:,1:3)))

% now rescale the analysis image: work with grape_crop : the handcropped field pic
%     cf.
http://au.mathworks.com/matlabcentral/fileexchange/42548consistent-imaging-with-consumer-cameras?s_tid=srchtitle
 % code from whitebalance.m, in /CameraColourCodes/..  &  ref. Akkaynak JoSA 2014
 % param.  f : Relative brightness of the WS. f = 1 may saturate most images;
%             default value 0.8.
f = 0.8;
WS = rgb_white; DS = rgb_black; % av RGB of White Sq & Black Sq (of ColourChecker card pic)
Rlayer = double(grape_crop(:,:,1));
```

```
Glayer = double(grape_crop(:,:,2)); Blayer
= double(grape_crop(:,:,3));
 % linear re-scale
Rlayer = f*(Rlayer - DS(1))./(WS(1) - DS(1));
Glayer = f*(Glayer - DS(2))./(WS(2) - DS(2)); Blayer
= f*(Blayer - DS(3))./(WS(3) - DS(3));
%
Rlayer(Rlayer>1)=1;
Glayer(Glayer>1)=1;
Blayer(Blayer>1)=1;
 % output white balanced image
grape_crop_wb(:,:,1) = Rlayer;  % nb these are double, not uint8 [0,
255]
grape_crop_wb(:,:,2) = Glayer;
grape_crop_wb(:,:,3) = Blayer; clear
f Rlayer Glayer Blayer WS DS

figure; imshow(grape_crop_wb); hold on
title('Cumulus                          Chy-II:                          white
balanced','FontSize',14,'FontWeight','bold')
% double plot: side-by-side compare figure;
subplot(1,2,1); hold on
imshow(grape_crop);  title('Original Picture'); subplot(1,2,2);
imshow(grape_crop_wb); title('Colour balanced Picture'); hold
off

%% 6. now mask this WhiteBalance image, to get Hue angle of circles
(13/1/16)
% get colour per grape-berry: scan all found circles figure;
h=imshow(grape_crop_wb);   %
[imgdata,flag] = getimage(h); % get the image data {CData} - into an
array [3 deep: R,G,B]
  % need this array for later analysis of the circles, as found
imgsize=size(imgdata); % down, then across imgdata=uint8(imgdata);
% for consistent calc below imgarea=imgsize(1)*imgsize(2);
cropedimgAll=uint8(zeros(imgsize));  %  set  up  array  (for  all  cicles)
hueg=zeros(length(radii),1); % array to hold hue angle (average) for ea.
grape berry %figure; hold on
cropedimgAll=uint8(zeros(imgsize(1),imgsize(2),3)); % dummy array to
hold new image
```

```
% cycle through each disc found:
for i=1:length(radii)
 %for      i=4:4      %5           %      Debug      ~      0      pixels?
cropedimg=uint8(zeros(imgsize(1),imgsize(2),3)); % set up array (for this
cicle)
% set up mask, for 1st disc, then try #2
     %[xx, yy]= ndgrid((1:imgsize(1))-centers(2,1),
(1:imgsize(2))centers(2,2));
[xx,  yy]= ndgrid((1:imgsize(1))-centers(i,2),
(1:imgsize(2))centers(i,1)); % may need to switch x,y axes, to match
i,j indexing in image
 %[xx, yy]= ndgrid((1:imgsize(1))-centers(1,2),
(1:imgsize(2))centers(1,1)); % circle #1
mask=uint8((xx.^2 +yy.^2) < radii(i)^2 ); for
j=1:3
    cropedimg(:,:,j)=imgdata(:,:,j).*mask; % need to filter each R,G,B
layer end
cropedimgAll=cropedimgAll + cropedimg; % add in the new cicle
 %imshow(cropedimgAll);
 %figure; imshow(cropedimg) % Debug %
get Hue of this circle, so need HSV:
cropedimghsv=rgb2hsv(cropedimg);
  cropedimgh=cropedimghsv(:,:,1); cropedimgh=cropedimgh*360; % get Hue,
in degrees
 npix=length(find(cropedimgh(:)>0));  %  get  #  pixels  in  this  circle
HueAv1=mean(cropedimgh(:))*imgarea/npix;  % Av hue of this circle: need
to rescale by # non-0 elements  HueStd1= std(cropedimgh(:));
HueStats = [i npix HueAv1 HueStd1]
%figure; stem(cropedimgh(:,:,1)) %Debug
hueg(i)=HueAv1; % accumulate the Hue angles
  %pause % examine each circle (testing)
 %clear cropedimg mask cropedimghsv cropedimgh cropedimgAll
end
%title('Cumulus Chy-01, WB:  circles found'); hold off

figure; hist(hueg); hold on
title('Cumulus          Chy-II,          WB:          Hue          angle
distribution','FontSize',14,'FontWeight','bold')
xlabel('Hue        angle        (White        balanced)','FontSize',14);
ylabel('Counts','FontSize',14); hold off
```

```
HueAvAll=mean(hueg) HueStdAll=
std(hueg)

%% 6.0.1 handle Outliers, if needed? (eg fingers, white sq, bright
background, leaves etc)
fprintf('\n >> Grape pictures; eliminate outlier colour balanced Hue
\n')
list=find(hueg<=130) % eliminate outliers (too white/bright )
hueg1=hueg(list);   figure; hist(hueg1) % check them
 title('Cumulus Chard II, Jan21: Hue (White balanced) angle
distribution','FontSize',14,'FontWeight','bold'); hold off
mean(hueg1)   std(hueg1)  clear list

%% 6.1  Other tasks: %
Export Vol Hist to Excel
binrange=linspace(0,150,25); % get Vol range from hist plot already
bincounts=histc(hueg,binrange); figure; bar(binrange,
bincounts,'histc')
[binrange', bincounts]  % get both as col vec VolHistData=[binrange',
bincounts];
csvwrite('20160121_time_Chy2_HueHist.csv',VolHistData);

% OR analyse Sigma/R-av vs t
% gsig=csvread('GrapeSigma.csv');
% figure; hold
on
plot(gsig(:,1), gsig(:,2), '.', 'MarkerSize', 30) axis([0
25 0.01 0.2])
title('Cumulus             Chardy,             Evolution             of
Variance','FontSize',14,'FontWeight','bold')
xlabel('day # (Jan 2016)','FontSize',14); ylabel('StdDev-R/ Mean-
R','FontSize',14); hold off
% >>>>>>>>
```

Appendix 6: OpenCV and Java codes for phone app

The OpenCV and Java codes for the phone app contain many thousands of lines of code and are not included in the report. Inquiries can be made with the National Wine and Grape Industry Centre (NWGIC) at Charles Sturt University.

Appendix 7: Picture taking protocol

To get the best measurement results with the app, photographs need to be taken with a little care. You must take care of the overall illumination falling on the grapes and the position of the smartphone with respect to the grape bunch. To measure the diameter of the berries, you need to use a known object (for instance a coin or a graduated scale) and place it near the grape when taking a photograph.

The best day to take the photographs is on an overcast day when the illumination falling on the grapes is uniform. If this is not possible, take the photograph of the bunch completely in the shade. If sunlight is falling on some of the berries, put yourself between the sun and the grape to cast a shadow on the grape you are photographing. Do not use a coloured translucent material such as an umbrella as it will put a colour cast on the photograph. The photographs below show what to avoid, on the left, and what to aim for, on the right.



Figure 56: Avoid non-uniform illumination: note the top of the bunch is in the shade compared to the bottom (left). Uniform illumination is better (right).



Figure 57: Another example of non-uniform illumination: some of the berries are lit brightly by the sun.

The human eye does not notice colour casts until the photograph is displayed or printed. Light sources of different colour temperatures [Burns] will usually cause colour cast problems; this is more evident in the shadows. Avoid taking photographs too early, around sunrise, as the shade will have a blue cast; or at sunset, as the shadow then will have a warm tone. Some examples of colour cast are shown below. These colour casts can be corrected later by performing a colour calibration (see below).



Figure 58: Blue colour cast in the original photograph (left). The same image after being colour-corrected using the ColourChecker card (right).

When taking a photograph, make sure that you hold the phone parallel to the grape bunch (i.e. in the same plane) and that the bunch fills the screen. If the camera is not parallel the image will be skewed: the app will have more trouble finding circles. Some examples are shown below.



Figure 59: An example where the camera is held too high.